An Intraperitoneal Implantable Drug Delivery Device for the Treatment of Ovarian Cancer

by

Hongye Ye

B.S.E. Biomedical Engineering
University of Michigan, Ann Arbor, 2007

Submitted to the Harvard-MIT Division of Health Sciences and Technology
in partial fulfillment of the requirements for the degree of
Doctorate of Philosophy in Medical Engineering and Medical Physics
at the
MASSACHUSETTS INSTITUTE OF TECHNOLOGY
February 2014
©2014 Massachusetts Institute of Technology 2014.
All rights reserved
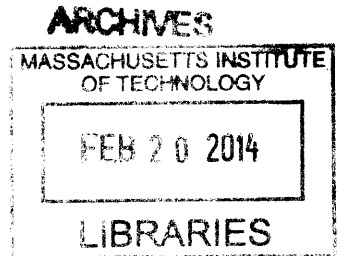
Signature of Author: ....
Harvard-MIT Division of Health Sciences and Technology
Sept 23, 2013

Certified by: ....
Michael J. Cima, PhD
Koch Professor, Professor of Material Science Engineering
Director of Lemelson-MIT Program
Thesis Supervisor

Certified by: ....
Robert Langer, PhD
Institute Professor
Professor of Chemical Engineering and Bioengineering, MIT
HST Committee Chair

Accepted by: ....
Emery N. Brown, MD, PhD
Director, Harvard-MIT Program in Health Sciences and Technology
Professor of Computational Neuroscience and Health Sciences and Technology

1

An Intraperitoneal Implantable Drug Delivery Device for the Treatment of Ovarian Cancer

by

Hongye Ye

Abstract:

Ovarian cancer is the fifth leading cause of cancer-related deaths in women and the deadliest gynecologic cancer. The current standard treatment for advanced ovarian cancer includes a minimally invasive cytoreduction surgery, followed by intravenous (IV) or intraperitoneal (IP) chemotherapy with cisplatin and taxol. Clinical trials showed that the IP cisplatin treatment regimen was able to prolong overall survival by 16 months but only 42% of subjects completed all cycles of the IP therapy. The primary reason for the early termination of the IP treatment is catheter-related complications. The implantation of the catheter is also a complex procedure that can only be performed at premier centers by trained personnel. An alternative for IP administration that eliminates catheter-related complications and simplifies IP drug administration would therefore allow more patients to enjoy the benefits of IP therapy.

A drug delivery device for use in a mouse model was developed as a tool to prove that maintaining a low constant cisplatin concentration in the peritoneal cavity and serum would improve the treatment outcome and reduce drug-related toxicity in ovarian cancer, compared to periodic IP bolus drug infusion. The device demonstrated highly linear and easily tunable *in vitro* release and exhibited excellent *in vitro-in vivo* correlation. Investigations of the device pharmacokinetics *in vivo* proved that the device was able to maintain a low and constant cisplatin concentration both locally in the peritoneal cavity and in the serum over up to six weeks. *In vitro* cytotoxicity of continuous cisplatin dosing with various human ovarian cancer cells lines was demonstrated. An *in vivo* xenograft SKOV-3 tumor model was established and optimized to reflect the distribution of ovarian cancer metastases in humans. The device achieved effective tumor growth retardation without systemic toxicity. An IP bolus injection scheme with a similar area-under-curve (AUC), however, caused severe bone marrow depletion. The results verified that the treatment efficacy correlates with the AUC but not the peak concentration, C_{max}. These promising preclinical results highlight the potential of this new therapeutic regimen to change the course of ovarian cancer care and warrant the need for designing a human device before proceeding to human trials.

Thesis Supervisor:
Michael J. Cima, PhD
Koch Professor, Director of Lemelson Program, MIT

Thesis Committee Chair:
Robert Langer, PhD
Institute Professor of Chemical Engineering and Bioengineering, MIT

Thesis Readers:
Michael J. Birrer, MD, PhD
Professor, Department of Medicine, HMS, DF/HCC

Marcela G. del Carmen, MD
Associate Professor, Department of Obstetrics, Gynecology and Reproductive Biology, HMS
Associate Professor, Gynecologic Oncology, MGH

Acknowledgement

I would like to thank my advisor, Professor Michael Cima for his unwavering support and mentorship over the past five years. His structure of having weekly meetings provided not only an opportunity to get regular feedback on our work and keep us on track, but also a chance for us to practice effective communication and presentation skills. I would like to thank my thesis committee chair, Professor Robert Langer, for all the thought-provoking questions along the way during the course of my PhD. I would also like to thank my thesis committee members who are also our collaborators on this project, Dr Michael Birrer and Dr Marcela Del Carmen for their kind guidance, extensive knowledge in their various fields and constructive recommendations. It was truly an honor to be able to work with them.

The PhD journey was certainly a path of hardship and endurance. I am very glad to have very good company throughout this journey. To all my lab mates, Lenny and Barb, Chris, Jen, Honglin, Yoda, Yibo, Byron, Alex, Vincent, Qunya, Urvashi, Kevin, Jay, Yuan, Laura, Matt, Negar, Greg, Katerina, Anna (Turskaya), Anna (Rodriguez-Chavez), Joan and Nuria, thank you all for the joy that you have brought me during this long journey. Without my dear lab mates who made the environment so cheerful, helpful and comfortable, I would not have the courage to walk until the end. I learned a lot from everyone, particularly from Chris, Jen and Jay. Chris and Jay are both extremely knowledgeable, helpful and patient, and have set themselves as very good role models for me. Jen was like a big sister to me, someone who taught me skills and influenced me with her positive spirit. Laura was my best buddy at work and we went through a lot of happy and sad times in the last two years of my PhD. Dr Young Jeong Na had also helped me a lot when I was feeling lost in the earlier phase of my PhD. It was really fun working with him.

I am super grateful to have found a group of very good friends during the five long years away from home. Ninghan, Wang Jia, Mingjuan, Jayce, Joanne, Terence, Yinjin, Yu Bo, Gu Chen, Yoong Keok, Wang Yang, Songyu, Richie, Shengyong, Zhen Xin, Xiaosai, Qunya, Greg and Alberta, Chun Yang, Shirleen and Guoliang, Kongjie, Jit Hin, Trina, Wui Siew, Huili, Alice and many more... everyone of you mean a lot to me.

Many things happened to me during these years in MIT, especially in the last year. Good and bad things. I would never forget all the happy times that we had together and how all my friends and lab mates helped me tide over the bad times. Life is a roller-coaster ride, and I am fortunate to have such a group of friends who rode with me during these years.

I have learned a lot during my years in MIT, academics being the least. As I continue to walk the path of life, I will continue to experience things in life, but the years in MIT will definitely be a significant stage of my life.

Last but not least, I will always love you my dearest Mummy and Lao Ba. This is for the two of you.

Contents

List of Figures

13

List of Tables

1 Background

1.1 Ovarian cancer etiology

Ovarian cancer is one of the most common types of cancer in females. It is the fifth leading cause of cancer-related deaths in women and the deadliest gynecologic cancer[1]. There were 14,436 deaths in 2009 and a projected incidence of 22,240 and 14,030 deaths in 2013[1]. About three-quarters of the patients present with peritoneal metastasis at the time of diagnosis [2,3] and the five-year survival for such patients is merely 26.9%[1]. This is largely because ovarian cancer is relatively asymptomatic at its early stages with rare cases of incidental early diagnosis due to other diseases or symptoms[2]. The tumor cells can metastasize to within the vast capacity of the pelvis and the ovaries after stage III. By the time patients present with symptoms, such as loss of weight, abdominal bloatedness and early satiety, they are usually at the later phases of the disease, with metastasis into the peritoneal cavity. Although patients with low-risk, stage I cancer can expect to have a five-year-survival rate of greater than 90%, approximately 75% of ovarian cancer patients present only in stage III and IV, which have survival rates of 30-50% and 13% respectively[4-6].

1.2 Ovarian cancer pathogenesis and genetics

There are two main theories involved in the pathogenesis of epithelial ovarian cancer: the incessant ovulation and the gonadotropin hypothesis[7]. The incessant ovulation suggests that with repeated ovulation, the ovarian epithelium undergoes repeated wounding and proliferation cycles. These cycles of repair process increases the chance of neoplasm and tumor formation[8]. In the gonadotropin theory, it is postulated that the gonadotropin secreted during rounds of ovulation also stimulates the ovarian surface epithelial cells and induces cell transformation[9]. Both models

are supported by data from both humans and animals. Although ovarian cancer displays defects in many genes (AKT, EGFR, ERBB2, RAS, PIK3CA, MYC, TP53 etc[7]), ovarian cancer has a strong correlation to an inherited mutation in either BRCA-1 or BRCA-2[6]. Mutations in these two genes account for 10% of ovarian cancers in the United States[10]. It is thought that about 90% of hereditary ovarian cancers arose from an inherited mutation in BRCA-1 on chromosome 17q[11]. BRCA-1 and -2 genes are involved in the DNA damage repair and transcriptional regulation. The fact that tumorigenesis in patients requires both the presence of a BRCA family mutation and a somatic inactivation of the remaining wild-type allele, shows that BRCA genes are tumor suppressors. BRCA-1/2 mutations are also associated with a higher risk of breast cancer, prostate cancer and so on[12] . Women with mutations may develop cancers at an early age, leading to psychological distress and loss of both quality and quantity of life. Genetic screening for BRCA-1/2 may help detect early ovarian cancers. It was demonstrated that preventive bilateral oophorectomy or salpingo-oophorectomy may reduce the risk of ovarian cancer by 53%[13].

1.3 Cytotoxic mechanism of cisplatin
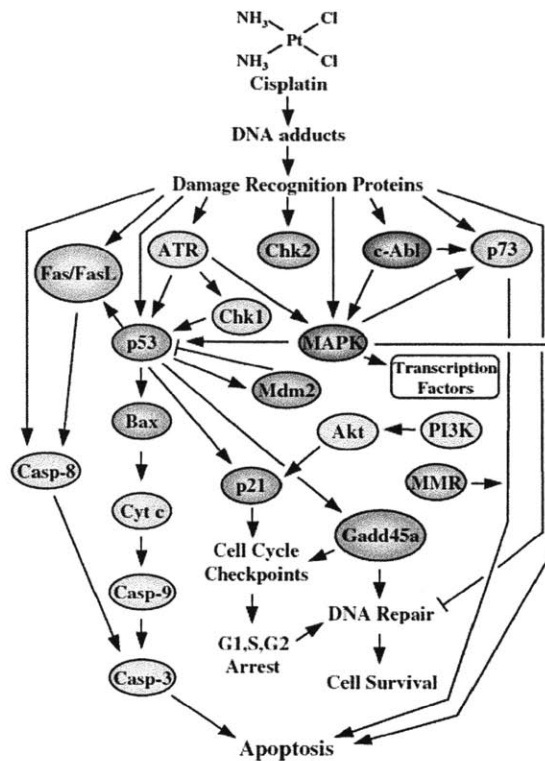
Figure 1.1 A schematic showing the various pathways involved in mediating cisplatin-induced cellular effects. Common apoptosis markers such as Casp-3, Casp-9, p53 and MAPK are involved. *Source: Cisplatin: mode of cytotoxic action and molecular basis of resistance by Z. H. Siddik*

Cisplatin is a well established, highly effective chemotherapeutic agent, commonly used in the treatment of ovarian, testicular, head and neck, small cell lung cancer and other cancers[14,15]. The anti-cancer property of the drug was discovered in 1965 by Rosenberg[14,16]. Cisplatin is a neutral molecule with a platinum core, two chloride and two ammonia groups. Cisplatin causes cells to undergo apoptosis by binding to DNA to form Pt-DNA adducts that will trigger various pathways that either repair the DNA damage or activate the cell's self-destruction mechanism (apoptosis). Figure1.1 provides an overview of the various pathways involved in apoptosis

triggered by the formation of the Pt-DNA adduct[15].
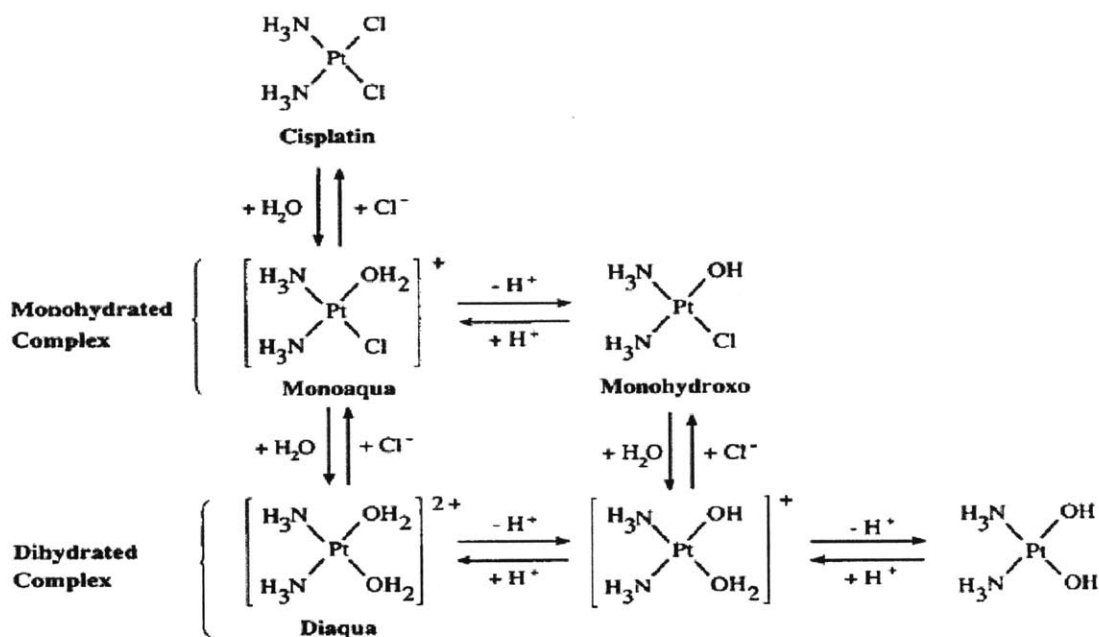
Figure 1.2 Cisplatin and its mono- and di-hydrated complexes. *Source: Cisplatin, transplatin, and their hydrated complexes: Separation and identification using porous graphitic carbon and electrospray ionization mass spectrometry by H. C. Ehrsson et al.*

Cisplatin, being a neutral molecule, has to undergo multiple steps of hydration in order to activate its side groups for binding with the charged DNA[15]. Figure 1.2 shows the hydration steps involved – each step consist of the replacement of one of its chloride ligands for a water molecule[17]. Figure 1.3 describes the steps that cisplatin molecule goes through after entering a cell. A cisplatin molecule in the bloodstream of a patient stays in its un-hydrated form due to the high chloride concentration in the blood (approximately 100 mM)[18]. Cisplatin in the blood is highly susceptible to binding with the proteins found in bloodstream, especially those with thiol side groups such as the albumin[19-21]. Studies have shown that one day after IV cisplatin administration, 65 – 98% of the drug had bound with proteins found in the body, deactivating it[22]. The cisplatin that either diffuses or is actively transported into the cells via Cu-transporters

20
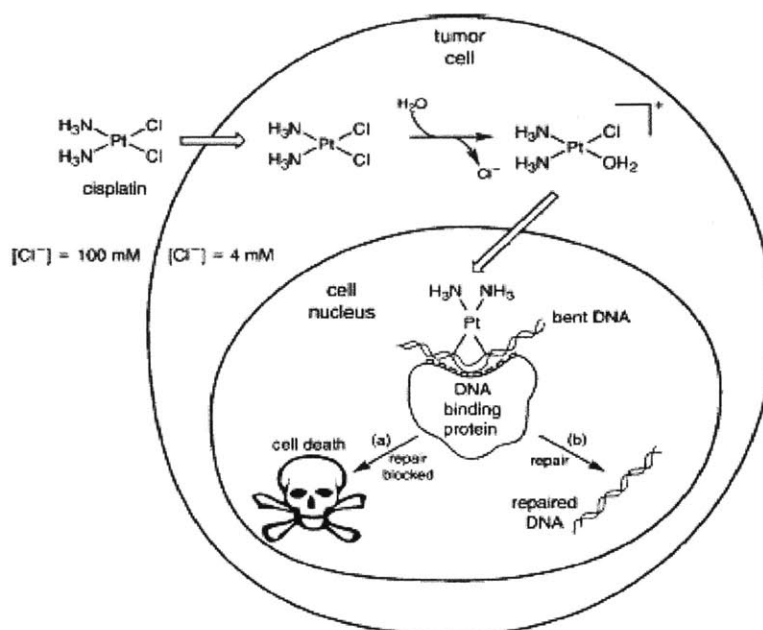
Figure 1.3 A schematic showing the path of cisplatin after it enters a cell. *Source: The discovery and development of cisplatin by R. A. Alderden et al.*

(CTR1) enters an environment with relatively low chloride concentration of 4-20 mM[14,23]. This low chloride concentration drives the equilibrium towards forming the hydrated forms of cisplatin[17]. Researchers have reported that 98% of the Pt-DNA adducts in the cells are formed by monohydrated cisplatin molecules and it is the hydrated complexes that are cytotoxic and reactive with DNA[17,24].

1.4 Cisplatin resistance

Cisplatin resistance is generally considered to be multifactorial. It is usually due to the following four factors[14,25,26]:

1. Reduced accumulation of the drug

2. Inactivation of the drug by thiol-containing molecules

3. Improved Pt-DNA adduct repair

4. Increased cisplatin tolerance and disruption of the cell death pathways

21

[Cl⁻] → $[Cl^-]_{intracellular} \approx 2\text{-}30\ mM$

$[Cl^-]_{extracellular} \approx 100mM$
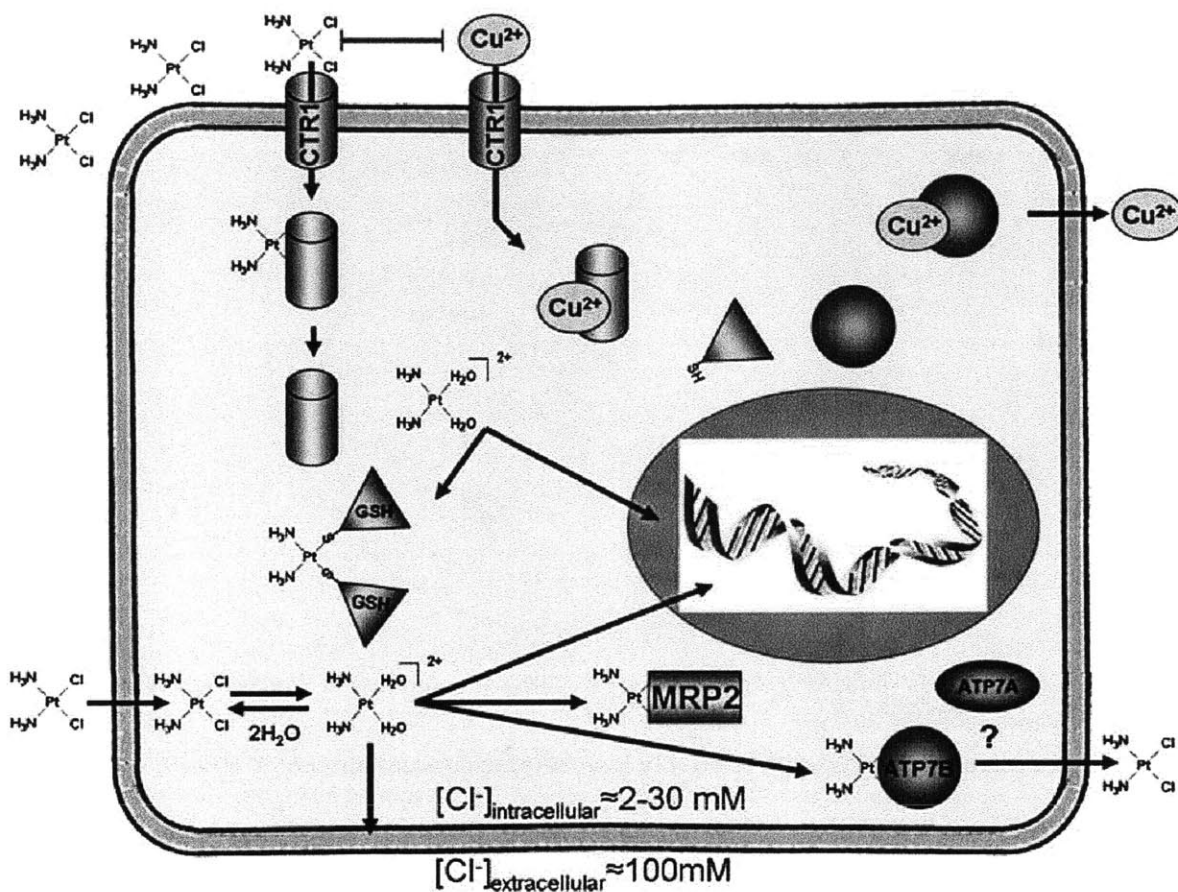
Figure 1.4 Cisplatin transport in and out of a cell. The uptake of cisplatin by a cell could be through both diffusion through the cell membrane or an active copper transporter (CTR1). Once inside the cell, cisplatin could bind to a thiol-rich molecule or enter the nucleus to bind to DNA. Binding of cisplatin to thiol-rich molecules such as glutathione reduces the amount of cisplatin available for DNA binding and therefore decreases the sensitivity of a cell to cisplatin. Multidrug resistance-associated protein-2 (MRP2) has been associated with the enhanced efflux of cisplatin from a cell. *Source of diagram: Biochemical mechanisms of cisplatin cytotoxicity by V Cepeda et al.*

Different cells may exhibit cisplatin resistance through different combinations of the above factors. The reduction in the concentration of drug within the tumor cells could be a result of decreased drug uptake or increased drug efflux[15]. There is evidence for both mechanisms and a reduction of 20 – 70% has been documented in the literature[27]. The decrease in influx of cisplatin is likely related to the reduction in active transport of cisplatin into the cell; the increase in efflux

is reported to be associated to the multidrug resistance-associated protein-2 (MRP2). The

increase in the production of thiol-rich molecules such as glutathione (GSH) has been reported in

the literature[27]. The elevation of such molecules inside the cell causes increased binding of

cisplatin and inactivation of cisplatin. This therefore reduces the free cisplatin available for DNA

adducts formation (Figure 1.4).

The formation and persistence of the Pt-DNA adduct is directly related to the success of turning

on the apoptosis pathway. An enhanced repair would switch off apoptosis. The nucleotide

excision repair (NER) is the major pathway involved in repairing the Pt-DNA adduct. It is

evident that cellular defects of the NER pathway lead to cisplatin hypersensitivity; restoration of

the NER pathway re-establishs a normal level of cisplatin sensitivity[28,29]. In the clinic, resistance

develops when the tumor cells do not undergo apoptosis at clinically relevant drug

concentrations[15]. It is observed that cisplatin resistance is much higher in refractory diseases in

patients and would require cytotoxic concentrations of 50-100 times higher drug concentration

than drug sensitive tumor cells[25,30].

1.5 Current treatment options for ovarian cancer

The current standard treatment for advanced ovarian cancer includes cytoreduction surgery

where the bulk of the tumor is removed (most of the time via minimally invasive laparoscopic

surgery), followed by intravenous (IV) or intraperitoneal (IP) chemotherapy with a platinum-

based agent such as cisplatin[4,31,32]. Patients who opt for IP chemotherapy receive 100mg/m^2 of

cisplatin solution through an in-dwelling catheter once every three weeks, for six cycles[33]. The

catheter and a subcutaneous port, to which it is connected to, are implanted during the

cytoreduction surgery. Two 5mm incisions are made at the upper right and lower right quadrants

of the abdomen following the debulking of large visible tumors. The tip of the catheter is

tunneled subcutaneously to the incision in the lower right quadrant of the abdomen where it will enter the peritoneal cavity. The port is then inserted through the incision at the upper right quadrant and sutured subcutaneously. A schematic is shown in Figure 1.5[34].
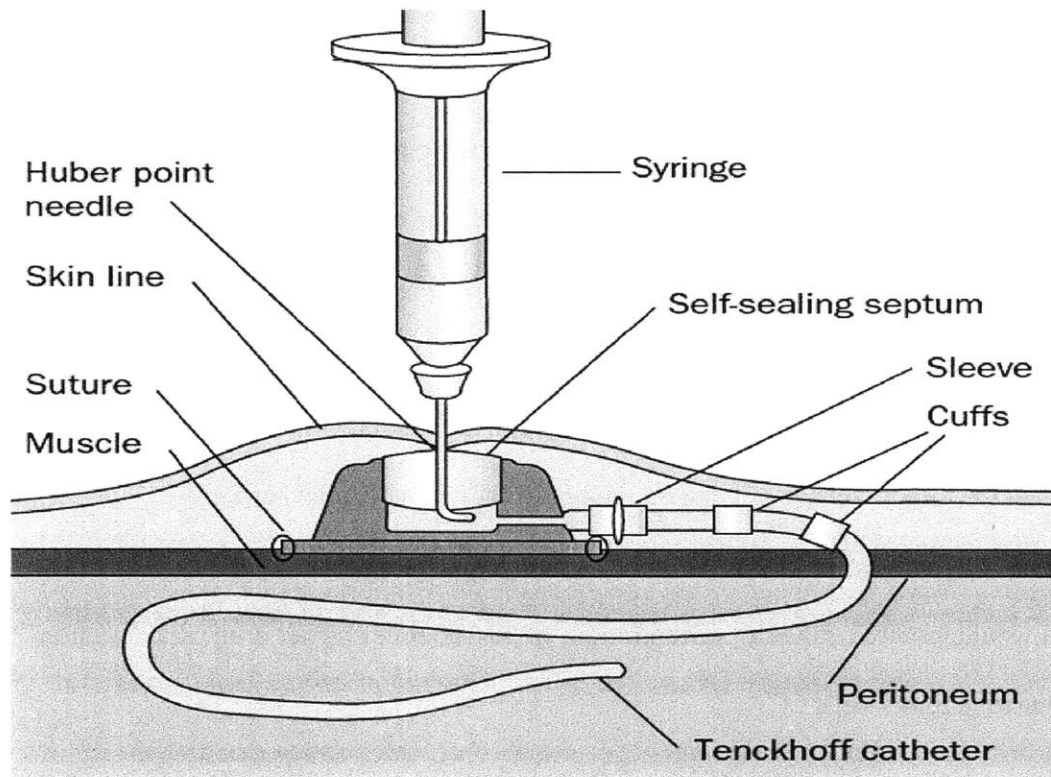
Figure 1.5 A schematic (not to scale) showing the various components of the catheter port. The cisplatin solution is injected via a syringe once every 3 weeks through the catheter port, into the peritoneal cavity of the patient. *Source of diagram: Intraperitoneal antineoplastic drug delivery: rationale and results, Maurie Markman*

A patient on an intraperitoneal chemotherapy treatment regimen receives an infusion of 2-L of cisplatin solution through the port and into the peritoneal cavity once every three weeks. The implantation site is prone to infection and inflammation over the entire period of 18 weeks of treatment, and the long catheter is susceptible to obstruction[35]. Pharmacokinetic studies have shown that the peak concentration of cisplatin in the peritoneal cavity reaches a level 20 times that in the systemic compartment, and the total area-under-curve concentration of cisplatin is 12

times that of systemic circulation if cisplatin is administered directly into the peritoneal cavity[34,36]. The Gynecology Oncology Group (GOG) has conducted three large randomized phase III trials, comparing IV cisplatin treatment regimens to IP cisplatin treatment[33,37-39]. The three trials are outlined in Figure 1.6[37].

Study	Intravenous Regimen	IP Regimen
SWOG 8501/ GOG 104, Alberts et al[5]	Cisplatin 100 mg/m^2 IV Cyclophosphamide 600 mg/m^2 IV Q 3 wks × 6	Cisplatin 100 mg/m^2 IP Cyclophosphamide 600 mg/m^2 IV Q 3 wks × 6
GOG 114/ SWOG 9227, Markman et al[8]	Cisplatin 75 mg/m^2 IV Paclitaxel 135 mg/m^2 IV Q 3 wks × 6	Carboplatin (AUC 9) IV q 28 days × 2 Cisplatin 100 mg/m^2 IP Paclitaxel 135 mg/m^2 IV Q 3 wks × 6
GOG 172, Armstrong et al[10]	Cisplatin 75 mg/m^2 IV; Paclitaxel 135 mg/m^2 IV Q 3 wks × 6	Paclitaxel 135 mg/m^2 IV Cisplatin 100 mg/m^2 IP Paclitaxel 60 mg/m^2 IP on day 8 Q 3 wks × 6

GOG, Gynecologic Oncology Group; HR, hazard ratio; IV, intravenous; Q, every.

Figure 1.6 An outline of three large randomized phase III clinical trials conducted by the Gynecologic Oncology Group (GOG). *Source: Intraperitoneal Chemotherapy – Why the Fuzz? By Walter H. Gotlieb*

The GOG had found that the IP cisplatin treatment regimen was able to prolong overall survival from 49.7 months in IV treatment to 65.6 months (p=0.03)[33]. However, while 83% of subjects completed all cycles of the IV therapy, only 42% of subjects completed all cycles of the IP therapy. The primary reason for early termination of the IP treatment is catheter-related complications[33,35]. An alternative for IP administration that eliminates catheter-related complications would thus allow more patients to benefit from IP therapy. Furthermore, many

medical practitioners in smaller centers are unable to recommend this treatment modality due to the lack of familiarity among clinicians with peritoneal administration and catheter-placement techniques[33]. The New York Times reported on March 11, 2013 that this complex procedure can only be performed at premier centers by trained personnel. As a result, most ovarian cancer patients missed out on their optimal treatment which could have added a year or two to their lives[40]. The paper published by Dr Bristow also proved that the 5-year survival for patients that received National Comprehensive Cancer Network (NCCN) guidelines adherent care was significantly better than patients who received non-NCCN guidelines adherent care (41.4% vs 37.8% for white patients and 33.3% vs 22.5% for black patients)[41]. A new treatment regimen that eliminates the need for a catheter, is inexpensive and is simple to administer would be favorable for both clinicians and patients.

1.6 Cisplatin and its characteristics

Cisplatin is sensitive to light, and degrades quickly in biological fluids at body temperature[42]. Cisplatin binds to serum proteins irreversibly with an initial half-life of 2.58 hours and a disappearance (regardless of degradation or protein binding) half-life of 1.27 hours in human plasma at 37°C[43,44]. The volume of distribution is defined to be the theoretical volume that the total amount of administered drug were to occupy to provide the same concentration as it currently is in the blood plasma. A higher volume of distribution indicates that the drug concentration in the blood is lower than it should be and that most of the drug is distributed out of the circulatory system and inside the tissues. It was reported that in mice that received 5 mg/kg of cisplatin solution IV, the volume of distribution of free cisplatin was found to be 6.2 - 16.4 mL/g at steady-state[45, 46].

26

1.7 Cisplatin assay method

The quantification of cisplatin could be performed using high-performance liquid chromatography (HPLC) and/or inductively-coupled plasma mass spectrometry (ICP-MS). Cisplatin does not fluoresce under UV illumination, therefore, pre-column or post-column derivatization is required for quantification with HPLC containing UV detectors.

Cisplatin, after derivatization with diethyldithiocarbamic acid (DDTC), can be quantified in a linear range between 0.05 µg/mL - 10 µg/mL in plasma ultrafiltrate[47]. A similar method described by Lopez-Flores et al. (2005) measures cisplatin concentration in plasma, cancer cell and tumor samples with a linear range of 0.5 µg/mL - 10 µg/mL[48]. ICP-MS is capable of measuring platinum, the core atom of each cisplatin molecule, at very low concentrations when combined with HPLC. Using HPLC-ICP-MS, Cairns et al. (1994) reported achieving a detection limit of 0.6 pg/mL[49,50]. Hann et al. (2003) were able to detect cisplatin, mono- and di-aqua cisplatin in aqueous samples and diluted urine of a cancer patient by HPLC-ICP-MS with limits of detection of 0.74 ng/mL, 0.69 ng/mL and 0.65 ng/mL respectively[51-53].

1.8 *In vivo* imaging technique

Since the discovery of luciferin and its ability to emit light in the 1960s, luciferase had become a widely popular reporter gene for cell culturing systems and oncological studies[54]. Many cancer cell lines were transfected or transduced with a firefly luciferase reporter gene or fluorescent reporter gene for cell *in vitro* or *in vivo* monitoring and tracking [55]. Both bioluminescence (BLI) and fluorescence (FLI) are viable ways providing quantitative analysis of cell numbers and location. However, BLI is more sensitive than FLI and the results does not get confounded by autofluorescence[56]. The luciferase reporter gene insert/transfect allows the tumor cells to produce luciferase enzymes. In the presence of luciferin, the luciferase metabolize luciferin and ATP

(magnesium is also required) to give off luminescence of emission wavelength in the range of 421 – 623 nm (Figure 1.7)[54].
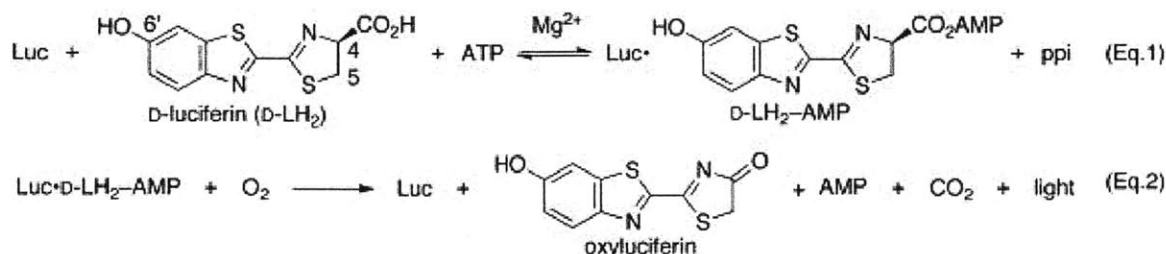
Figure 1.7 The chemical reaction for light emission from luciferin. This reaction requires both ATP and oxygen. Bioluminescence is therefore a measure the number of living cells only. *Source: Wikipedia*

Oxygenated hemoglobin and melanin in the skin attenuates light in the blue-green region, allowing the near infra-red region of light of luciferin to pass through skin for detection[54]. The luminescence detected allows for a non-invasive method to track tumor growth profile *in vivo* at each time point.

1.9   Principles of proposed device

A reservoir-based drug delivery device is fabricated for the delivery of drug directly into the peritoneal cavity. The device is loaded with solid drug and drug release is accomplished by diffusion through orifice(s) in the device. The diameter of each orifice is precisely controlled via micromachining to ensure desired release rate. Fick's First Law of Diffusion was used to estimate the rate of drug release from the device:

$$\dot{m} = -A * D \frac{C_S}{\Delta x}$$
(Equation 1)

where $\dot{m}$ is the mass diffusion rate(mass per unit time), A is the area of the release orifice(or orifices), D is the diffusion coefficient of the drug in the diffusion medium, C_S is the solubility of

the drug and Δx is the diffusion distance (assumed to be the depth of the orifice). These reservoir-based devices allow for simple control of the release rate by engineering the size and/or number of orifices.

The reservoir-based device presented in this thesis works by allowing peritoneal fluid to enter the device, dissolve the powdered drug, and releases the drug in solution. It is shown below that cisplatin stability is surprisingly preserved with the device during *in vivo* use. Presumably, the stability is superior over solutions of cisplatin because the drug is in the solid form within the device. This allows for maximum drug efficacy upon release, even months after implantation

1.10 Existing technology and clinical practice

The current treatment regimen requires surgeons to implant a catheter connected to a port (such as the BardPort®) during the cytoreduction surgery. Two 5mm incisions are made at the upper right and lower right quadrants of the abdomen following the debulking of large visible tumors. The port is inserted through the incision at the upper right quadrant and sutured subcutaneously. The tip of the catheter is tunneled subcutaneously to the incision in the lower right quadrant of the abdomen where it will enter the peritoneal cavity. A patient on intraperitoneal chemotherapy treatment regime receives an infusion of 2-litres of cisplatin solution through the port once every three weeks, into the peritoneal cavity. The implantation site is prone to infection and inflammation over the entire period of 18 weeks of treatment and the long catheter is susceptible to obstruction[35].

1.11 Other drug delivery platforms for the treatment of ovarian cancer

The reported depot approaches to delivery of cisplatin or other chemotherapeutic drugs for the treatment of ovarian cancer involve polymeric particles[3,57,58]. Drug laden particles are

administered to the desired site and release the drug over a period of time. These approaches essentially view the particles as a new formulation of the drug and aims to extend the biological half-life of the drug as it is being released continuously for an extended period. The first similarity that these polymeric particles share is that this approach requires a significant amount of polymeric material to be present in the formulation to reliably control the release of the cytotoxic agent. The mass of polymer often significantly exceeds the mass of drug in such formulations. The administration of these formulations is also irreversible. Thus, if the dosage is administered for the entire therapy, physicians cannot remove the drug if the therapy is not tolerated. The physicians must then take a repeated administration approach, which is similar to the current IP bolus administration regimen. This provides no solution to the current problem of catheter-related morbidities as intraperitoneal administrations of these formulations still has to take place through a catheter. A combination of the above two limitations could also result in the accrual of polymeric materials within the patient and could limit the frequency of administration. The device is, in contrast, implanted once and therefore poses no problem of a 'carry over' effect in terms of foreign material between administrations. A third constraint, as mentioned above, is that it is a formulation and not a device. The distinction is that the release from a formulation is strongly affected by the chemistries of the drug and polymeric material. The rate of release, therefore, is limited once the materials are selected and changing the release rate is not a trivial problem. A device, however, is less dependent on the relative chemistries of the drug and device components. The rate of release can be tuned by varying the architecture of the device, independently of the payload and method of loading. Bulk polymers, such as polylactic acid used by Araki *et al.* result in non-zero order releases while a constant, zero-order release rate is often preferred in drug delivery. The use of liposomes has also emerged as a popular drug-carrying

vehicle in the recent years[59-61]. For the same reasons as above, these formulations may not be the ideal solution for the treatment of ovarian cancer.

A group from University of California, San Diego recently developed a type of CD44-targeting hyaluronan-based microparticle that can encapsulate cisplatin[62]. CD44 is a surface ligand that is expressed on some types of ovarian cancer cells, and hyaluronan is a natural ligand for CD44. These particles can only increase cisplatin uptake for CD44-positive ovarian cancer cell lines. Although these particles managed to prolong cisplatin half-life in the peritoneal cavity (when administered IP) compared to IP bolus injection from 18 minutes to 124 minutes, it is still dropping quickly. The device described in the study below will release constantly for up to 18 weeks, allowing cisplatin to constantly act on the tumor cells over the entire period.

Paclitaxel is another commonly used drug in the current ovarian cancer treatment. It is dosed IV 135mg/kg post-surgery over 24 hours[39] or IP 60mg/kg on day 8[33]. It is a hydrophobic small molecule that has a logP of about 3.5 (DrugBank, DB01229). There are several recent patents that incorporate paclitaxel into degradable polymer microparticles for drug release locally. Vook et al. (Patent No.: US 6855331 B2) developed a way of releasing hydrophobic drugs using the polylactic glycolic acid (PLGA) particles. The PLGA particles could only sustain a relatively linear release profile up to about Day 11 before there was a sharp drop in the release rate. Those microparticles could only release for up to 25% of the paclitaxel loaded into the microparticles before the plateau. Dang (Patent No.: 6479067 B2) developed a method of using poly(phosphoester) particles to release paclitaxel and other small molecules such as lidocaine, cisplatin and doxorubicin. The release of cisplatin from these microparticles is not very controlled: 45% of the loaded cisplatin was released through Day 1 in one of the in vitro release experiments, and another 30% was released in the subsequent 3 days. In another in vitro release

31

experiment with cisplatin, only 5% of cisplatin was released over 3 days, and almost no cisplatin

was released over the rest of the 14 days of *in vitro* release. The release of paclitaxel was the

most consistent among all the drugs mentioned. The only *in vivo* efficacy study performed was

with OVCAR-3 ovarian tumor cell line which compared microparticles containing palictaxel at a

dose of 10 mg/kg and 40mg/kg to free paclitaxel of 10 mg/kg and 40mg/kg. The results showed

that at 10mg/kg dose, there is no significant difference between the microparticle formulation

and free paclitaxel (70 and 60 days respectively); at 40mg/kg, the median survival of

microparticle formulation is about 110 days while that of free paclitaxel is about 70 days. This

dose is quite high compared with conventional dosing in mice. The standard maximum dose of

paclitaxel in the mouse model is 20mg/kg[63,64]. 50mg/kg has, however, been used to investigate

the neurophysiological and neuropathological damage in mice[65]. The dose of 20mg/kg is,

therefore, a better comparison between the efficacy of the microparticles and free paclitaxel.

A new approach is envisioned in which a device is fully deployed in the peritoneal cavity. The

surgeon drops the device(s) into the peritoneal cavity through the laparoscopic ports near the end

of cytoreduction surgery, instead of the tunneling procedure, before closing the wound. Such an

approach will eliminate catheter-related complications and improve surgeon acceptance.

Removal of the device, if necessary, can be accomplished by minimally invasive surgery using

laparoscopy. This study reports on preclinical results for local delivery of cisplatin in an animal

model of ovarian cancer.

There is a constant, ongoing research effort on the various chemotherapeutic drug formulations

to improve the efficacy (high retaining power in the vicinity of the tumor, targeted therapy and

so on) of the drugs. The proposed implantable reservoir-based device in this thesis is such a robust and versatile system that it could incorporate many different types of drug formulations in it, and release them at a constant, reproducible and predictable rate, to achieve maximum benefit for cancer patients in the near future.

This page is intentionally left blank.

2 Materials and methods

2.1 Materials and chemicals

Materials for *in vitro* release were obtained from VWR International (USA). Cisplatin, A2780 cell line, nickel(II) chloride, sodium hydroxide, sodium diethyldithiocarbamate trihydrate (DDTC), dimethyl sulfoxide and HPLC-grade methanol were obtained from Sigma-Aldrich (St. Louis, MO, USA). OVCAR3 cell line was obtained from ATCC. The HPLC column (ODS Hypersil, 250x4.6mm, 5μm) was purchased from Thermo-Scientific (USA). SKOV3-Luc (luciferase-positive) cell line and luciferin were obtained from Caliper LifeSciences (Hopkinton, MA, USA). Isofluorane was purchased from McKesson (San Francisco, CA, USA). Cell growth media, MTT assay, fetal bovine serum (FBS) were purchased from Invitrogen (NY, USA). BALB/c and nu/nu mice were purchased from Charles River (MA, USA). HPLC used is the LC 1200 series from Agilent. Serum separation tubes were purchased from VWR International (USA). Bouine solution is from Electron Microscopy Sciences (PA, USA).

2.2 Device fabrication

The devices used in this thesis were fabricated by microPEP, RI, USA and consist of an injection molded reservoir and cap. The devices are injection molded into a cylinder of 3 mm in diameter and 3.5 mm in height (Figure 2.1). The cap is a thin disc, 3 mm in diameter and 400 μm in thickness. A 180 μm orifice was laser drilled through the cap. Any material that can be extruded can be used to fabricate these devices. The devices used in this theses are fabricated using poly-L-lactic acid (PLLA) from SurModics Inc, MN, USA and liquid crystal polymer (LCP) synthesized by microPEP. Both materials are thermoplastics that are biocompatible. PLLA is a very well-known and commonly used biomaterial that is biodegradable. In our application, we

would not need the device to degrade *in vivo* over time. Therefore, the PLLA that we chose were

slow degradation PLLA polymer that will not change its properties over the time frame of 3

months *in vivo*. LCP is biocompatible but not biodegradable.

Figure 2.1 A picture and schematic of the mouse device used in this thesis.

Some devices required multiple orifices; the additional orifices were drilled on the forth-axis on the microCNC machine (Cameron Micro-machining Center, CA, USA). A fixture made out of
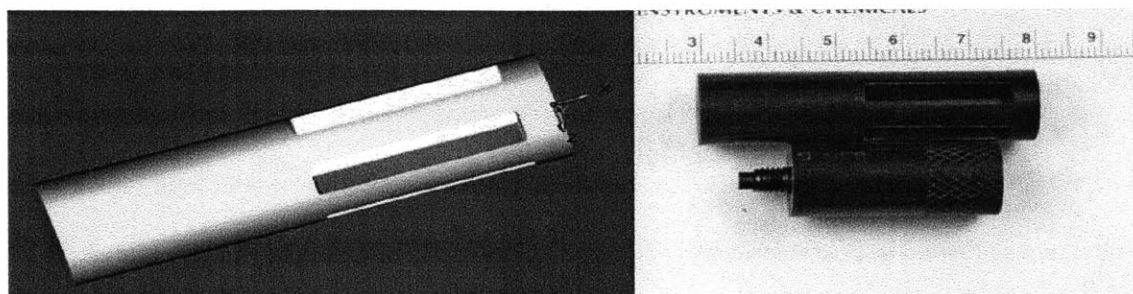
acetal copolymer was fabricated to hold six devices in place for drilling (Figure 2.2). The fixture consists of two parts: the holder and the screw head piece. Six devices are loaded into the holder. The screw head piece screws into the holder and presses the column of devices tightly together to prevent any movement during drilling. The forth axis collet clamps on the screw head piece while a tail stock fixes the fixture on the bare end of the holder (which acts as a center-drill) to make sure the fixture does not deviate from its axial position during the drilling process. The forth axis rotates the fixture, exposing its various slots to allow the drill bits to reach the devices stacked inside.

2.3 Device filling and preparation

5 - 10 mg of cisplatin powder was weighed out in weighing dishes and poured into each device with the aid of a fixture. A cap was then glued onto each device using a medical grade epoxy

Figure 2.2 Fixture used for drilling holes on the cylindrical wall of the device.

(Loctite M21-HP Hysol) and left overnight to cure. Devices that were implanted in animals were sterilized in ethylene oxide after drug loading and the activation steps were performed in a sterile hood with all materials sterilized prior to activation.

Each filled device was secured onto a strip of plastic with double-sided tape and submerged into a vial containing 1mL of PBS. The vial was vacuumed so that the air inside the device was replaced by PBS. This allowed the cisplatin drug to dissolve in the PBS and formed a saturated cisplatin solution inside the device for drug release.

2.4   *In vitro* release

Each device was loaded with cisplatin and activated as described above. The devices released drug into a vial of PBS solution at 37°C. The release solution was replaced at various time points to maintain a constant sink condition around the device. The volume of the release solution varied with the length of the time point (i.e. the longer the time point, the larger the volume of PBS). The release solution at each time point was then assayed with HPLC to measure the mass of drug that had been released. The cumulative mass of drug released was plotted versus time to obtain the *in vitro* release profile for the device.

2.5   High-performance liquid chromatography method

2.5.1   Reagent preparation

Working solutions of nickel (II) chloride in PBS and sodium diethyldithiocarbamate trihydrate (DDTC) in 0.1M sodium hydroxide were prepared at 0.1 mg/mL and 0.1 g/mL respectively. Nickel chloride was used as an internal standard while DDTC was used to conjugate cisplatin for UV detection on the HPLC machine

2.5.2   Sample preparation

The samples were diluted in PBS to a final volume of 450 μL, before adding 50 μL of nickel chloride and 100 μL of DDTC stock solutions. The sample was then incubated at 37°C for 30

minute before running on HPLC. The volume of DDTC could be reduced to 50 μL if the calibration range is less than 5 μg/mL. PBS is added to bring the final volume to 600 μL.

2.5.3 Cisplatin concentration calibration

The HPLC method was a slight modification from the method published by V Augey et al[47].

Stock cisplatin solution was prepared by dissolving a known amount of drug in PBS solution.

The stock solution is then serially diluted to concentrations between 0.1 μg/mL and 20 μg/mL.

100 μL of DDTC and 50 μL of internal standard were added to 450 μL of the various concentrations of cisplatin. The calibration samples were incubated for 30 min at 37°C and ran on HPLC with the below-mentioned parameters. A calibration was run on each day that the samples were run to reduce day to day fluctuations.

2.5.4 High-performance liquid chromatography parameters

A commercial HPLC system (Agilent 1200 LC) was used for cisplatin quantification. The HPLC works by separating a sample that is injected into the column at high pressure into its constituent components. The column separates the sample according to the properties such as hydrophobicity and size. The components leave the column after different retention times after being separated. An ultraviolet (UV) diode array detector will sense the various components at user-defined wavelengths as each component exits the column and plots a peak (an example shown in Figure 2.3).

The column was heated to 30°C and the sample holder was cooled to 4°C prior to the run. A mobile phase of 75% methanol (HPLC-grade) in water (HPLC-grade) was used with a flow rate of 1.4 mL/min. A 100 μL volume of cisplatin-containing sample was injected into the column. The Diode Array Detector (DAD) was set to detect both 250 nm and 254 nm. The area under the

curve (AUC) of the cisplatin peak that appears at 5.1 min on the 254 nm spectrum was normalized to the AUC of the internal standard peak at 6.0 min on the 250 nm spectrum. Figure 2.4 shows the user interface and the relevant settings on the ChemStation software for controlling the HPLC machine. A calibration curve was obtained by plotting the ratio of the cisplatin AUC to the internal standard AUC against a concentration range of 0.1 to 20 µg/mL. The flow rate could also be reduced to 0.7 mL/min for higher sensitivity. The cisplatin peak would then appear around 10 min for 254 nm and the internal standard peak at about 12 min for 250 nm.
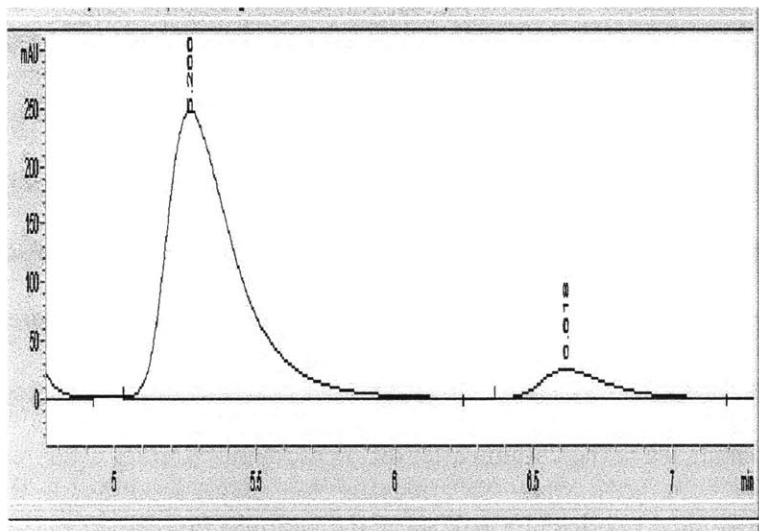
Figure 2.3 An example of the HPLC spectrum
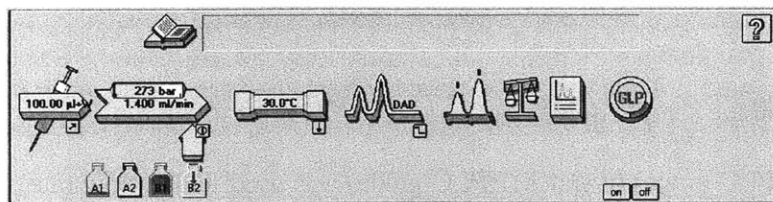
Figure 2.4 An example of the running conditions for the HPLC machine on ChemStation software.

2.6 Inductively-coupled mass spectrometry method

For samples with very low concentrations of cisplatin (less than 0.1 μg/mL), another cisplatin assay technique has to be used. The inductively-coupled plasma mass spectrometry (ICP/MS) uses strong plasma to ionize a molecule and break it up into its elements. It then uses the mass spectrometry to separate the elements for quantitative detection. The ICP/MS is reported to be able to measure the element platinum down to 0.74 ng/mL[66]. The ICP/MS protocol was provided by the Trace Metal Laboratory at Harvard School of Public Health. Up to 500 μL of liquid sample (serum or blood or peritoneal lavage) or 500 mg of solid sample (tumor or tissue) was mixed with 1 mL of concentrated nitric acid (BDH ARISTAR). The sample was incubated at room temperature for 48 hours, and 0.5mL of hydrogen peroxide was then added. The solution was allowed to sit for a few hours to allow any bubbling to die down. Distilled water was added to top up the solution to a final volume of 5 mL. The samples, along with a set of calibration samples, were then run on a Perkin Elmer Elan 6100 DRC-II ICP/MS machine in the Harvard School of Public Health, Trace Metal Laboratory. The concentration of elemental platinum was converted into cisplatin concentration.

2.7 *In vitro* cytotoxicity experiment

The cisplatin-susceptible cell line A2780 and cisplatin-resistant cell lines SKOV3 and OVCAR3 were used. RPMI 1640 with 20% fetal bovine serum (FBS) was used for culturing A2780 and OVCAR3, and McCoy's 5a with 10% FBS was used for SKOV3 propagation. The cells were seeded in 96-well plates at 10^4 cells/well. The cells were then incubated in cell culture media of cisplatin concentrations of 0.1 μg/mL to 10 μg/mL over different durations ranging from 2 hours to 7 days. The cisplatin-containing cell media was changed daily to prevent degradation of the drug in media over time. The control wells contain cells that were subjected to cell culture media

without cisplatin. Another set of control wells contain no cells. At the end of treatment period, the media for the respective wells was changed back to normal media and allowed to grow until day 8. Please refer to Figure 2.5 for a schematic of treatment periods. The MTT assay (3-(4,5-dimethylthiazol-2-yl)-2,5-diphenyltetrazolium bromide) was performed to obtain cell viability of all wells on Day 8. Background signal (wells that have no cells and only the MTT reagents) is subtracted from all wells containing cells. The percentage cell viability is calculated as a percentage of the untreated group at each time point.
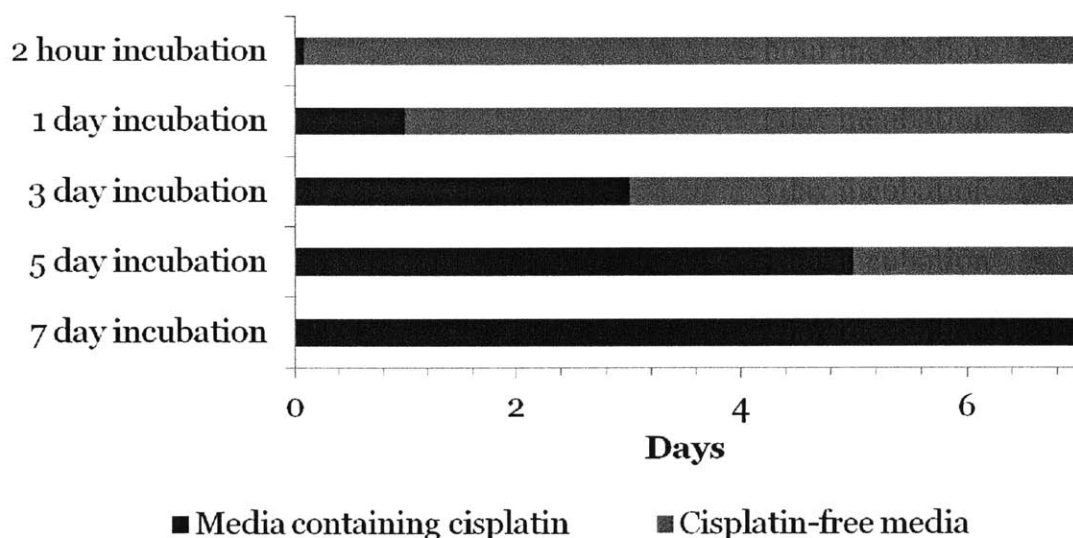
Figure 2.5 A schematic to explain the treatments received by cells of each group in the *in vitro* cell experiment.

2.8 *In vivo* pharmacokinetic study

Healthy, tumor-free mice were used to study the pharmocokinetics of the cisplatin *in vivo* as it was administered by an IP bolus injection or released from an implanted device. Devices of 1- or 3-orifice were implanted in their respective groups on day 0. The IP bolus group animals

received one dose of cisplatin intraperitoneally on day 0. The animals were sacrificed at various time points (n=3) after either device implantation or IP bolus injection, to harvest their peritoneal lavage and blood. Peritoneal lavage was obtained by injecting 1mL of sterile saline into the peritoneum and immediately withdrawing the solution. The blood samples were obtained via cardiac puncture and introduced into the serum separation tubes. Animals that were implanted with devices had their device(s) explanted after euthanasia. Each serum separation tube was allowed to clot for 30 min before centrifuging to separate serum from the blood. The lavage and serum samples were assayed for cisplatin concentration. All explanted devices were cracked open to release their contents into a 15 mL conical tube filled with 10mL of PBS. The tubes are vortexed and left in the 37°C incubator overnight to dissolve any drug remaining in the device. Samples from these tubes were collected and measured on the HPLC to obtain the amount of drug remaining inside each device. The amount of drug released is calculated by subtracting the amount of drug remaining from each device from the amount of drug loaded. All animal protocols were approved by the Division of Comparative Medicine at MIT.

2.8.1 Pharmacokinetic study over 7 days

One of the pharmacokinetics experiments aimed to investigate the changes in cisplatin drug concentration in the peritoneal cavity and the serum over a period of 7 days. The animals were divided into 2 groups: IP bolus injection (n=3) and device treatment group (n=3). The IP bolus injection group was injected IP with 10mg/kg of cisplatin solution. The animals were sacrificed at time points of 15 min, 30 min, 1 hour and 3 hours to obtain the peritoneal lavage and serum samples. The device group animals had five single-orifice devices implanted and were sacrificed at time points 1 hour, 3 hours, 1 day, 3 days, 5 days and 7 days.

2.8.2 Pharmacokinetic study over 42 days

The other pharmacokinetic experiment aimed to demonstrate the changes in cisplatin concentration in peritoneal cavity and serum compartments over period of 42 days (6 weeks). This corresponds to the duration of the treatment efficacy study. This pharmacokinetic experiment also elucidated the *in vivo* release rate for the device group over the duration of treatment and allowed comparison between *in vitro* and *in vivo* release rates. The animals were divided into 3 groups: IP bolus injection at 10 mg/kg (n=3), one-orifice device group (n=3) and three-orifice device group (n=3). The IP bolus injection group received a bolus IP injection of cisplatin solution at time = 0. The device groups each received an implant of cisplatin-containing PLLA device at time = 0. The animals in the IP bolus injection group were sacrificed at time points 15 min, 30 min, 1 hour, 3 hours, 8 hours, 1 day and 7 days. The 1-orifice device group animals were sacrificed at 2 days, 4 days, 7 days, 10 days, 14 days, 21 days, 35 days and 42 days. Peritoneal lavage and serum samples were collected at each time point. Devices were explanted at each time point.

All lavage and serum samples were sent to Harvard School of Public Health for ICP/MS analysis of cisplatin concentration. All explanted devices were cracked open to measure the amount of drug remaining.

2.9 *In vivo* experiments

2.9.1 *In vivo* Imaging System (IVIS) imaging method

The IVIS Spectrum Pre-Clinical *In vivo* Imaging System from PerkinElmer was used. The imaging technique is adapted from the method suggested by the manufacturer (Perkin Elmer)[67]. Luciferin stock solution of 15 mg/mL in sterile DPBS was prepared. The mice were anesthetized

44

with isofluorane before 10 μL/g was injected IP into each mouse. Imaging was performed 10 min after luciferin injection. The exposure time is 4.0 seconds with a small binning setting. The bioluminescence intensity (BLI) is measured on the Living Image® software. The BLI values were normalized to the BLI values on Day 14 (the start of treatment) and plotted against time to show relative changes in BLI over time.

2.9.2 *In vivo* bioluminescence calibration

Different numbers of cells were inoculated into the mice and luciferin was injected immediately. The animals were imaged 10 minutes after luciferin injection. The bioluminescence intensity (BLI) was plotted against the number of cells inoculated.

2.9.3 Complete Blood Count

All blood for complete blood count (CBC) was collected in Sarstedt tubes. The tubes were inverted four – five times after being filled with blood. The tubes were then delivered to the Massachusetts General Hospital (MGH) Center of Comparative Medicine for CBC analysis.

2.10 Tumor induction studies

IP cell inoculation method is adapted from the methods suggested by Connolly et al[55]. Cells were trypsinized, centrifuged and reconstituted to the desired concentration. Each nu/nu or SCID BEIGE mouse was inoculated with 10^6 to 10^7 SKOV3 luciferase-positive cells suspended in sterile PBS or complete media on Day 0. The luminescence intensity was measured twice a week and the tumors were allowed to grow for up to 35 days.

2.11 Treatment efficacy and toxicity studies

Cells were trypsinized, centrifuged and reconstituted to 10^6 per mL of sterile PBS or complete media. The mice were inoculated with 10^6 SKOV3 cells in 1 mL of solution on Day 0, and

treatment (either IP bolus injection at 5mg/kg, 10 mg/kg or intraperitoneal device implantation) was administered on Day 14. The devices were sterilized with ethylene oxide prior to implantation and activated in a sterile biological cabinet with sterile PBS. All animal care guidelines as listed in the animal protocol were followed. The animals were imaged two times a week, similar to the tumor induction study. The animals also received IP daily saline hydration. The animals in the toxicity study were sacrificed on Day 56 and their organs (kidney, liver, spleen) were removed immediately upon euthanasia to be fixed in 10% formalin overnight. Femurs were also excised from some animals, fixed and decalcified in Bouine solution for two weeks. The fixed samples were then sectioned and mounted on glass slides in the Histology Department of the Swanson Biotechnology Center in the Koch Institute, MIT. Hematoxylin and eosin staining is performed on the tissue slides to identify any signs of toxicity on the histological level. Pictures of the histology slides were taken in the Microscopy Facility of the Swanson Biotechnology Center in the Koch Institute, MIT. The Zeiss light microscope was used. Creatinine analysis is also performed (Creatinine Colorimetric Assay Kit, Cayman Chemical, USA) on the serum samples of selected animals to quantify the extent of kidney damage. The devices from the animals under device treatment were also retrieved during necropsy. The amount of drug remaining inside the device was measured with HPLC to calculate how much drug has been released (method same as in section 2.8).

This page is intentionally left blank.

3 Results

3.1 *In vitro* release experiments

3.1.1 Cisplatin Detection Assay

High-pressure liquid chromoatography (HPLC) was used to quantify cisplatin in the samples.

Cisplatin does not fluoresce under UV and must be bound to diethyldithiocarbamic acid in order

for the diode array detector to recognize its presence. This method was shown to be highly

reproducible and linear in the range of 0.1 µg/mL to 20 µg/mL with $R^2 = 0.9996$ (Figure 3.1).
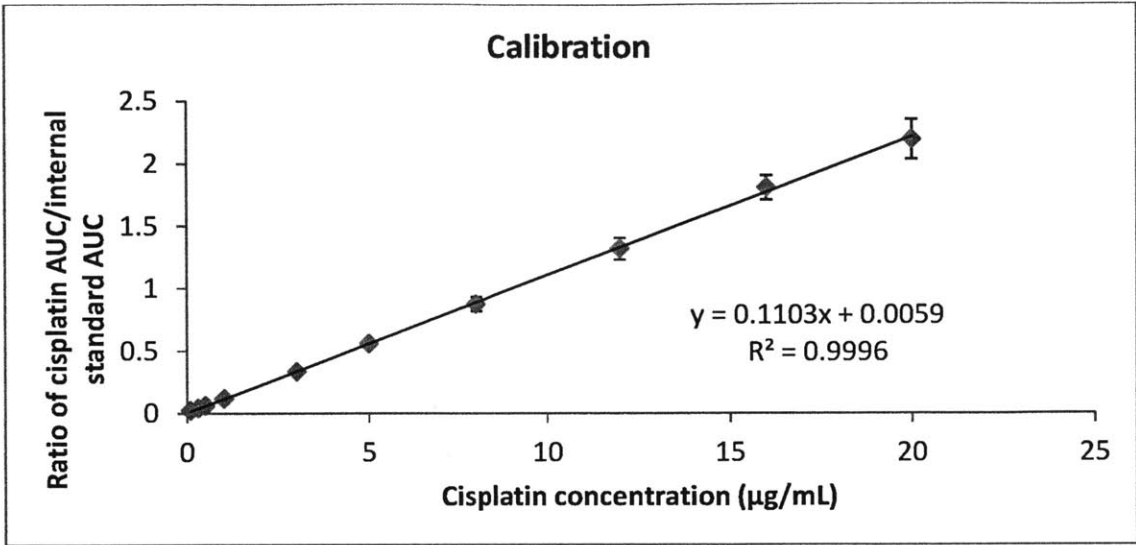
Figure 3.1 Cisplatin calibration curve obtained for a range of 0.1 µg/mL to 20 µg/mL. The calibration curve plots the ratio of the AUC of cisplatin peak detected at 254 nm and the AUC of the internal standard peak detected at 250 nm. The calibration curve is highly linear with an R^2 of 0.9996.

3.1.2 Device design
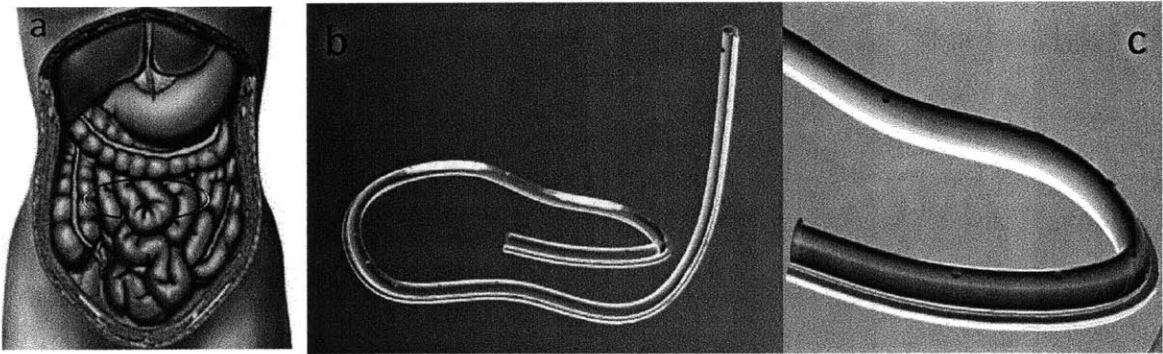
Figure 3.2 A schematic of the proposed human device. It comprises a thin, flexible tube that is able to hold itself in a particular conformation once implanted in the peritoneal cavity. a: The device is expected to hold its shape inside the peritoneal cavity. b: The flexible tube would have mechanical properties that are similar to soft organs to reduce trauma and damage to the soft organs in the peritoneal cavity. c: Orifices could be laser-drilled along the length of the tube to facilitate release of any therapeutic agent.

The proposed human device will be tubular with or without small orifices along the length of the device, depending on the permeability of the device material to cisplatin. Figure 3.2a depicts how the device would reside inside the body. The human device is envisioned to be made of an elastomer and could be biocompatible (such as silicone or polyurethane) or biodegradable (such as poly(glycerol sebacate[68]). The biodegradable materials have the advantage of requiring only a single surgery of implantation, without the need to retrieve the device after releasing its payload. Preliminary data has shown that PGS could be fabricated in a curved conformation (Figure 3.3), be straightened during implantation through a laparoscopic port, and curl back into its pre-determined conformation upon implantation. The device could either be sutured to the posterior surface of the anterior abdominal wall or be left free-floating in the peritoneal cavity.
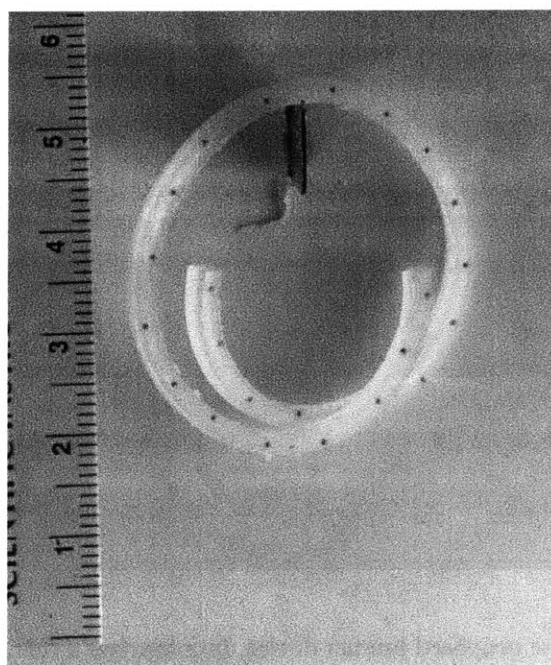
Figure 3.3 A tubular device made into a curved conformation with poly(glycerol sebacate) (PGS). It was hung from a point and was able to maintain its curved conformation. Steel balls were added to allow for radio-opacity during x-ray after implantation.

3.1.3 *In vitro* cisplatin release

The aim of this experiment was to investigate the release of cisplatin from devices of various numbers of orifices. The devices released cisplatin into in PBS at 37°C.
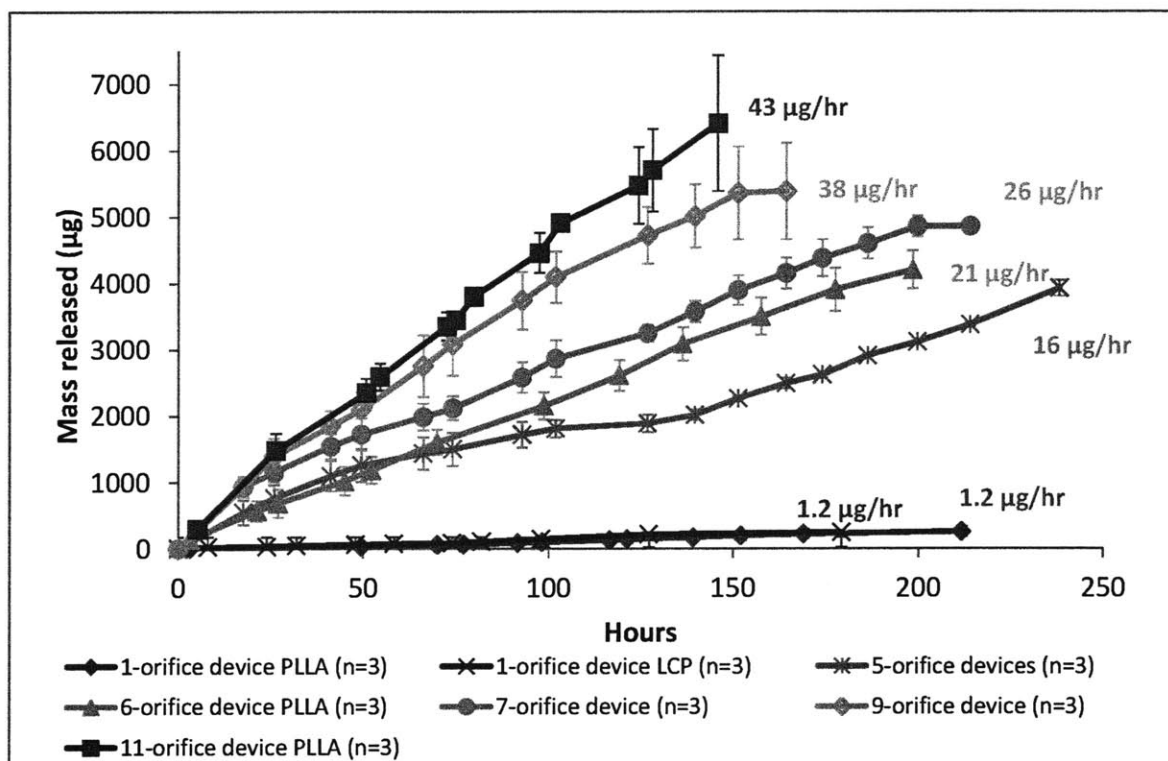
Figure 3.4 *In vitro* release profiles for devices of various orifices at 37°C in PBS. The 1-orifice PLLA and LCP devices had the same release rate of 1.2 µg/hour, the 5-orifice device released at 16 µg/hour, the 7-orifice device released at 21 µg/hour, 7-orifice released at 26 µg/hour, 9-orifice released at 38 µg/hour and the 11-orifice released at 43 µg/hour. These release rates were obtained by best-fitting the linear relationship through the origin.

The resulting release profiles (Figure 3.4) show that the devices released cisplatin at a constant, reproducible rate that scales with the number of orifices. . The single-orifice device released cisplatin at a rate of 1.3 µg/hour, 6-orifice device released at 21 µg/hour and the 11-hole device released at 43 µg/hour *in vitro*. In a separate *in vitro* release experiment, the 5-orifice device released at a rate of 16 µg/hour, 7-orifice device released at 26 µg/hour and 9-orifice released at 38 µg/hour. Figure 3.5 shows that the release rate varied linearly with the number of orifices. A

51

linear equation fitted to the data could be used to calculate expected *in vitro* release rate for any number of orifice.

Expected release rate *in vitro* = 4.3672 * (number of orifice) – 4.1703　　　　　(Equation 2)
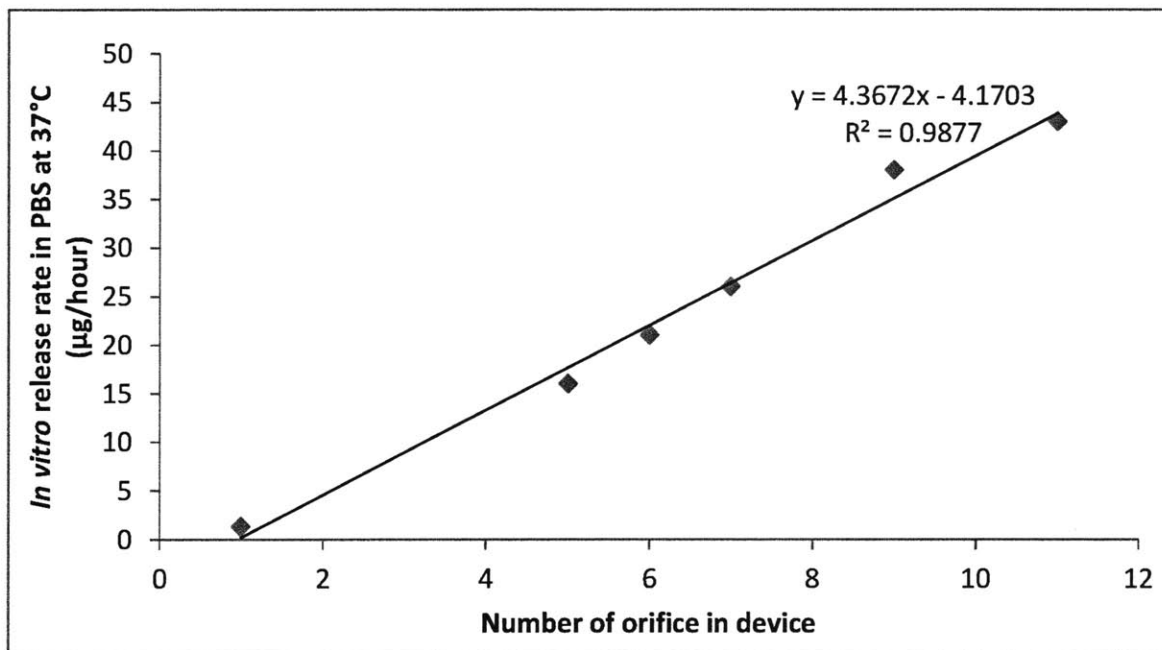
Figure 3.5 A plot of the measured *in vitro* releases rate in PBS at 37°C against the number of orifice in device. The *in vitro* release rate is linearly proportional to the number of orifices on the device ($R^2 = 0.9877$).

3.2　*In vivo* pharmacokinetics study

3.2.1　Pharmacokinetics over 7 days

A pharmacokinetics study was performed to examine the drug concentration in the serum and peritoneal cavity in mice after either a 10mg/kg cisplatin IP bolus injection or an IP implantation of five single-orifice devices. This experiment elucidated the local (peritoneal cavity) drug

concentration and serum drug concentration in the physiological environment. The results

(Figure 3.6) reveal that for IP bolus injection the serum cisplatin concentration spiked at about 7

µg/mL and quickly decreased to below detection limit (0.1 µg/mL) in about 3 hours. The

implanted devices, however, were able to constantly maintain a very low serum and peritoneal

concentration of about 0.1 µg/mL over 7 days.
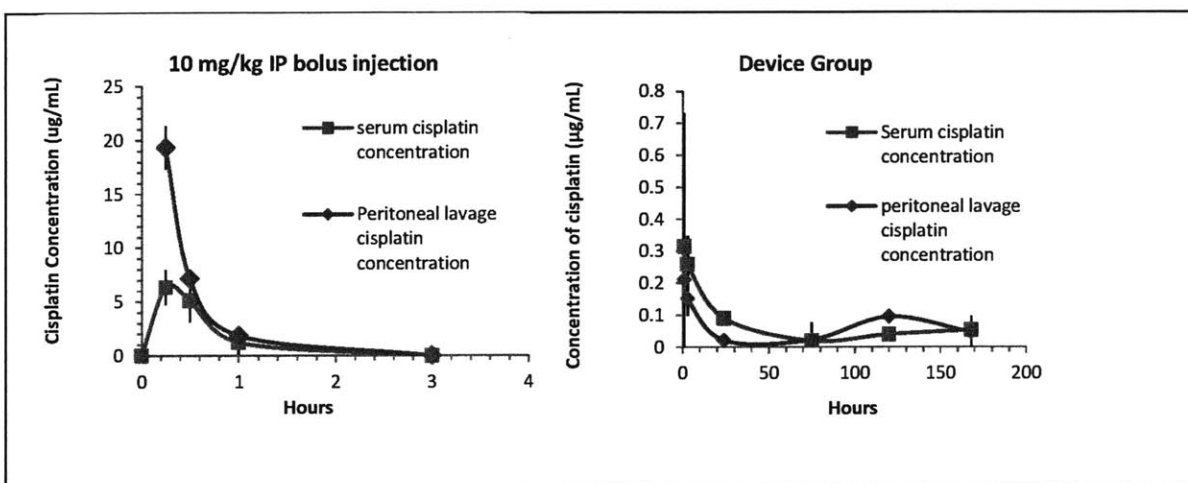
Figure 3.6 Pharmacokinetic study of 5 1-orifice device over 7 days and 10 mg/kg IP bolus injection over 3 hours. The IP bolus injection resulted in a large spike in cisplatin concentration in the serum which quickly attenuated over 3 hours. The high concentration of cisplatin injected IP also quickly diminished in 3 hours. The cisplatin concentrations in both the serum and peritoneal cavity were maintained at a low and relatively constant level over 7 days in the 5 1-orifice device group.

3.2.2 Pharmacokinetics over 42 days

A second pharmacokinetic study was performed over a longer period of 42 days with both 1-

orifice and 3-orifice devices. This experiment was designed to elucidate the *in vivo* release rate

of the devices for a duration that is more relevant to the treatment period of 42 days in mice. It

also investigated the changes in local and serum drug concentration over the 42 days to help

approximate an appropriate release rate for the efficacy study. The results in Figure 3.7 show that

the 3-orifice device released at a rate that is very similar to the expected *in vitro* release rate of a

53

3-orifice device initially. However, the release rate of the device dropped drastically after about 7 days. The 1-orifice device, on the other hand, was able to release cisplatin throughout the period of 42 days with a linear profile. The release rate of 1.0 μg/hour (24.6 μg/day as shown in Figure 3.7) was very similar to its *in vitro* release rate of 1.2 μg/hour. This strong *in vitro-in vivo* correlation allows for a reliable prediction of *in vivo* release rate based on its *in vitro* release rate. The 1-orifice device was chosen because its expected release rate was very similar to the dose of the weekly 5 mg/kg IP bolus injection in mice (as shown in Figure 3.7).

Cisplatin Released Pharmacokinetics

$y = 214.35x$

$y = 28.8x$

$y = 24.626x$

- ■ 1-orifice, in vivo (n=3)
- ◆ 3-orifice, in vivo (n=3)
- — • 3-orifice, in vitro
- ● IP bolus dose (weekly 5mg/kg)
- — — 1-hole, in vitro
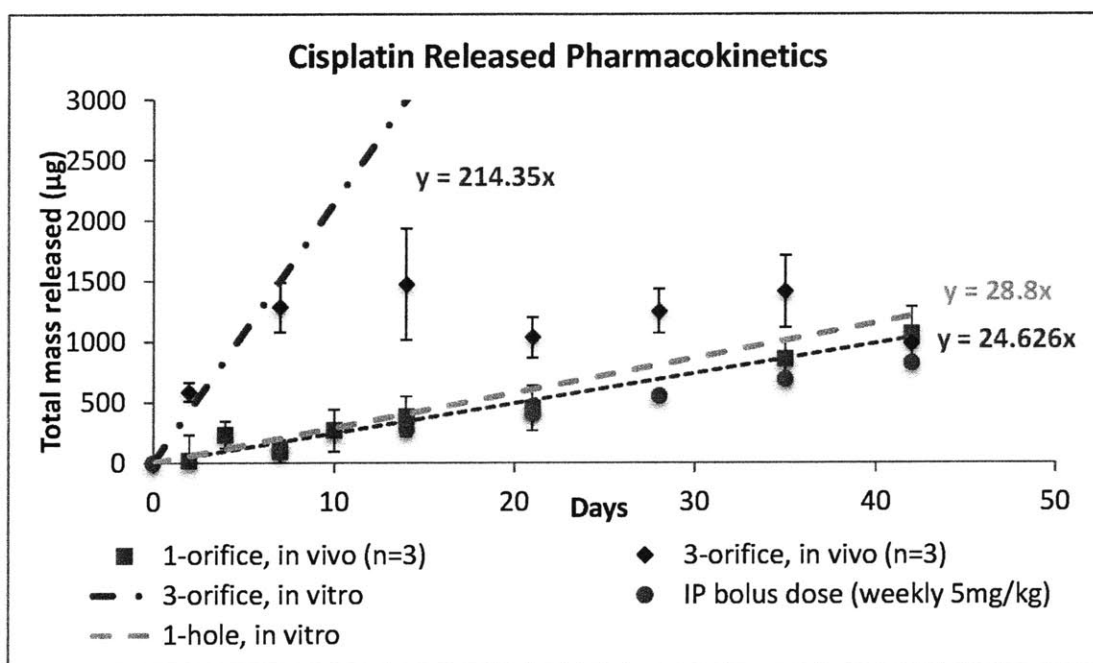
Figure 3.7 The pharmacokinetic study for the amount of cisplatin released by the devices over 42 days. The 3-orifice device released at a rate that was very similar to the expected *in vitro* release rate initially, but the release rate dropped drastically after about 7 days. The 1-orifice device was able to release cisplatin constantly throughout the period of 42 days with a linear profile. The released rate of 1.0 μg/hour (24.6 μg/day) was very similar to its *in vitro* release rate of 1.2 μg/hour. The weekly 5 mg/kg IP bolus injection in mice was also plotted (green).

Recall that sterile PBS was drawn into the device during the device activation step. The powdered drug present inside the device dissolved in this small volume of PBS to form a

saturated solution inside the device. One possible explanation for the premature termination of release from the 3-orifice device is that upon implantation of the activated 3-orifice device, as cisplatin diffuses out of the device, peritoneal proteins, proteoglycans and other molecules or cells also diffuse into the device. The presence of such molecules may reduce the solubility of cisplatin inside the device over time, and thus lowering the cisplatin release rate from the device. The faster the expected release rate (due to greater number of orifices), the faster the peritoneal proteins diffuse into the device and the faster the drop in cisplatin solubility occurs. The diffusivity of cisplatin in the peritoneal fluid may also be decreased due to the presence of peritoneal protein and proteoglycan molecules. The release was therefore hindered as the concentration of peritoneal proteins build up inside the device. A reduced cisplatin solubility inside the device and/or a decrease of cisplatin diffusivity leads to an attenuated release rate according to Fick's First Law.

$$\dot{m} = -A * D \frac{c_s}{\Delta x} \qquad \text{(Equation 1)}$$

These factors resulted in a sharp decline in release rate *in vivo* for the 3-orifice device in just 7 days when enough of the peritoneal proteins have entered the device to cause this decrease in release rate. This diffusion of peritoneal proteins occurred much more slowly in the 1-orifice device. Assuming the rate of diffusion of the peritoneal proteins is proportional to the cisplatin release rate, the 1-orifice device would be able to release continuously for up to 52 days. The calculations are shown below:

3-orifice device release rate *in vitro* is estimated to be 8.9 µg/hour based on Equation 2.

Assuming the release rate *in vitro* and *in vivo* is very similar as proven above, the release rate of the 3-orifice device should also be about 8.9 µg/hour.

Assuming the rate of diffusion of the peritoneal proteins is proportional to the cisplatin release rate,

(8.9 μg/hour) * (7 days) = (1.2 μg/hour) * (number of days)

Number of days that the 1-orifice device would be able to release continuously for = **52 days**

A larger reservoir in the device would allow for a longer period of release as it will take a longer time for the protein concentration inside the device to reach the critical concentration that affects release rate. For instance, a 3-orifice device would require the device that is able to provide a 8.9 μg/hour/1.2 μg/hour = 7.4 times larger volume of saturated cisplatin solution in PBS for it to release continuously for about 52 days. Hereinafter, the volume of saturated PBS solution has to be scaled up along with the desired release rate in order to sustain the release for a set duration. The *in vivo* release rates will therefore be tuned in our animal efficacy studies by implanting multiple 1-orifice devices instead of a single multiple-orifice device. Further investigations are necessary to elucidate the mechanism for release rate reduction.

The cisplatin concentration in the peritoneal cavity and serum collected in this experiment were also measured. The cisplatin concentrations in these samples were lower than the detection limit of the HPLC and therefore had to be sent to the Harvard School of Public Health for ICP/MS analysis. Both the serum and lavage samples were filtered using a 10 kDalton filter prior to the cisplatin assay to ensure that only free cisplatin, unbound was measured by ICP/MS. Free, unbound cisplatin was of interest because it was shown to be inverse proportional with cell viability and was therefore the relevant form for causing cytotoxicity[69]. Figure 3.8 shows that the 10 mg/kg IP bolus injection resulted in a sharp peak in serum and peritoneal cisplatin the same way as the previous experiment had shown. The 1-orifice device demonstrated that it was able to

release continuously for the entire duration of 42 days. The peritoneal and serum cisplatin was maintained at a constant value of above 20 ng/mL throughout the treatment period. This finding was also consistent with the results from the previous pharmacokinetic experiment where 5 1-orifice devices resulted in about 100 ng/mL of cisplatin in the serum and peritoneal lavage. This further proved that the 1-orifice device was able to release continuously for at least 42 days, and was able to maintain a constant cisplatin concentration in both the serum and peritoneal cavity.
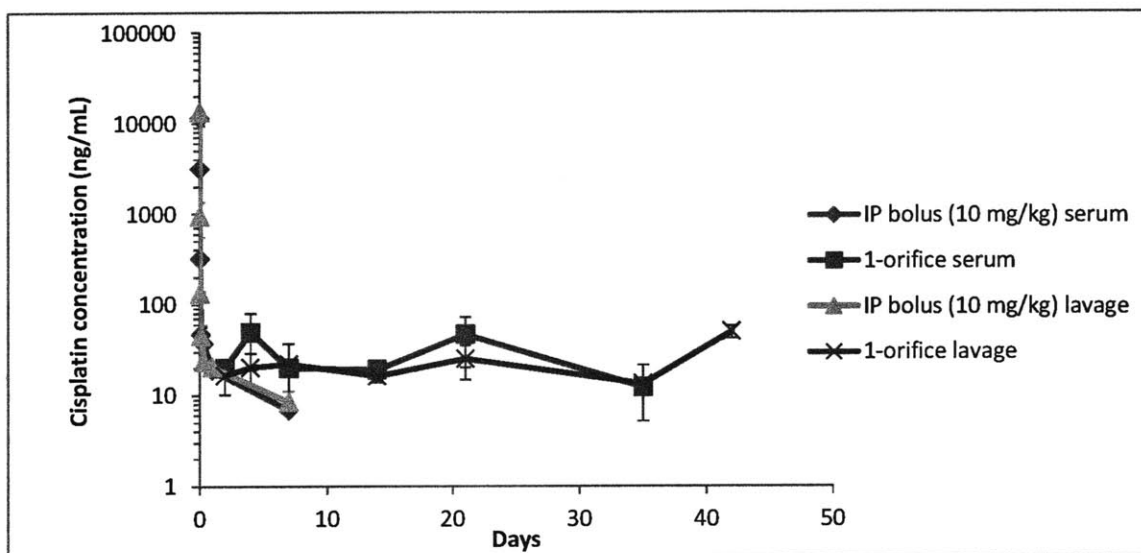
Figure 3.8 Pharmacokinetic study conducted over 42 days to measure the cisplatin concentration in the serum and peritoneal lavage samples (n=3). The IP bolus injection group showed a peak in cisplatin concentration in both serum and peritoneal lavage at 15 min. The 1-orifice device proved that it was able to release cisplatin continuously over the entire 42 days, maintaining the cisplatin concentration in the serum and peritoneal cavity at a relatively constant value of 20 ng/mL.

3.3 *In vitro* cytotoxicity experiment

The objective of this experiment was to prove *in vitro* that low cisplatin concentration maintained over a long period of time is at least as cytotoxic as a short burst of high cisplatin concentration. It also provides an estimate for the minimum concentration of cisplatin that the device needs to maintain in the local environment to kill both the cisplatin-sensitive and the cisplatin-resistant ovarian cancer cell lines.

This *in vitro* cytotoxicity experiment involved culturing three types of epithelial ovarian cancer cells in various concentrations of cisplatin over various periods of time (Figure 3.9). SKOV3 and OVCAR3 are cisplatin resistant and A2780 is cisplatin-susceptible ovarian cancer cell line. 10 μg/mL is used as a positive control because it was shown that 10 μg/mL for 2 hours is the critical condition to kill ovarian tumor cells[70]. The results shows that for all three ovarian cancer cell types, a minimum concentration of 0.1 μg/mL to 0.5 μg/mL over 7 days is to be maintained to achieve significant cytotoxicity against all three types of ovarian cancer cells tested. That is an area-under-curve (AUC) of 0.7 μg-day/mL to 3.5 μg-day/mL-day to achieve cytotoxicity. The 1-orifice device is capable of maintaining 20 ng/mL of cisplatin in the mouse peritoneal cavity over 42 days (Figure 3.8) that is an AUC of 0.87 μg-day/mL. This AUC falls on the lower end of the range of the desired AUC. An increase in the device release rates over the 42 day treatment period may result in a higher efficacy.

SKOV3 (n = 16)

OVCAR3 (n = 16)

A2780 (n=16)
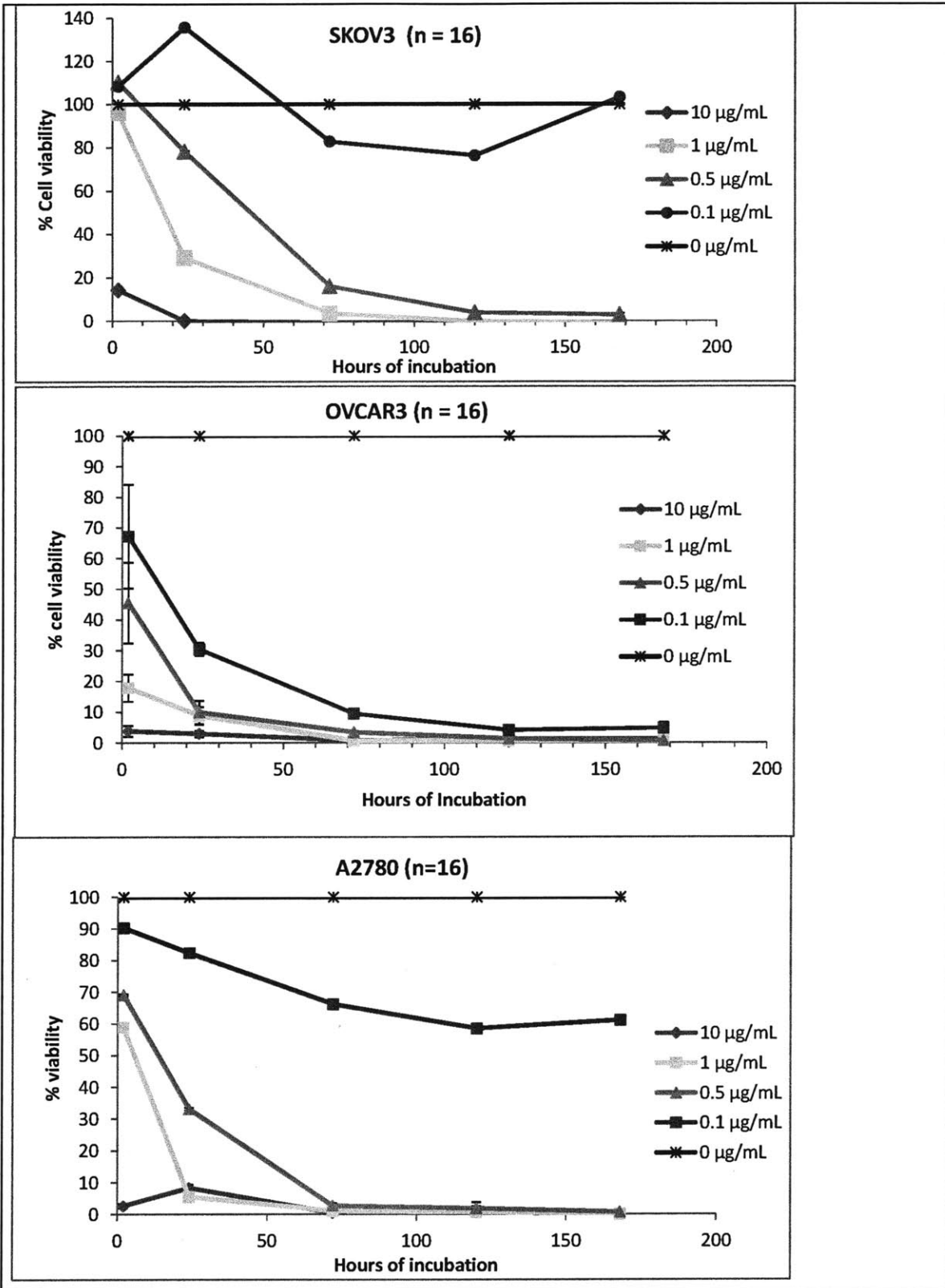
Figure 3.9 *In vitro* cell viability study to examine the viability of three ovarian cancer cell lines after being treated with various cisplatin concentrations up to 7 days. The three plots demonstrated the percentage viability compared to the untreated control wells after various duration of cisplatin treatment. For SKOV3 and A2780 cell lines, a minimum concentration of 0.5 µg/mL maintained over 7 days is sufficient to eliminate all the tumor cells. For OVCAR3 cell line, a minimum of about 0.1 µg/mL is required to kill all the cancer cells in 7 days.

3.4 *In vivo* bioluminescence calibration

This study aims to verify a linear relationship between the number of cancer cells and the

bioluminescence intensity (BLI). Figure 3.10 shows that there is a linear relationship between the

intensity of bioluminescence and the number of cancer cells present *in vivo*.
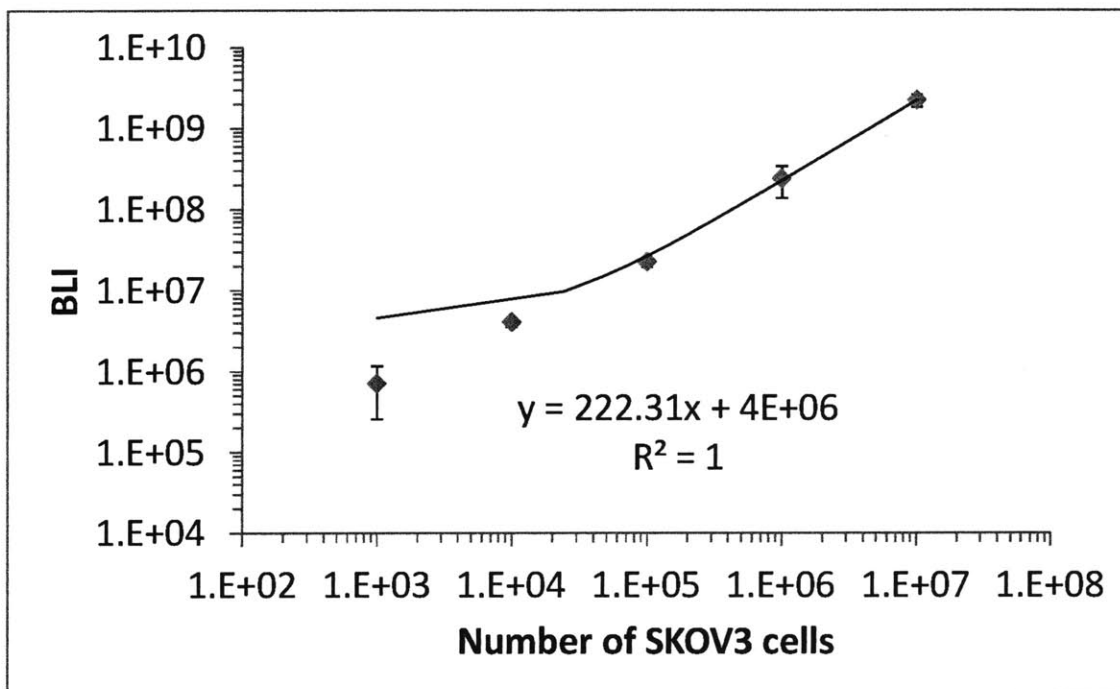
Figure 3.10 Bioluminescence calibration *in vivo*. Cells of 10^3 to 10^7 cells per animal were injected IP and the BLI was measured immediately after. The plot of BLI against the number of cells injected was plotted on a log-log scale. There was a very good linear correlation between the BLI and the number of cells injected, with a linear fit of $R^2 = 1$.

It is to be noted, however, that Figure 3.10 measures BLI from a solution of single cells or small

cell clusters dispersed in complete media solution. This strong correlation between tumor cell

60

number and BLI may change when BLI is measured for tumors instead of a solution of single cells. Tumors develop angiogenesis and the formation of extracellular matrix *in vivo* which is absent in a solution of single cells. Tumors may also develop necrotic cores over time and these dead cells will no longer contribute to the BLI signal, resulting in a less linear correlation between tumor mass and BLI as the tumor sizes increase. Stress response from the animals under chemotherapeutic treatment may also alter the luciferase expression that may lead to deviation from this linear trend.

3.5   Tumor induction study and tumor model optimization

SKOV3 was used as the tumor model for testing our device release regimen. The SKOV3 cells purchased from Caliper Life Sciences had a luciferase gene insert via a CMV promoter. Caliper Life Sciences reported that the transfection of luciferase is stable for up to 13 generations. The SKOV3 cisplatin-resistant cell line was chosen as one of the animal models. This cell line was obtained from the ascites fluid of a human epithelial ovarian cancer patient, and therefore is a good representation of metastatic tumors of the ovaries in the peritoneal cavity. Only cells of less than 10 generations were used for all the animals to ensure that the luciferase gene insert had not been lost with the generations and the BLI measured will be more representative of the tumor cell numbers. Various numbers of cells (5×10^5 to 10^7 cells per mouse) were inoculated in two different strains of mice (nu/nu and SCID BEIGE mice) and the tumor growth profiles were tracked over time.

3.5.1 5 and 10 million cells per mouse in nu/nu mice

This tumor induction study was performed with human ovarian cancer cells as the xenograft and nu/nu mice as the host to validate the animal model and to elucidate the tumor growth profile. Nude mice lack thymus and hence are unable to produce T-cells. They are therefore considered to be immunodeficient and will be able to tolerate the introduction of a human cell line. This study aimed to establish the tumor animal model for the subsequent drug treatment efficacy and toxicity study. Figure 3.11a shows that there was an initial drop in the bioluminescence value with 5 million and 10 million cells per mouse inoculated. This is presumably the result of only some of the cells surviving after being attacked by the host animal's immune system abet a deficient one. The tumor cells that survived seeded at various locations in the peritoneal cavity, achieved cellular adhesion, angiogenesis and stabilized by about 7 days. The tumors began to grow exponentially from about Day 20 onwards according to the figure.

Patients who receive chemotherapeutic treatment in clinical situation are administered the drugs after an optimally debulking surgery where the only tumors that remain are small, diffused tumors less than 1cm in diameter. It was realized that this model brought about few but large tumors towards the later part of the experiment (Figure 3.11b). This does not mimic the clinical scenario well. A smaller cell inoculation number may lead to a more ideal xenograft tumor model.

Another problems encountered with this nu/nu mouse model was that only about 60% of the animals developed tumors despite having a relatively large injection number of 10^7 SKOV3 cells per mouse. We postulated that this was probably a result of the remnant immune system of the nude mice attacking the foreign human cancer cells in the peritoneal cavity, eliminating them. Another strain of mice that is more immune-compromised than the nu/nu would be preferred.

3.5.2 0.5 and 1 million cells per mouse in SCID BEIGE mice

A

Luminescence Intensity vs. Days

- —♦— 10^7 cells injected in nu/nu (n=4)
- —■— 5x10^6 cells injected in nu/nu (n=5)
- —*— 10^6 cells injected nu/nu (n=2)
- —▲— 10^6 cells injected in SCID BEIGE (n=5)
- —✕— 5x10^5 cells injected in SCID BEIGE (n=5)
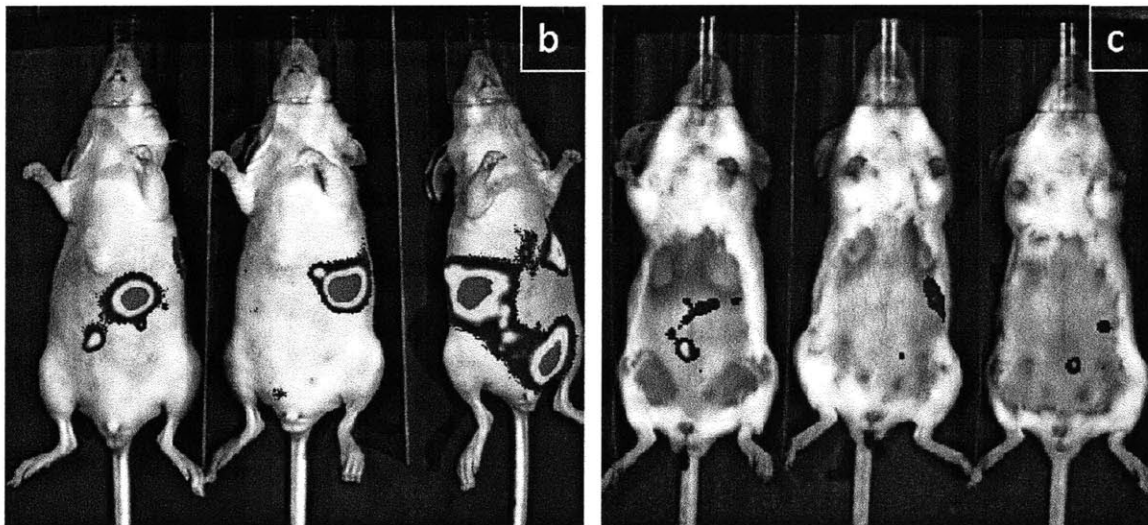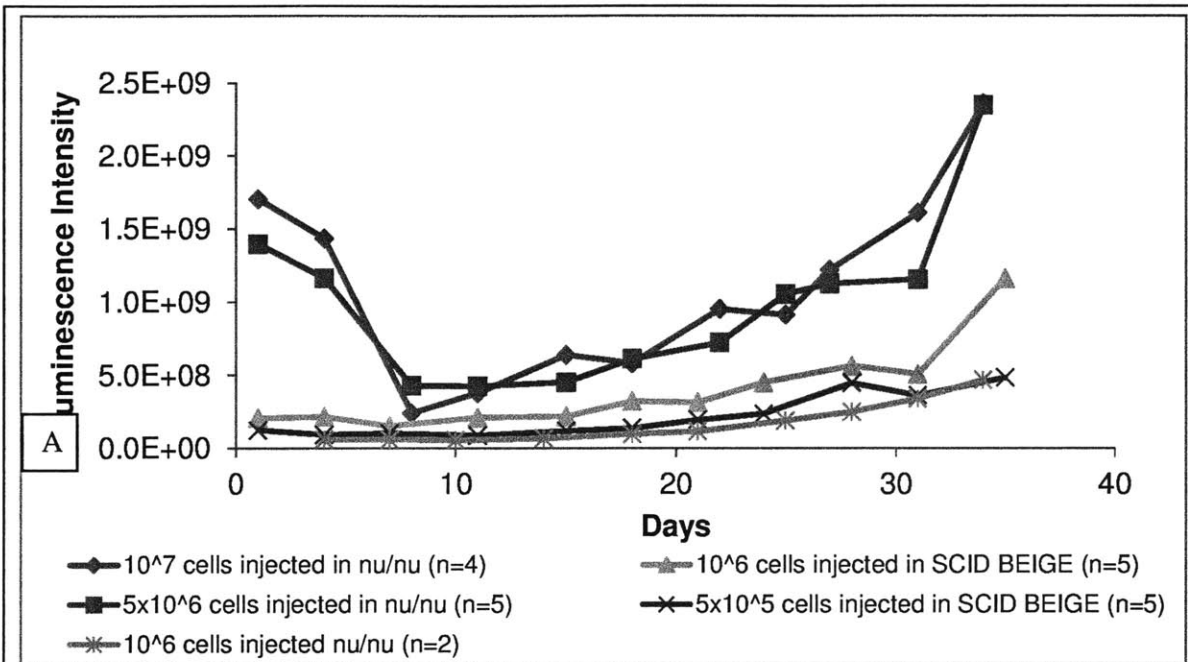
Figure 3.11 a: Bioluminescence intensity (BLI) of the tumor induction experiment for various mouse strains and various inoculation cell numbers. b: The bioluminescence image of nu/nu mice that received 10^7 cells/mouse on day 35. c: The bioluminescence image SCID BEIGE mice that received 10^6 cells/mouse on day 35. The latter resulted in smaller and more dispersed tumors.

The number of SKOV3 cells injected per mouse was reduced and the strain of mice was changed from nu/nu to the SCID BEIGE mice in an attempt to improve the animal model. The Fox Chase SCID BEIGE mice possess both the SCID ($Prkdc^{scid}$) mutation as well as the BEIGE ($Lyst^{bg}$) mutation. The SCID mutation results in severe combined immunodeficiency affecting both the T and B lymphocytes, while the BEIGE mutation results in defective natural killer cells. The combination of these mutations make this strain of mice an excellent host for a xenograft and have great potentials in improving the tumor uptake rate.

We inoculated 10^6 or 0.5×10^6 cells per mouse and monitored the tumor growth over time. Figure 3.11a shows that with a reduced number of cells inoculated in SCID BEIGE mice, tumors developed and took-off with a similar pattern as that of higher cell number inoculation. The initial decrease in bioluminescence signal in the first week was absent, justifying that 10^7 cells/mouse might had been excessive. The tumors stabilize by about Day 14 and 'took off' exponentially after Day 20. Figure 3.11b and 3.11c compare how the tumors looked like at Day 35 for both 10^7 and 10^6 cells/mouse. There was clearly a reduction of tumor size and the tumors were better dispersed in the peritoneal cavity at 10^6 cells/mouse.

The tumor uptake rate in SCID BEIGE was, however, not improved. There were still only about 60% of the mice that developed tumors. A later experiment described in section 3.6.2 involving treatment of these SCID BEIGE mice revealed that due to their severely defective immune system, they were significantly less tolerant to cisplatin treatment and the study had to be terminated prematurely. It was decided that these severely immune-compromised mice may not be good representations of the clinical situation as patients receiving chemotherapy are usually

not so severely immune-deficient prior to the therapy. Given the lack of improvement in the tumor uptake rate and the severe intolerance to treatment, the SCID BEIGE mice were not chosen as the host for the xenograft model.

3.5.3 1 million cells per mouse in nu/nu mice

A lower cell inoculation number of 10^6 per mouse was used on nu/nu mice (instead of 5 and 10 million). This was to investigate the growth profile and uptake percentage of nu/nu mice and compare them to that of the SCID BEIGE mice. The tumor progression in nu/nu did not differ from that in SCID BEIGE (Figure 3.11a). The tumor uptake rate was also 60%. It was therefore decided that the nu/nu mice with 10^6 cancer cells per mouse will be the final model for the treatment efficacy and toxicity studies that followed.

3.5.4 Tumor growth and adipose tissue association

One observation from these *in vivo* experiments was that most of the tumors were attached to adipose tissues in the peritoneal cavity, for example, adjacent to the spleen and the mesenteric fats. This observation is coherent with the paper published by the University of Chicago in 2011[71]. In this paper, it was reported that ovarian cancer cells in human patients preferentially home to and proliferate in the omentum fat tissues. Co-cultures of adipocytes and SKOVip1ovarian cancer cells showed a physical transfer of fluorescently-tagged lipids to the ovarian cancer cells. Co-cultures also induced lipolysis in the adipocytes and β-oxidation in the ovarian cancer cells, suggesting that lipolysis is a source of energy for the proliferation of the ovarian cancer cells. The group also observed an up-regulation of fatty-acid binding protein 4 (FABP 4) in metastatic ovarian cancer cells in the omentum compared to primary ovarian cancer cells. All the evidence indicates that the presence of adipose tissue improves the proliferation of ovarian cancer cells.

Bioluminescence is not a precise measurement of the tumor load in animals. However, it is not feasible to sacrifice a significant number of animals at every time point to track tumor growth. Moreover, even if the tumor masses were measured at each time point, the small tumors embedded in the peritoneal fats could easily be missed. This would result in false negatives and inaccurate tumor mass measurements especially at the earlier time points when the tumors were too small to be seen by eye. Therefore, bioluminescence tracking is a reasonably accurate method for determining the time to start administering treatment and the end point of the treatment. The treatment efficacy was ultimately confirmed by tumor mass measurement at the end of the treatment period of 42 days.

3.6 Treatment efficacy and toxicity studies

The main purpose of the treatment efficacy and toxicity study was to verify if the device treatment was able to control tumor size as well as, or even superior to the IP bolus treatment regimen. The toxicity that resulted from the treatment had to also be less severe than that of the IP bolus treatment regimen. Multiple treatment efficacy and toxicity studies were performed with different strains of mice, different cancer cell inoculation numbers, IP bolus injection of different doses and devices of various numbers of orifices. The optimal dose with the lowest toxicity without compromising on the treatment efficacy will be elucidated.

3.6.1 Nu/nu mice with 10^7 cells per mouse

The nu/nu mice were inoculated with 10^7 tumor cells on Day 0 and treatment was started on Day 14. The animals were divided into 5 groups:

1. 6-orifice device group,

2. 11-orifice device group,

3. IP bolus injection of 10 mg/kg at once per week (1X/wk) group,

4. IP bolus injection of 10 mg/kg at once per 3 weeks (1X/3 wks) group and

5. Control (untreated) group.

The results (Figure 3.12a) demonstrated that the 6-orifice device was unable to control tumor growth as the BLI rose along with the untreated controls over time. The 11-orifice devices were able to restrain tumor growth better than the control group as well as the IP bolus injection (once per 3 weeks) group. The IP bolus injection (once per week) group was able to suppress tumor growth the best. However, kidney histology obtained from these animals indicated that the weekly IP bolus injection caused more toxicity than the 11-orifice device group (as illustrated in Figure 3.13). We focused mainly on the extent of kidney damage as nephrotoxicity is a well-documented toxicity caused by cisplatin[72-76]. Hematoxylin and eosin stain for 10x magnification in Figure 3.13 shows that there was significant kidney tubular regeneration in the kidneys from the IP bolus injection (once per week) group as circled out in black. This implied the presence of past tubular damage as a result of the treatment, and the kidney's attempt to compensate by remodeling and reconstructing. Higher magnification of 25x also revealed protein casts in the proximal and distal tubules, indicating that there was permanent damage to the tubules. This resulted in necrosis and tubular cell death with protein leakage into the tubules.

The amount of drug remaining in each explanted device was also measured using HPLC. The amount of drug that was released was calculated based on the initial amount of drug loaded into each device. The total amount released divided by the number of days that the device was implanted for provides the average release rate for each device. The average release rate for the

devices in the 11-orifice group was 62.1 ± 47.9 µg/day (or 2.59 µg/hour). This was substantially slower than that observed during the *in vitro* release for the 11-orifice devices which was 43 µg/hour as shown in Figure 3.4 in section 3.1.3 of this thesis. According to what we found out from the pharmacokinetic study over 42 days (section 3.3.2), this was likely because the 11-orifice device released quickly over the first few days and the release rate declined rapidly for the rest of the treatment period. The calculated release rate for these 11-orifice devices, average over the entire duration of treatment, would therefore be lower than its expected release rate.

Tumor vasculature from three groups - the control, the 11-orifice device and IP bolus injection (once every three weeks) - were stained using immunofluorescence CD31+ antibodies. This work was done with the help of Yuan Xue. CD31+ antibodies are used to identify endothelial cells on the blood vasculature system. Figure 3.12b shows that in the 11-orifice device group (marked as 'device' on the figure) there was a significant reduction in blood vessel formation, or angiogenesis. This indicates poor development of tumors in the presence of device treatment. The IP bolus (once every three weeks) group showed a comparable amount of angiogenesis as compared to the untreated control group. This observation is also consistent with the bioluminescence measurement where the tumor growth profiles of these two groups were similar to each other. This was the first set of data that proved that device treatment regimen could control tumor growth and hinder the formation of blood vessels inside the tumors better than the IP bolus treatment regimen. Thus, the 11-orifice device was able to achieve treatment efficacy with minimum renal damage and was proven to be the ideal treatment modality throughthe preliminary *in vivo* studies.
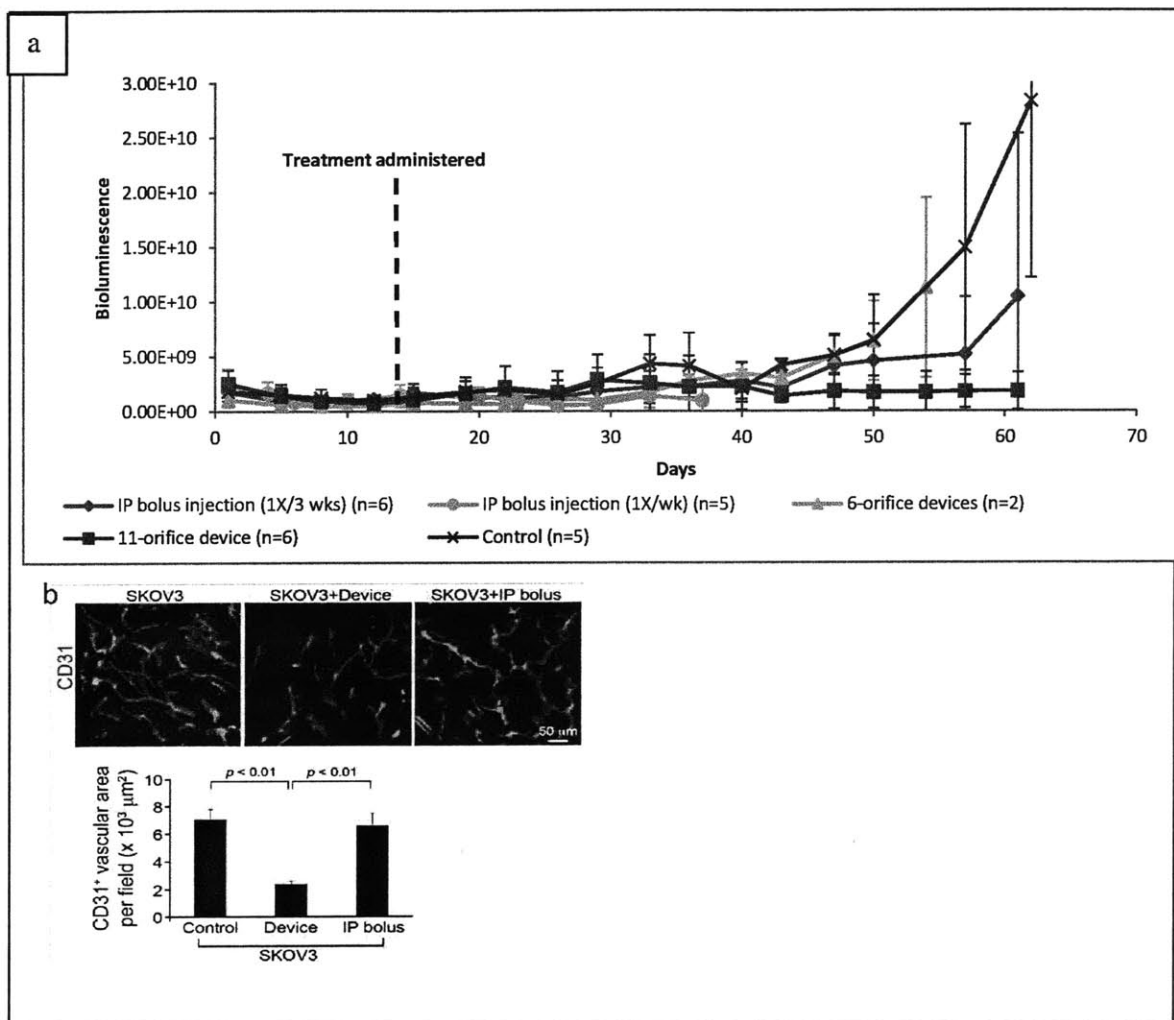
Figure 3.12 Bioluminescence intensity (BLI) and CD31+ staining of the tumors. a: BLI was plotted over time. Day 0 was the day of cancer cell line inoculation; Day 14 was the start of treatment administration (device implantation or IP bolus injections). The animals in the control group were untreated. b: CD31+ stain of the tumor vasculature and fluorescence signal strength comparison of the 3 groups: control, 11-orifice device, and IP bolus injection once every 3 weeks.
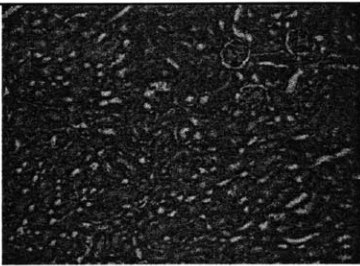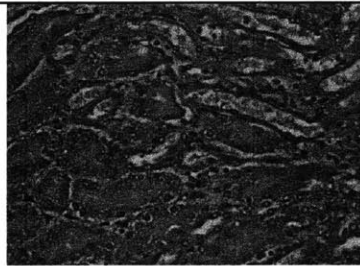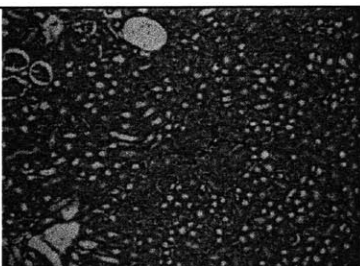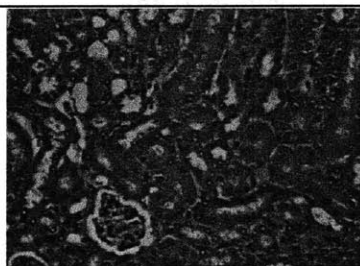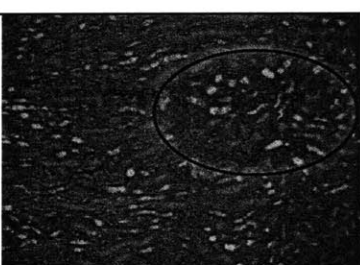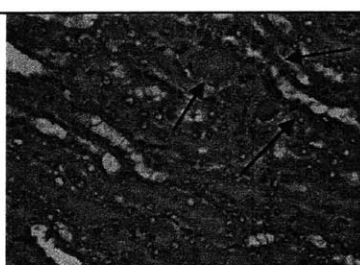
Magnification	10X	25X
Control		
11-orifice device		
IP bolus injection (1 dose per week)		

Figure 3.13 H&E staining of the kidney samples obtained from animals from the respective groups at end point. The IP bolus injection (1 dose per week) group showed significant tubular regeneration (circle) and the presence of protein casts (arrows). The 11-orifice device group showed normal kidney structures compared to the control group.

3.6.2 SCID BEIGE mice with 10^6 cells per mouse

This study was conducted to investigate the treatment efficacy of a tumor model with reduced tumor burden on SCID BEIGE mice. Each SCID BEIGE animal was inoculated IP with 10^6 cells. Assuming that a lower drug concentration is required in the peritoneal cavity to achieve a similar

treatment outcome as compared to the previous experiment (section 3.6.1), devices of 5- and 7-orifice was chosen. The animals were divided into the following groups:

1. 5-orifice device group

2. 7-orifice device group

3. Blank device group

4. Control (untreated) group

The blank device group was included to verify that any toxicity or treatment outcome was not an effect of a sham device or the surgical procedure of implanting the device.
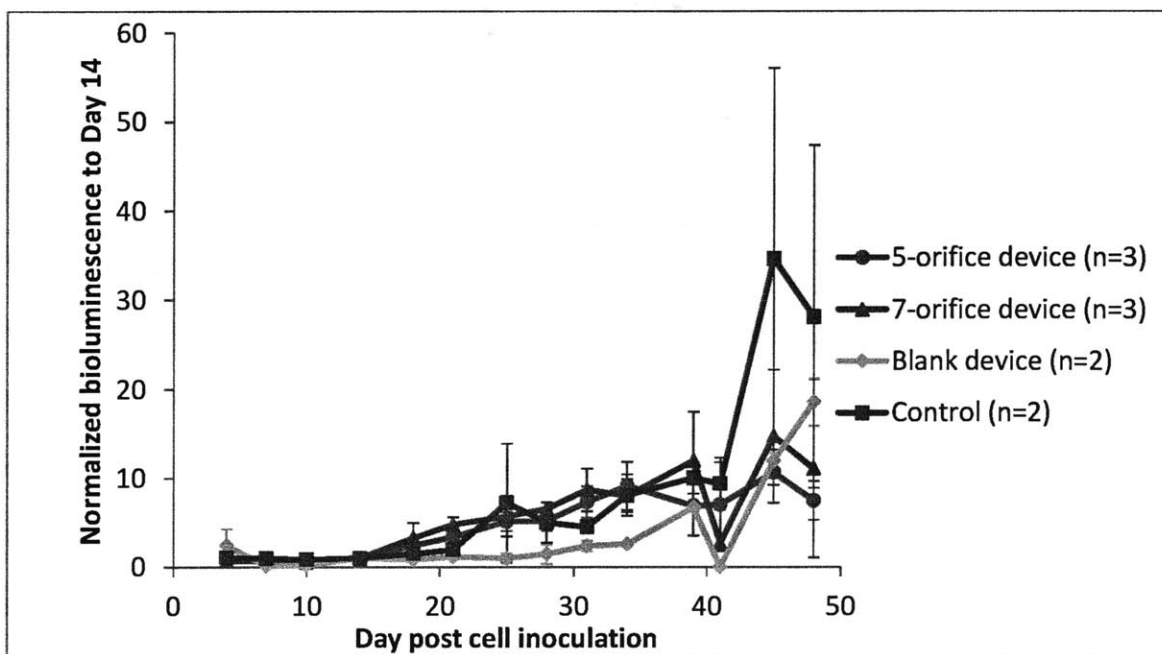
Figure 3.14 Bioluminescence intensity (BLI) normalized to the day of the start of treatment (day 14). The BLI for 5- and 7-orifice device groups seemed to have no significant difference from the blank device and control groups. However, a later tumor mass measurement showed a significantly lower tumor mass in the 5- and 7-orifice device groups compared to the blank device and control groups. The BLI seemed to be over-estimating the tumor burden.

The normalized bioluminescence of these animals as illustrated on Figure 3.14 shows that the 5- and 7-orifice devices were not very effective at suppressing tumor growth compared to the blank

72

devices. There was no significant difference between the BLI values of the 5- and 7-orifice device to that of the control animals either, especially given the relatively small n value in the control group. However, tumor mass data that we obtained at autopsy showed a significant difference between the device-treated groups and the control group ($p < 0.05$). Figure 3.15 shows that both the 5- and 7-orifice group had tumor mass of less than 20 mg, while the blank device and control groups had an average of 214 mg and 314 mg respectively. This result did not agree with the normalized bioluminescence data and raised the postulation that the BLI could be falsely high in the presence of effective treatment. This phenomenon will be further discussed in section 3.7.
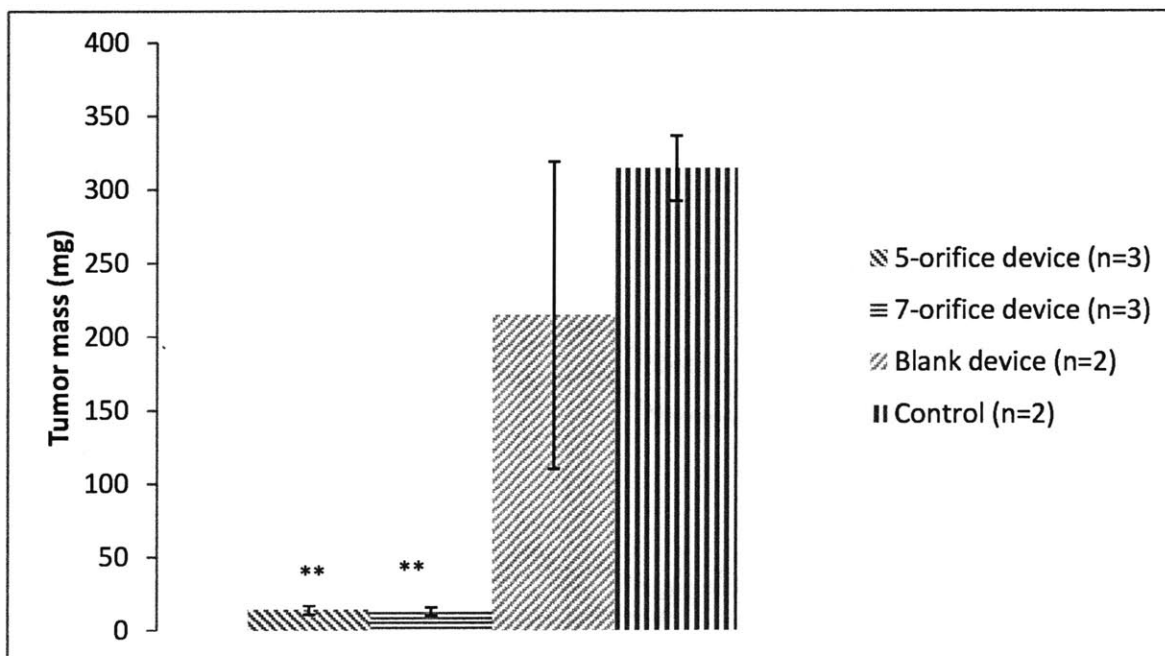
Figure 3.15 Tumor mass plot for the SCID BEIGE 10^6 cells/animal treatment efficacy study. The 5- and 7-orifice device groups showed significantly treatment compared to the blank device and control group. (*: $p < 0.05$, **: $p < 0.01$, ***: $p < 0.001$)

The normalized animal body weight plot in Figure 3.16 was an indication of the general well-being of the animals with respect to the day before the start of the treatment (day 14). The body weight was used as an approximation of the treatment toxicity. Figure 3.16 reveals that the

animals that received device treatment (both the 5- and 7-orifice groups) lost weight rapidly over the 14 days after the start of treatment. Therefore, even though the 5- and 7-orifice devices were able to inhibit tumor growth, they were also too aggressive for the SCID BEIGE mice. The previous tumor model with 10^7 cells inoculated per nu/nu mouse was able to withstand the 5- and 11-orifice devices, therefore, it was deduced that the SCID BEIGE mice were less tolerant to cisplatin treatment compared to the nu/nu mice due to the degree of their immunodeficiency. As previously mentioned in section 3.5.2, SCID BEIGE mice were used in an attempt to increase the tumor uptake rate of the mice. However, in this experiment, there were still about 40% of the mice that did not develop tumors after cell inoculation. Subsequent experiments would be conducted using the nu/nu mice as hosts for the xenograft since the SCID mice brought about no improvement to the tumor uptake rate, and were less tolerant to cisplatin treatment.
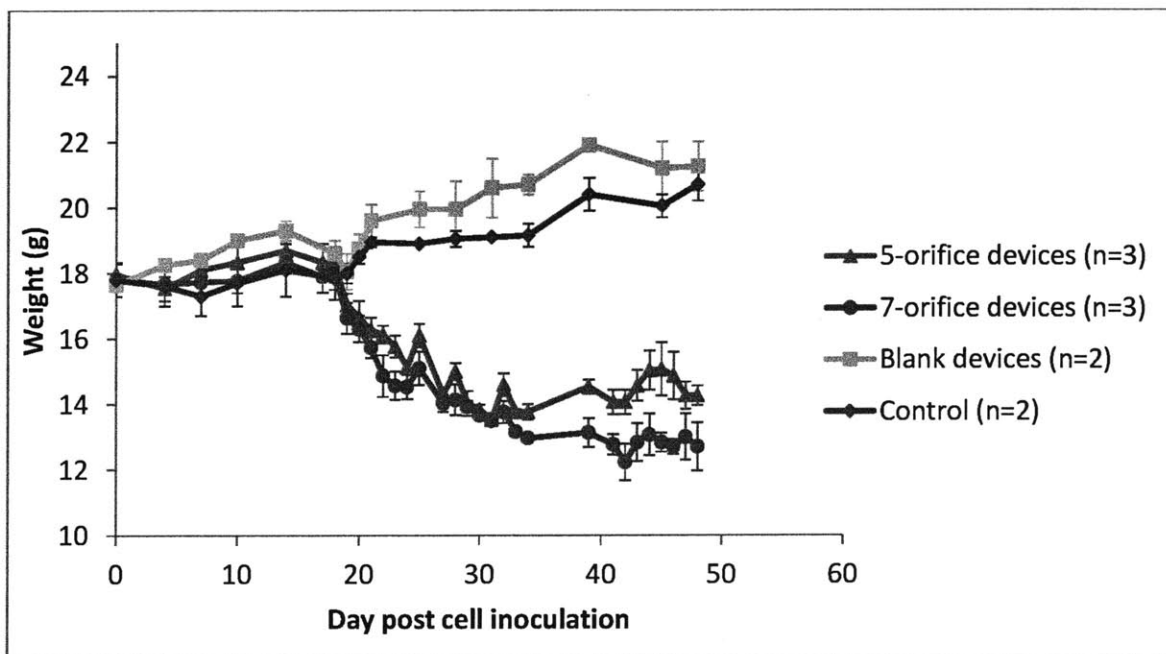
Figure 3.16 Body weight plot over time for the SCID BEIGE 10^6 cells/animal study. The 5- and 7-orifice device groups lost weight significantly compared to the blank device and control groups.

74

3.6.3 Nu/nu mice with 10^6 cells per mouse

Each nu/nu mice were injected with 10^6 SKOV3 human ovarian cancer cells on Day 0. The animals were imaged twice every week. After the last imaging time point before Day 14 (usually Day 12), the animals were assigned into the following groups such that the average BLI per group was very similar to each other.

1. 1-orifice device group

2. 3-orifice device group

3. 5-orifice device group

4. 7-orifice device group

5. 5 mg/kg weekly IP bolus injection group

6. 10 mg/kg weekly IP bolus injection group

7. Control group (no treatment)

This batch of data was obtained by performing three separate studies with different groups, but the control animals were pooled together to obtain a fair basis for comparison. Table 1 outlines the treatment scheme for all the groups.

Groups		Treatment Scheme
Control		The animals did not receive treatment.
Device	1-orifice device	A device was implanted in the peritoneal cavity on Day 14.
	3-orifice device	
	5-orifice device	
	7-orifice device	
IP bolus injection	10 mg/kg weekly	Cisplatin bolus doses was administered IP once per week, starting from Day 14.
	5 mg/kg weekly	
Subcutaneous		Cisplatin was administered subcutaneously daily at 20 µg/day.

Table 1 Treatment scheme for each group for the nu/nu 10^6 cell/animal treatment efficacy study

Figure 3.17 shows the normalized bioluminescence over time for all the groups of animals. The

bioluminescence was normalized to the last imaging time point before the start of treatment (day

12) to obtain a relative tumor progression profile after treatment had started. The 1-orifice device

showed the best treatment outcome among all the device treated groups, according to the BLI.

Both the 5 mg/kg and 10 mg/kg IP bolus injection groups showed good tumor burden reduction

compared to the untreated control group. The daily 20 µg/day subcutaneous injection group

showed the least tumor reduction among all the groups that received treatment. Tumor masses

were obtained at the end of the study (day 56) during autopsy (Figure 3.18). A comparison of the

tumor mass of all the animals that survived until the end of the treatment period of 56 days

demonstrated significant tumor reductions in the 1-orifice device group, the 7-orifice device

groups and the weekly 5 mg/kg IP bolus injection group compared to the control group. No

tumor mass was recorded for the weekly 10 mg/kg IP bolus injection group because all the

animals in that group had died before completing the 56 day treatment period. Figure 3.18a

shows the tumor mass in milligrams plotted with standard error. Figure 3.18b shows the tumor

mass box and whiskers plot. Each box in the box and whiskers plot shows the middle 50

percentile and the horizontal line in the box indicates the median. The error bars represent the

range of the data. The dot in each box marks the mean.

It is to be noted that there was a lack of correlation between the tumor mass and the BLI signal of

the 7-orifice group. This was the same phenomenon as observed in section 3.6.2 and will be

discussed in greater details in section 3.7.
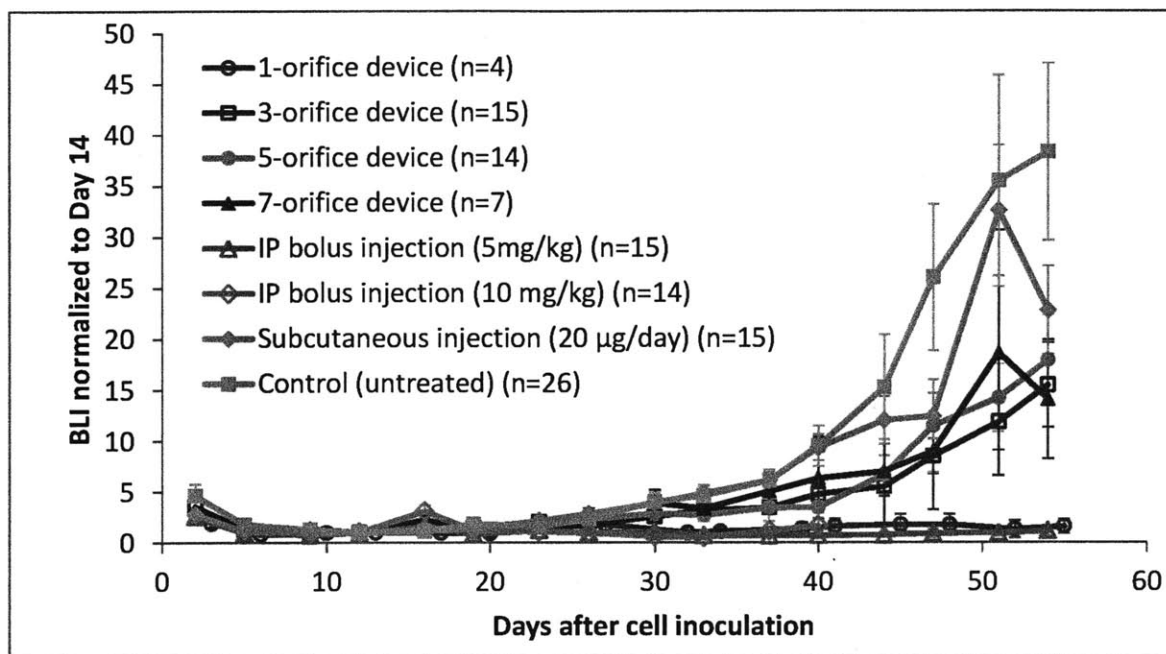
Figure 3.17 Bioluminescence intensity (BLI) of the animals normalized to the BLI of the start of treatment (Day 14). The 1-orifice device, weekly 5 mg/kg and 10 mg/kg IP bolus injection groups showed the lowest BLI over the treatment period. The 3-, 5- and 7-orifice device groups showed moderately high BLI compared to the controls. The subcutaneous 20 µg/day group showed the least treatment efficacy according to BLI.

The Kaplan-Meier survival curve revealed that the weekly 10 mg/kg IP bolus injection group showed the highest toxicity among all the groups, with a median survival of 25 days and all animals died by day 43 (Figure 3.19). The animal weight plot (Figure 3.20) also showed that with each IP bolus injection dose every week, the body weight dipped two to three days post-dose. This 10 mg/kg weekly dose was clearly too toxic *in vivo*. The 7-orifice device group was the next lethal group with a median survival of 30 days. The 7-
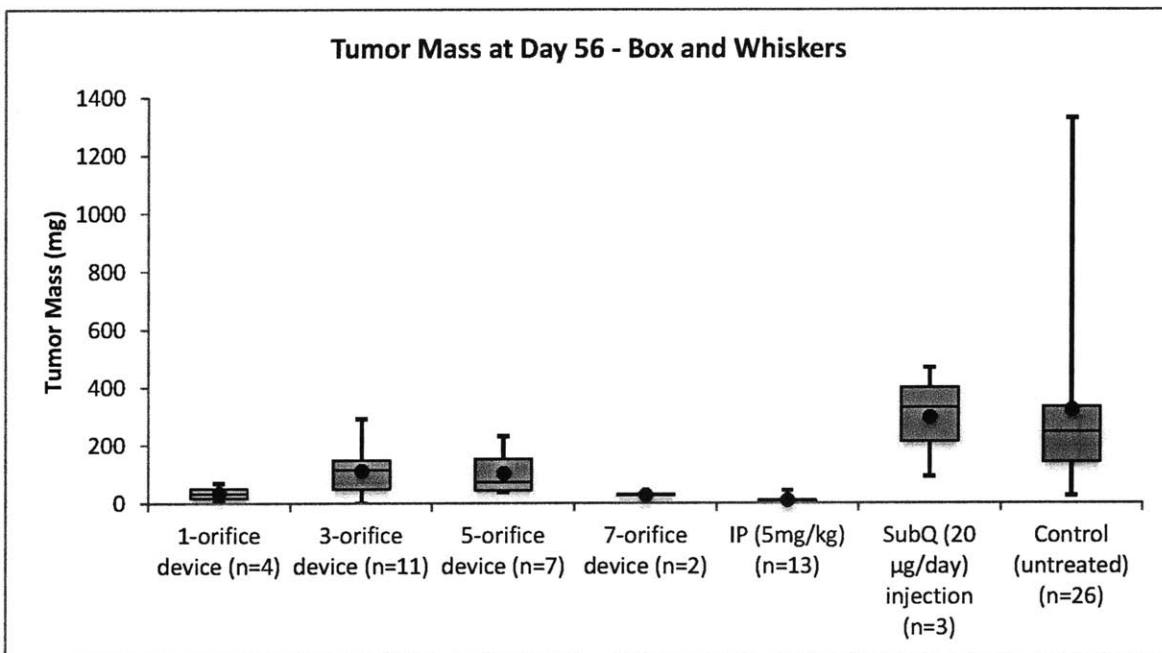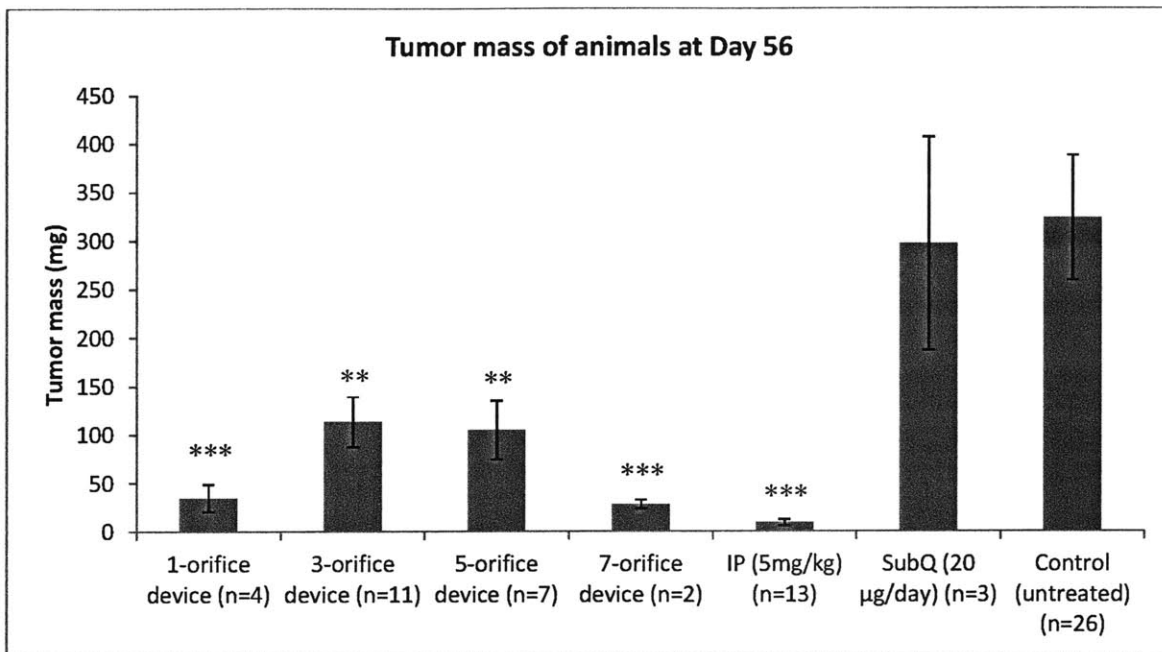
Figure 3.18 Tumor mass (mg) plots for the various experimental groups. A: Tumor mass in mg with standard errors for the various groups. B: Tumor mass in mg in a box and whiskers format. The box represents the middle 50 percentile, the bar in the middle of the box represents the median and the dot represents the mean. The error bars represent the range of the data. (*: $p < 0.05$, **: $p < 0.01$, ***: $p < 0.001$).

orifice device, as explained by the results of the pharmacokinetic study, probably had a high rate of release of cisplatin over the first few days of the treatment. The release rate was reduced greatly for the rest of the treatment period due to the fast diffusion of peritoneal proteins into the device, hindering release beyond a few days post-implantation.. Although the 7-orifice device group was able to result in a significant tumor mass reduction compared to the control group, the high initial release of drug from the device was too toxic for the animals according to the Kaplan-Meier curve. The animal body weight plot also suggested the presence of toxicities that resulted in severe weight loss over time. A slower but more sustained release is preferred.

The 3- and 5-orifice device groups provided some tumor reduction, with only moderate decrease in BLI and moderate tumor mass reduction compared to the control group (Figure 3.17 and 3.18). This was likely a result of having an initial release over the first few days of the treatment that eliminated some tumor cells, but having almost no treatment administered over the rest of the treatment period which allowed for tumor mass to increase over time. The high initial dose, on the other hand, induced toxicities in some animals, resulting in a loss of body weight over time (Figure 3.20).

The body weight plot shows that with increasing number of orifice, there was an increase in toxicity. The pharmacokinetic study proved that with an increase in the number of orifice in the device, there was a higher initial dose but over a shorter period of time – increasingly similar to a bolus dose. By comparing the body weight plot of the 1-, 3-, 5-, and 7-orifice device groups, it could be deduced that the bolus dosing regimen definitely causes more toxicity to the body system compared to a slow, prolonged release profile.

The daily subcutaneous injection group was created to mimic a subcutaneous pump for delivery of cisplatin. The subcutaneous dose, 20 μg/day, was chosen as it is approximately the same total dose as the weekly 5 mg/kg dose for mice of an average body weight of 27 grams. The results indicated that the subcutaneous group, not only did it not treat the tumors in the animals (Figure 3.18), but was also toxic to the animals. The average body weight of the subcutaneous injection group continued to decrease over the entire course of treatment (Figure 3.20c), with a median survival of 44 days (Figure 3.19). A subcutaneous pump that delivers a low dose of cisplatin daily would therefore perform worse than even the IP bolus injection of cisplatin in patients.

The most efficacious dose regimens that did not lead to severe weight loss were the single-orifice device group and the weekly 5 mg/kg IP bolus injection group. The weekly 5 mg/kg IP group, despite showing no significant weight loss, showed significant bone marrow toxicities upon histological examination which will be explained in greater detail.
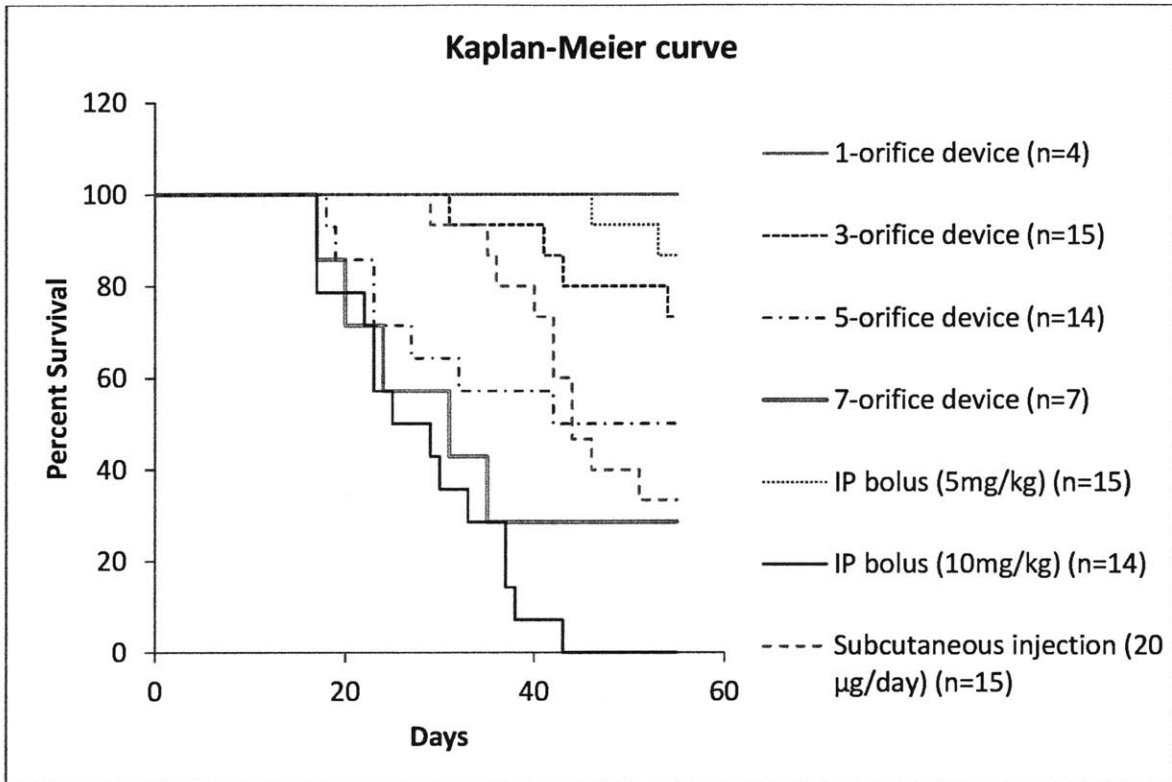
Figure 3.19 Kaplan-Meier curve for animal survival. The 1-orifice device group showed the highest survival among all the treated groups, followed by the weekly 5 mg/kg IP bolus, the 3-orifice device group and the 5-orifice device group. The subcutaneous 20 µg/day injection group had a median survival of 44 days. The 7-orifice device group had a median survival of 30 days. The weekly 10 mg/kg IP bolus injection group had the shortest median survival of 25 days.

a

Percent weight loss normalized to Day 14

10
5
0
-5
-10
-15
-20
-25
-30

0   20   40   60

Days after cell inoculation

→◆— 1-orifice device (n=4)

→▲— 3-orifice device (n=15)

→✳— 5-orifice device (n=14)

→☐— 7-orifice device (n=7)

→✕— 5mg/kg weekly IP bolus injection (n=15)

→⊙— 10mg/kg weekly IP bolus injection (n=14)

→●— SubQ 20 μg/day injection (n=15)

→■— Control (n=19)

b

Percent weight loss normalized to Day

10
5
0
-5
-10
-15
-20
-25
-30

0   10   20   30   40   50   60

Days after cell inoculation

→◆— 1-orifice device (n=4)

→▲— 3-orifice device (n=15)

→✳— 5-orifice device (n=14)

→☐— 7-orifice device (n=7)

→■— Control (n=19)

82

Figure 3.20 The body weight of the animals were plotted over time. A: Body weight of all the animals in this experiment. B: All device treated groups with the control group. The body weight of the device-treated animals dropped initially on day 14 after the start of treatment. The body weight of the 1-orifice device group bounced back to pre-treatment weight for the rest of the treatment period. With increasing number of orifice, the initial weight drop was larger – dose response was observed. This also proved the hypothesis of slow prolonged release of cisplatin causes less toxicity than a fast burst of cisplatin release. C: The IP bolus injection group, the subcutaneous 20 μg/day group and the control group. Both IP bolus groups showed cycling of the body weights, with a dip in body weight after each weekly IP dose. The subcutaneous injection group suffered from constant toxicity as the average weight decreased continuously over time.

Bone marrow toxicity

Cisplatin is a chemotherapeutic agent that works by binding onto unwound DNA strands, leading to cell apoptosis. DNA would only unwind during transcription and cell replication, therefore, cisplatin acts most effectively on rapidly proliferating cells, such as the cancer cells, hair follicle cells, epithelial cells that line the gastrointestinal tract, and the bone marrow cells[16].

83

Normal bone marrow contains numerous pleuripotent stem cells which are blood progenitor cells. These cells replicate to maintain the number of stem cells in the bone marrow as well as differentiate into committed stem cells called the lymphoid and myeloid cells. The lymphoid stem cells are the multipotential colony forming unit (CFU) for B and T lymphocytes (CFU-L on Figure 3.21). The myeloid stem cells are multipotential colony forming unit (CFU) for granulocytes, erythrocytes, monocytes and megakaryocytes (CFU-Gemm on Figure 3.21)[77-80].
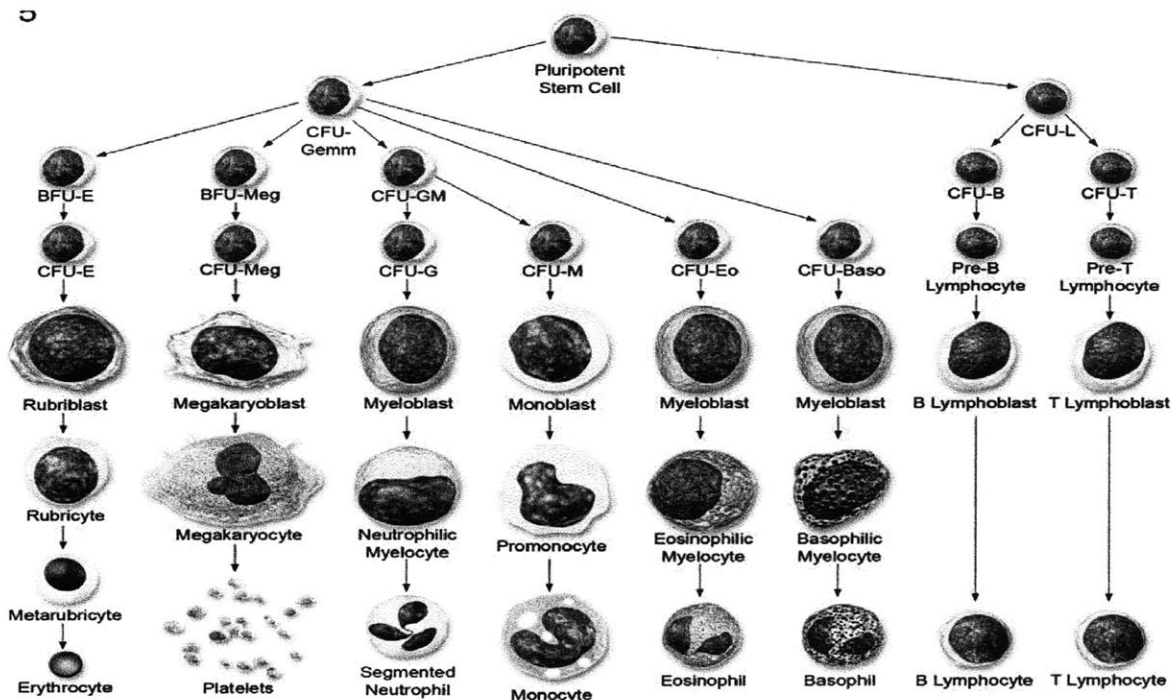
Figure 3.21 This figure showed the cell lineage of the bone marrow cells. The pleuripotent stem cell differentiates into either the colony forming unit lymphoid (CFU-L) cells or colony forming unit myeloid (CFU-Gemm) cells. The lymphoid cells will differentiate to become either the B or T lymphocytes. The myeloid cells will differentiate to become either the erythrocyte, megakaryoocyte (which will fragmentate to become the platelets), neutrophils, monocytes, eosinophils or basophils. Diagram drawn by David Sabio, cited from a paper by Travlos.

The bone marrow has an extensive blood supply with the hematopoietic tissue surrounded by vascular sinuses. Upon maturation, the hematopoietic cells are transported via these sinuses into the circulatory system. When these stem cells or/and myeloid and lymphoid cells are eliminated
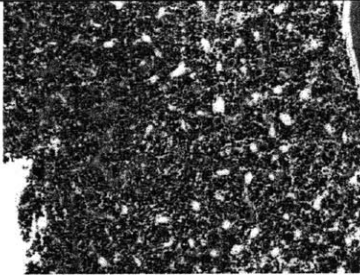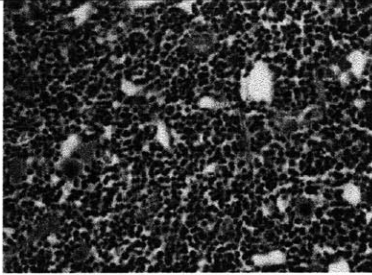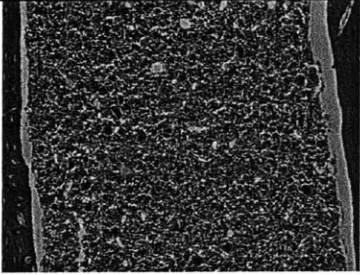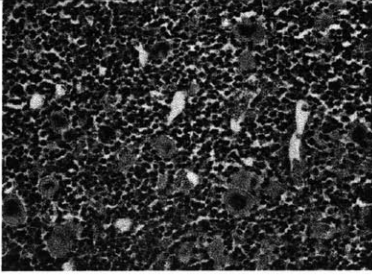
by the chemotherapeutic agent, there is a significant reduction in the number of cells in the bone marrow. The blood capillaries in the bone marrow then expand to fill up the void spaces in the bone marrow. The clusters of matured erythrocytes (red cells without nucleus) in the histology picture marked the blood sinuses. Beside the apparent reduction in bone marrow cellularity, the expansion of these clusters of erythrocytes also implies an expansion of blood vessels in the presence of bone marrow destruction.

There may be wide animal-to-animal, variation of sampling site, and age-related differences between samples, therefore, it is very important to compare potential treatment-related findings against appropriate concurrent control samples[81]. Figure 3.22 shows the hematoxylin and eosin stained bone marrow histology for the various groups. The bone marrow in the animals from the control group was packed with bone marrow cells with small pockets of blood sinuses. The 1-orifice device group was very similar to that of the control group and showed no significant bone marrow depletion. However, the IP bolus injection (5 mg/kg) group showed significant reduction in the bone marrow cell number as seen in the 10x magnification. On examination at a higher magnification, there was clearly a presence of blood vessel expansion and a depletion of normal bone marrow progenitor cells. Similar bone marrow toxicities after IP bolus cisplatin injections have also be reported[59].

This result was consistent with the results from complete blood count (CBC) as shown in Figure 3.23. Due to the depletion of lymphoids which differentiate to produce lymphocytes, there is a decrease in the number of lymphocytes in the animals in the weekly 5 mg/kg IP bolus injection group. It is to be noted that as the hosts are nu/nu mice which have deficient T lymphocytes, the baseline value of lymphocyte count may be lower than what is expected of a healthy non-immunodeficient animal. It is therefore crucial for comparison of the treated groups to the

control groups to obtain a relative toxicity. In this case, the p value between the control group and the 1-orifice device group is 0.527 and the p value between the control group and the weekly 5 mg/kg IP bolus injection group is 0.010. Based on even higher magnification of bone marrow histology (data not shown), there is also a reduction of not just lymphoid, but erythroids as well. Given that the life span of a red blood cell in mice is 40.7 ± 1.9 days[82], the loss of erythoid might not be reflected as anemia in the CBC report. The CBC was performed at day 56, 42 days after the onset of treatment. This might not have given the animals enough time for the effect of erythroid depletion to precipitate as a lowered red blood cell count in CBC. CBC showed no significant differences between groups in the counts of other cell types.

Group	10x magnification	25x magnification
Control group		
1-orifice device group		

3-orifice device group		
Weekly 5 mg/kg IP bolus group		
Daily subcutaneous (20 µg/day) group		
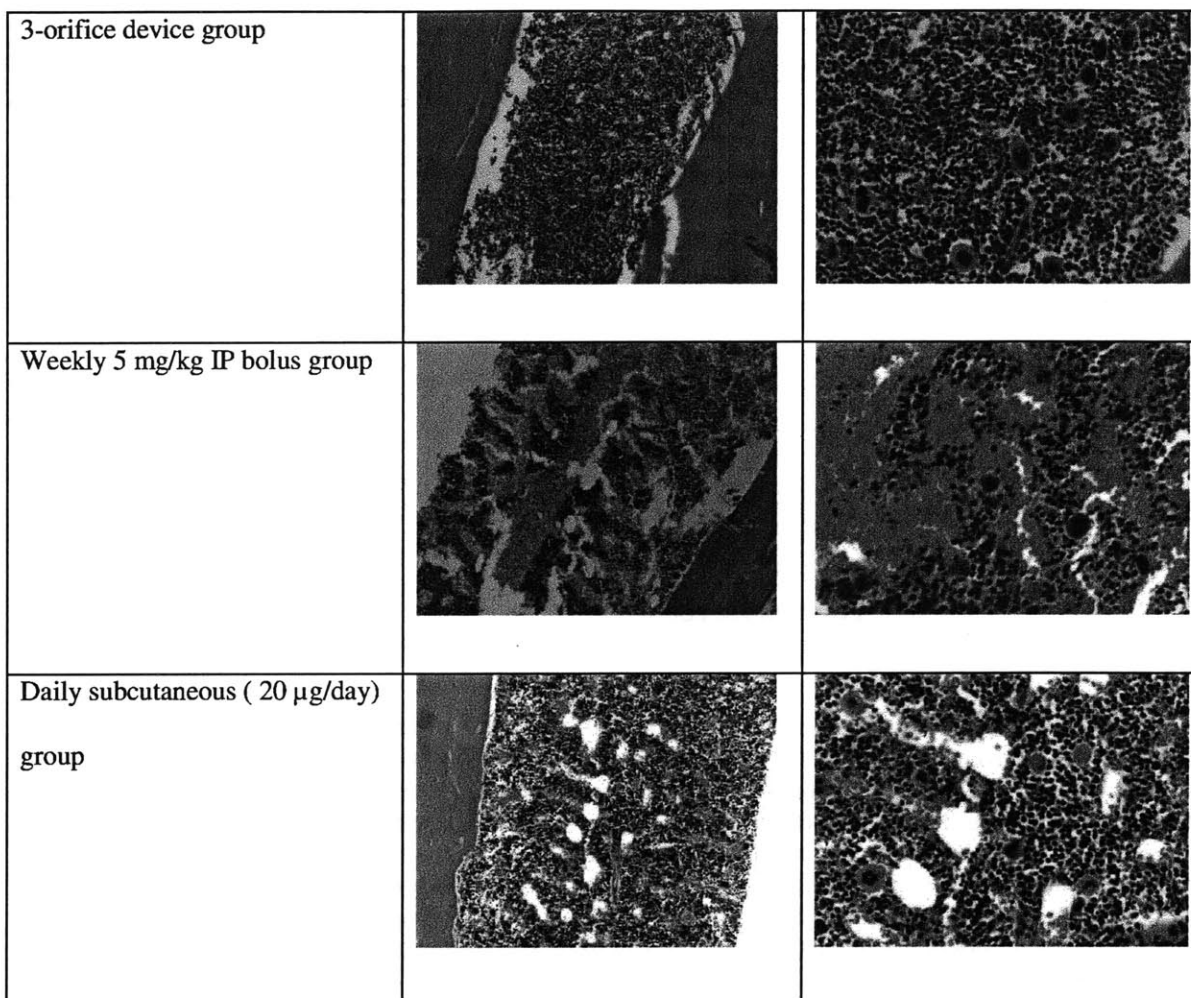
Figure 3.22 This figure shows the H&E histological slides of the bone marrows of the various groups. The control group showed the bone marrow of a normal nu/nu mouse. There are abundant bone marrow stem cells with pockets of vascular sinuses. The 1-orifice device and 3-orifice device groups showed similar bone marrow cellularity as that of the control group. The empty spaces between the bone tissue (light pink) and the hematopoietic stem cells on the 10x magnification images were considered normal histological artifacts. The weekly 5 mg/kg IP bolus group showed a significant reduction in the number of bone marrow progenitor cells (loss of cells with nuclei that are stained purple). This loss of bone marrow stem cells resulted in the expansion of the vascular sinuses. Numerous large pockets of mature red blood cells (red cells that do not have nuclei) marked the size and location of these vascular sinuses. The subcutaneous daily 20 µg/day group also experienced some, but less severe, bone marrow suppression as shown by the decreased cellularity and increased vascular sinus spaces.
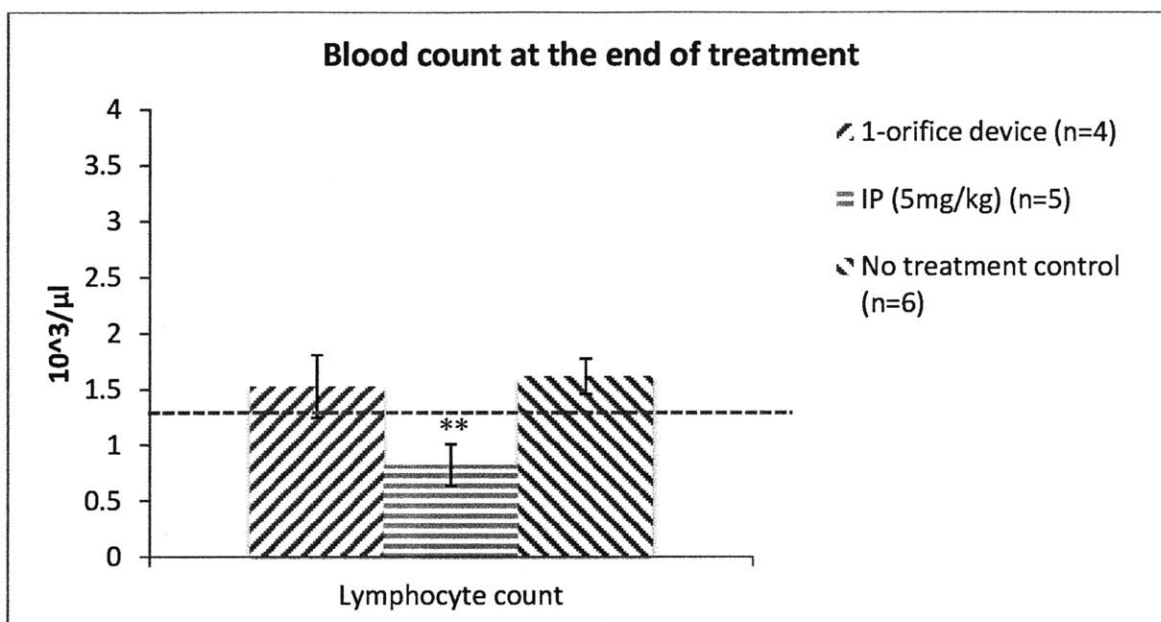
Figure 3.23 Complete blood count (CBC) conducted at the end of the treatment period (day 56) for the 1-orifice device, weekly 5 mg/kg IP bolus injection and the no treatment control group. The results showed that there was a significant decrease in the lymphocyte count (lymphocytopenia) in the weekly 5 mg/kg IP bolus injection group. This was consistent with the histological findings. As there was a loss of bone marrow stem cells (myeloid cells and lymphoid cells), the production of blood cells also decreased. This was especially shown through the lymphocyte counts as lymphocytes had a much shorter life span of a few days compared to the red blood cells of about 40 days. The other counts in the CBC showed no significant differences between groups. (*: $p < 0.05$; **: $p < 0.01$; ***: $p < 0.001$)

Creatinine is a metabolic by-product from the breakdown of creatine phosphate. It is excreted from the body by the kidneys and an elevated serum creatinine value indicates renal insufficiency. As mentioned in section 3.6.1, nephrotoxicity as a result of cisplatin treatment had been widely reported. However, creatinine assay performed on the serum samples showed that no significant nephrotoxicity was detected in all groups except the subcutaneous group (Figure 3.24). The two red lines mark the upper and lower bound of the normal range. Kidney histology also verified that there was remodeling and scarring of kidney tissues only in the subcutaneous injection group, but no damage to the kidneys to the other groups (Figure 3.25).

88

The 1-orifice device group and the weekly 5 mg/kg IP bolus injection group have a similar

cumulative drug dose or area-under-curve (AUC) in the peritoneal cavity, but have a vastly

different drug peak concentration (C_{max}) as shown in Table 2.

	1-orifice device group	Weekly 5 mg/kg IP bolus injection group
Area-under-curve (AUC) in the peritoneal cavity over the 42 day treatment period	0.83 µg-day/mL	0.60 µg-day/mL
Cisplatin peak concentration (C_{max})	No cisplatin concentration peaks	6.5 µg/mL once every week

Table 2 Table showing the calculated area-under-curve (AUC) and the peak cisplatin concentration (C_{max}) in the peritoneal cavity over the treatment period of 42 days for the 1-orifice device group and the weekly 5 mg/kg IP bolus injection group.

The AUC of the 1-orifice device group is approximately 0.83 µg-day/mL and the weekly 5

mg/kg IP bolus injection group is approximately 0.60 µg-day/mL over the 42 day treatment

period according to Figure 3.8. The 1-orifice device group demonstrated a relatively constant

drug release profile *in vivo* with no C_{max}; 5 mg/kg IP bolus injection group is estimated to have a

peak cisplatin concentration of 6.5 µg/mL in the peritoneal cavity (half of that of the 10 mg/kg)

with every week. The experiment in this section showed that despite having a different C_{max},

with a similar AUC, the two treatment regimens were able to result in a similar treatment

efficacy in terms of both the normalized BLI intensity and the tumor mass at the end of treatment.

This demonstrated that treatment efficacy correlates with AUC instead of C_{max}. This experiment

also proved that the device treatment regimen of delivering a low dose of cisplatin continuously

over a prolonged period of time is superior to the spikes of IP bolus injection treatment regimen

as it results in less toxicity, given a similar treatment efficacy. Recall from section 3.3 that the

efficacious cisplatin AUC was 0.7 µg-day/mL to 3.5 µg-day/mL. It is therefore consistent that

the 1-orifice device is suppressing tumor growth with an AUC of 0.83 µg-day/mL. The dose of

the device treatment regimen could be further optimized by implanting multiple 1-orifice devices

to ensure a higher but continuous release over the entire treatment period of 42 days.
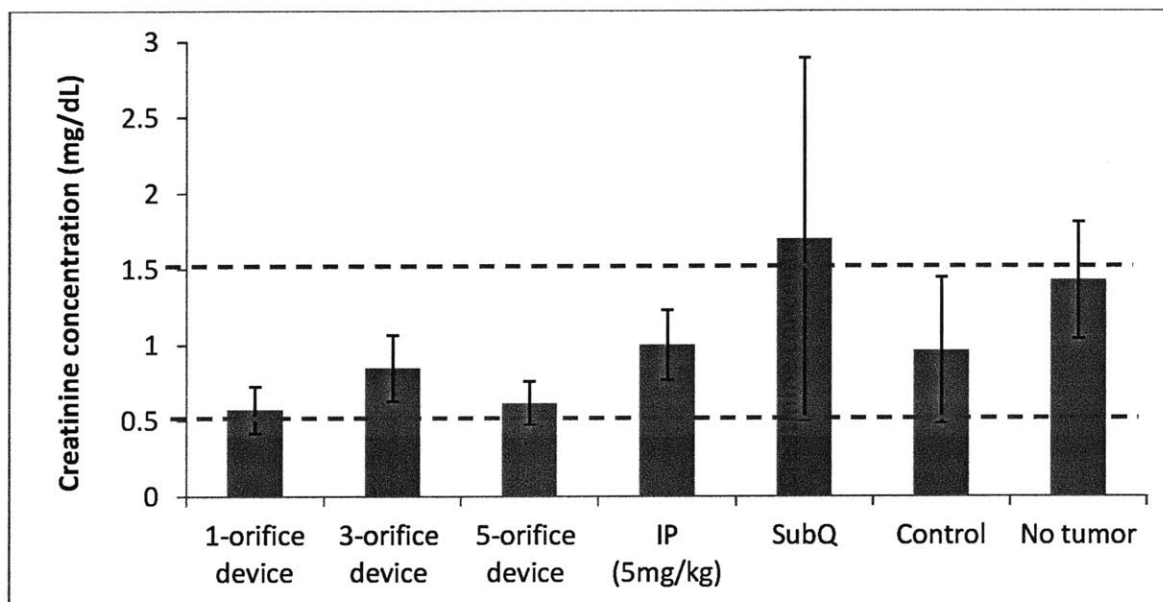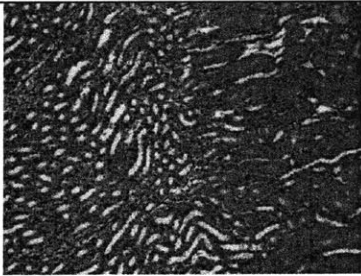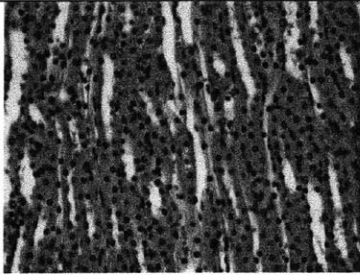
Figure 3.24 Serum creatinine concentration of the various groups showed that all groups, except the subcutaneous daily 20 µg/day injection group, had no significant kidney damage. The subcutaneous injection group showed a slightly elevated serum creatinine concentration.

Group	10x magnification	25x magnification
Control group		

1-orifice group		
3-orifice group		
Weekly 5 mg/kg IP bolus group		
Daily subcutaneous (20 µg/day) group		
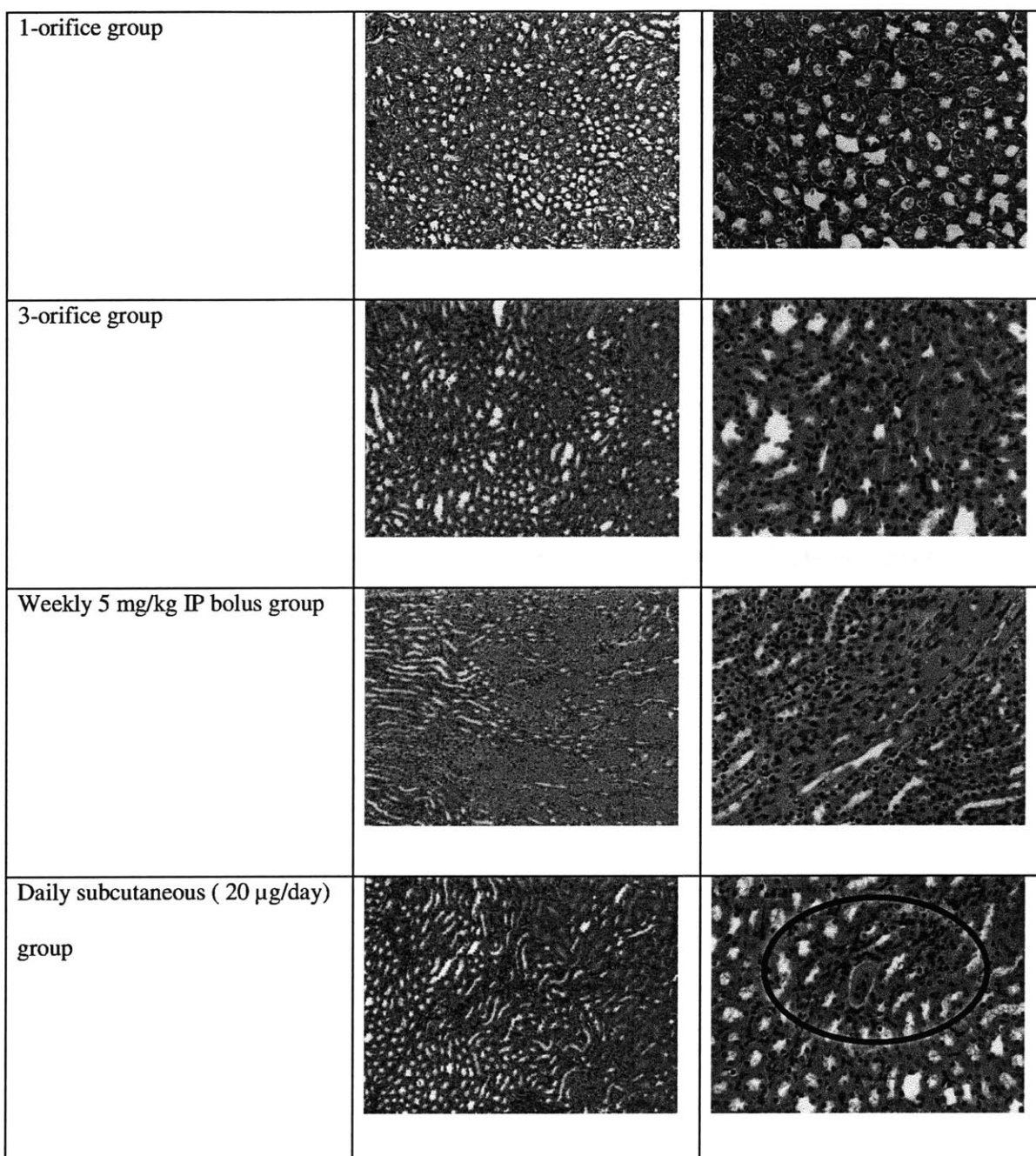
Figure 3.25 The control group showed the normal histology of kidney proximal and distal tubules on both 10x and 25x magnifications. The 1-orifice, 3-orifice and weekly 5 mg/kg IP bolus group all showed the same normal kidney histology as the controls. However, the daily subcutaneous (20 µg/day) group showed signs of tubular cell death with fragmented nuclei in a protein cast as circled in black. This is consistent with a higher-than-normal serum creatinine level in the daily subcutaneous group.

3.6.4 Multiple 1-orifice devices

The aim of this experiment was to explore the various doses for obtaining the optimal release rate to achieve the maximum efficacy without causing toxicity. The animals were grouped into the following groups:

1. 1-orifice device

2. 3 1-orifice devices

3. 5 1-orifice devices

4. Weekly 5 mg/kg IP bolus injection group

5. Control (untreated)
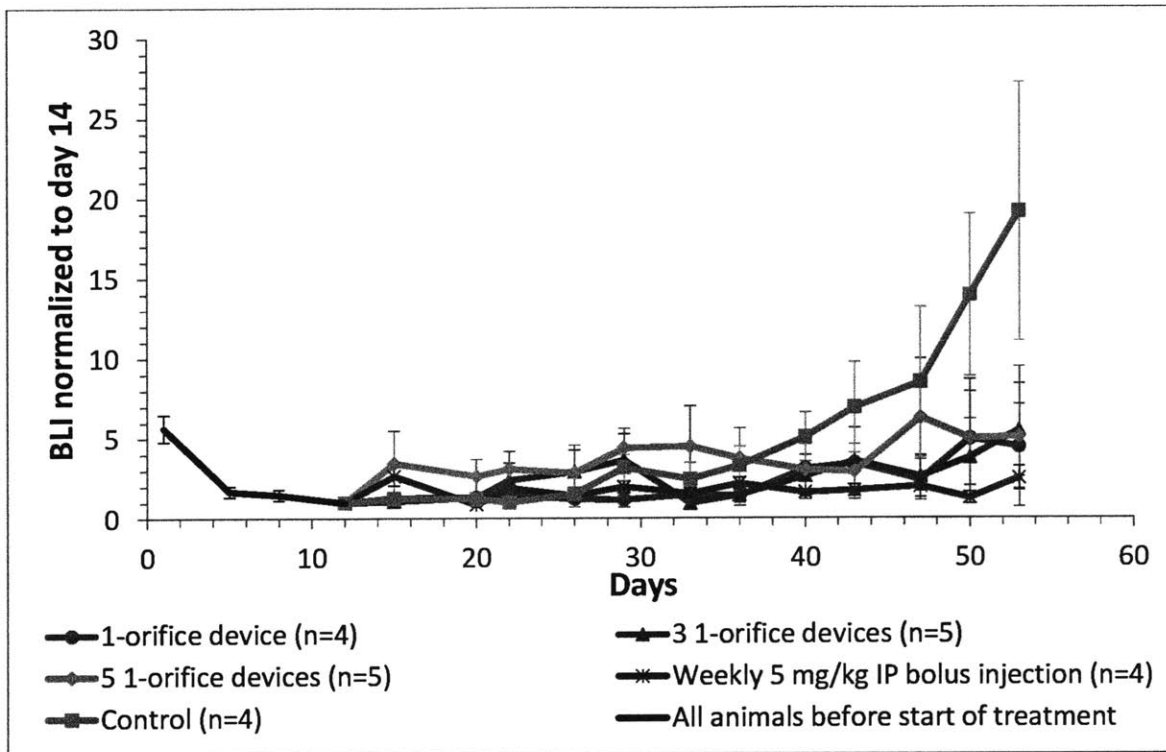
Figure 3.26 The normalized bioluminescence intensity of the multiple 1-orifice device study. The single, 3 and 5 1-orifice devices showed similar bioluminescence intensity (BLI) at day 53. The weekly 5 mg/kg IP bolus injection group showed the lowest BLI at the end of the study.

The bioluminescence in Figure 3.26 shows that there was no significant difference among the bioluminescence intensity of the single, 3 and 5 1-orifice devices groups. The weekly 5mg/kg IP bolus injection group showed the lowest BLI intensity and the untreated control group displayed a significantly higher BLI intensity.
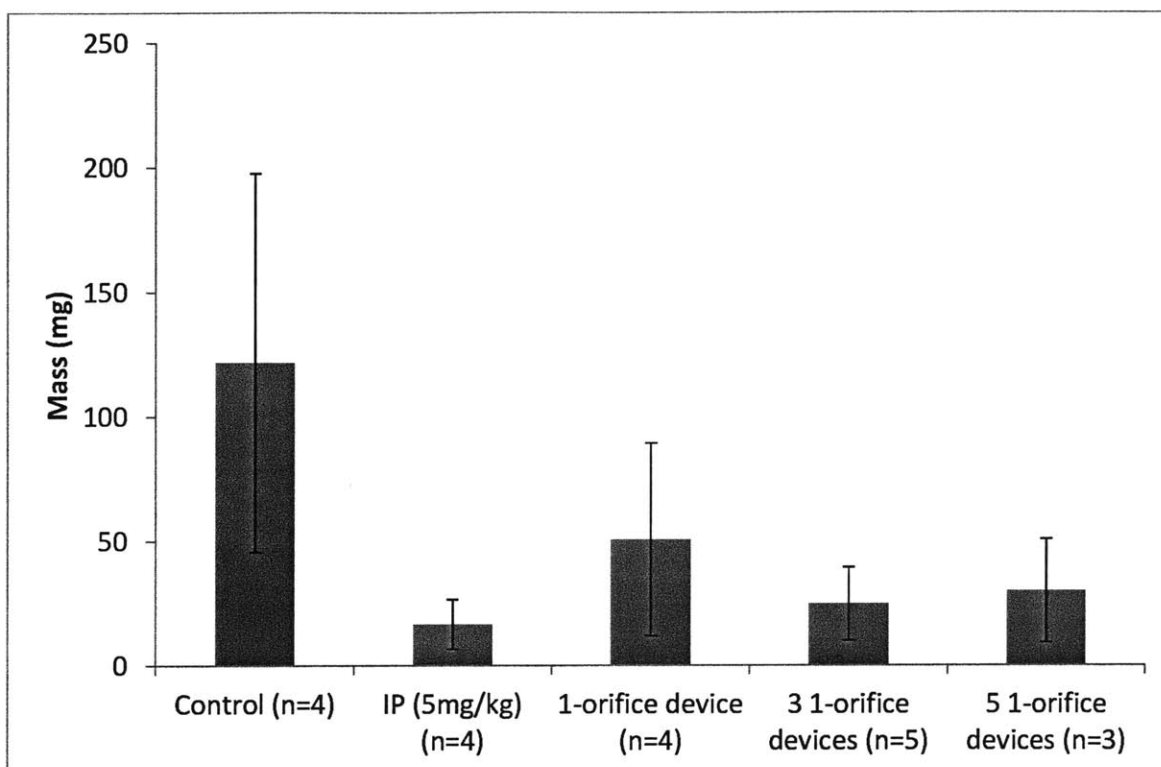
Figure 3.27 Tumor mass at the end of the treatment. The weekly IP (5 mg/kg) group, the 3 and the 5 1-orifice devices groups showed the lowest tumor burden.

The groups with the lowest tumor burden were the weekly 5 mg/kg IP bolus injection group, the 3 1-orifice devices group and the 5 1-orifice devices group according to Figure 3.27. A dose response was observed in terms of tumor mass with the 3 and 5 1-orifice devices groups showing a larger tumor growth suppression. The toxicity caused by the 5 1-orifice device treatment was, however, not ideal. Two out of the five animals in the 5 1-orifice devices group had to be euthanized due to severe weight loss on day 24. The release rate of 3 1-orifice devices may be the most efficacious dose for treating tumor in this tumor model. It is to be noted that none of the treatment groups had a p value of less than 0.05 with the control group due to the relatively small sample size (n value).
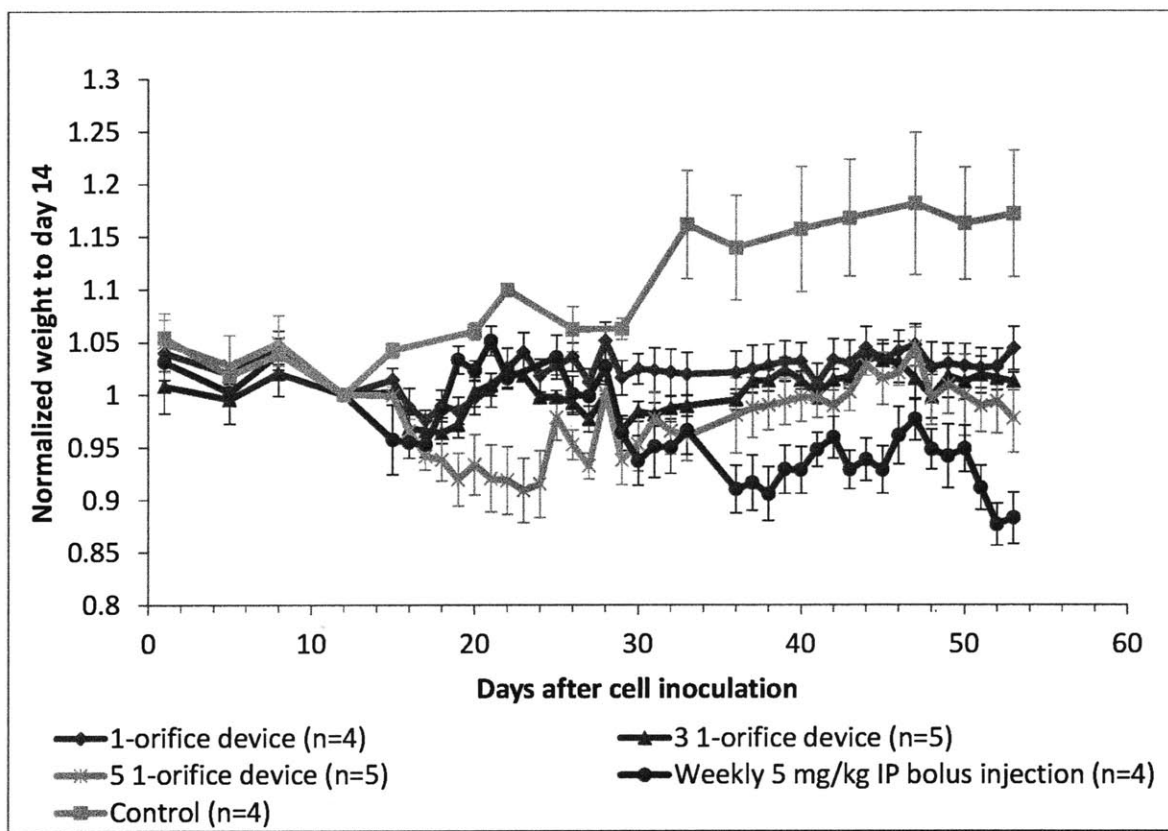
Figure 3.28 Body weight of the animals normalized to the day of start of treatment (day 14). This plot shows that the weekly IP bolus injection group animals experienced the largest weight drop by the end of the treatment period.

The normalized body weight plot showed the highest toxicity in the IP bolus injection group with the lowest normalized body weight among all the groups (Figure 3.28). The normalized body weight of the 5 1-orifice devices group decreased around day 14 to day 24, but rebounded after the euthanasia of the two sick animals.
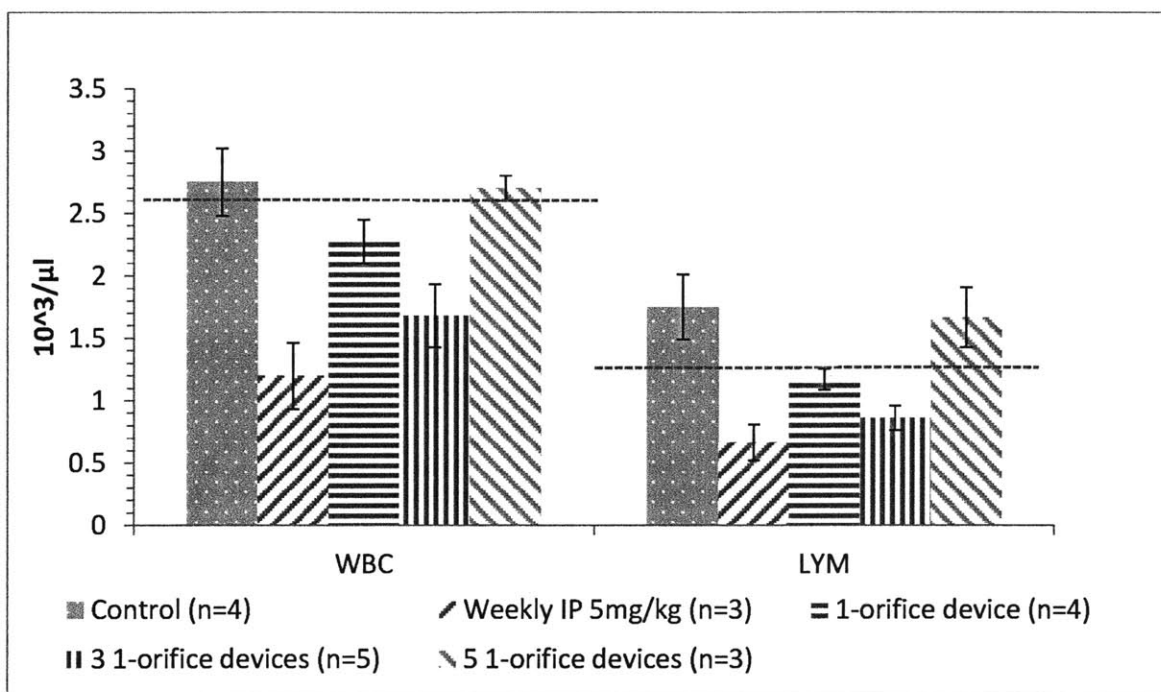
Figure 3.29 The complete blood count (CBC) of the animals on day 53. The weekly 5 mg/kg IP bolus injection group had the most severe reduction in white blood cell (WBC) count and lymphocyte (LYM) count. The red lines marks the lower end of the normal range. The 5 1-orifice devices group has a higher WBC and LYM count than expected despite having a mortality rate of 40%.

Complete blood count (CBC) in Figure 3.29 shows that of the animals survived until day 53, the IP bolus injection group experienced the most significant reduction in white blood cell (leukopenia) and lymphocyte count (lymphocytopenia) as compared to the control group. It was puzzling that despite the mortality rate in the 5 1-orifice group, there was no significant leukopenia or lymphocytopenia. A possible reason could be that the animals that had to be euthanized early experienced an acute, non-bone marrow related toxicity (for instance, nephrotoxicity) due to the high release rate. Kidney and bone marrow histology that are currently being undertaken will elucidate a possible hypothesis to this observation.

3.7 Up-regulation of the luciferase gene in the presence of chemotherapeutic treatment

It had been previously observed in section 3.6.2 and 3.6.3 that in some cases, the bioluminescence intensity (BLI) over-estimated the actual tumor mass *in vivo*. This was usually accompanied by a loss of body weight to that animal, indicating an assault to its body system. The SKOV3 luciferase-expressing cell line used in this animal model was a cytomegavirus-driven luciferase gene insert. This cytomegavirus (CMV) promoter was added as an proximal enhancer to achieve a high-level luciferase expression in mammalian cells[83]. This CMV promoter is known to be responsive to a variety of stimuli that activate various signaling pathways, such as the NFκB and p38 MAPK that are involved in viral replication[84,85]. As a result, inflammatory cytokines or cell stress-related molecules that plays a role in these pathways may alter the expression of the CMV promoter[86].

Similar observations over BLI over-estimating the actual tumor mass had been reported in the literature. One group discovered that an up-regulation of a CMV-driven green fluorescent protein (GFP) was observed after treatment with IV 8mg/kg of cisplatin *in vivo*[87]. Another group of researchers tried treating a few different CMV-driven luciferase-expressing cell lines with doxorubicin (a DNA-damaging agent), paclitaxel (a microtubule-stabilizing agent) and staurosporine (a protein kinase inhibitor) both *in vitro* and *in vivo*[88]. The results showed that there was a transient up-regulation of the CMV-driven luciferase expression post-treatment. This was, however, not observed at the same drug dosage in SV40-driven luciferase expressing cells[88]. Their data proved that despite the increase in photon flux to about 150% of the control samples, there was significant apoptosis (as indicated by increased caspase-3 activity) along with a decrease in cell viability.

In vivo experiments performed with a subcutaneous xenograft of a CMV-driven luciferase expressing cell line also demonstrated that despite a retarded tumor growth with doxorubicin treatment, the BLI increased over time. This increase in BLI was transient and eventually became reflective of the actual tumor burden 24 days after the IV injection of doxorubicin (as shown in Figure 3.30 C)[88]. Doxorubicin was especially relevant to the observations reported in

this thesis because similar to cisplatin, doxorubicin is also a DNA-damaging chemotherapeutic
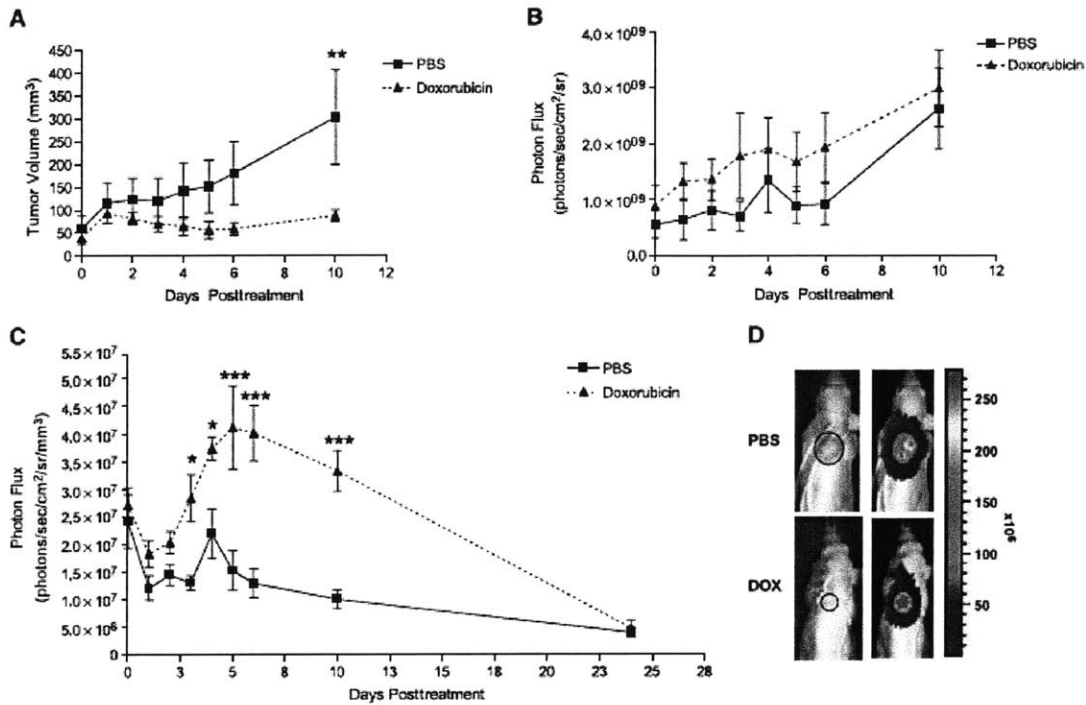
Figure 3.30 An *in vivo* experiment demonstrating the transient increase in luciferase expression. A: Tumor volume of the subcutaneous xenograft of 22RV1-CMVluc cells in nude mice over time. The animals were treated with either 200 µL of PBS or 200 µL of 1 mg/mL doxorubicin on Day 0. B: BLI over time measured from the same subcutaneous xenograft mice. C: BLI normalized to tumor volume over time. D: An example of PBS-treated and doxorubicin-treated animals on Day 6. The PBS-treated animal had a tumor volume of 220 mm^3 while the doxorubicin-treated animal had a tumor volume of 50 mm^3. *Source: Svensson et al. Cancer Research (2007)*

agent. The pathways involved in the up-regulation of CMV promoter are likely to be similar as

well.

The same group of researchers also discovered that the p38 mitogen-activated protein kinase

(MAPK) pathway was involved in the up-regulation of the CMV-driven luciferase expression.

They showed that an inhibitor of the p38 MAPK pathway (SB203580) was able to normalize the

up-regulation of luciferase activity when combined with doxorubicin or staurosporin[88]. This

99

result was not surprising given that it was also reported that p38 MAPK activation played a role

in the cell cycle checkpoint function after DNA damage[89].

The SKOV3 xenograft used in this thesis is also a CMV-driven luciferase expressing cell line. All these results from the literature helped to explain the observation of high BLI signal and the over-estimation of tumor burden by BLI in some device treatment groups. It is especially noted in section 1.3 that one of the apoptosis pathways that cisplatin turns on is the MAPK pathway. It could be deduced that the up-regulation of CMV promoter, and its associated observation of a higher-than-normal BLI value, could be indicative of the presence of apoptosis and cytotoxicity as a result of the cisplatin treatment.

The IP bolus injection groups were also expected to be experiencing this transient luciferase up-regulation since there was an effective treatment. This transient up-regulation, however, may not always be captured on the twice weekly IVIS imaging time points. It depends on the number of days between the IVIS imaging and the last IP bolus injection. Figure 3.31 shows an example of the weekly 5 mg/kg IP bolus injection group where this BLI peaking after each dose of cisplatin was captured, as indicated by the red arrows. Each BLI imaging time point occurred two days after each IP bolus dosing of cisplatin.
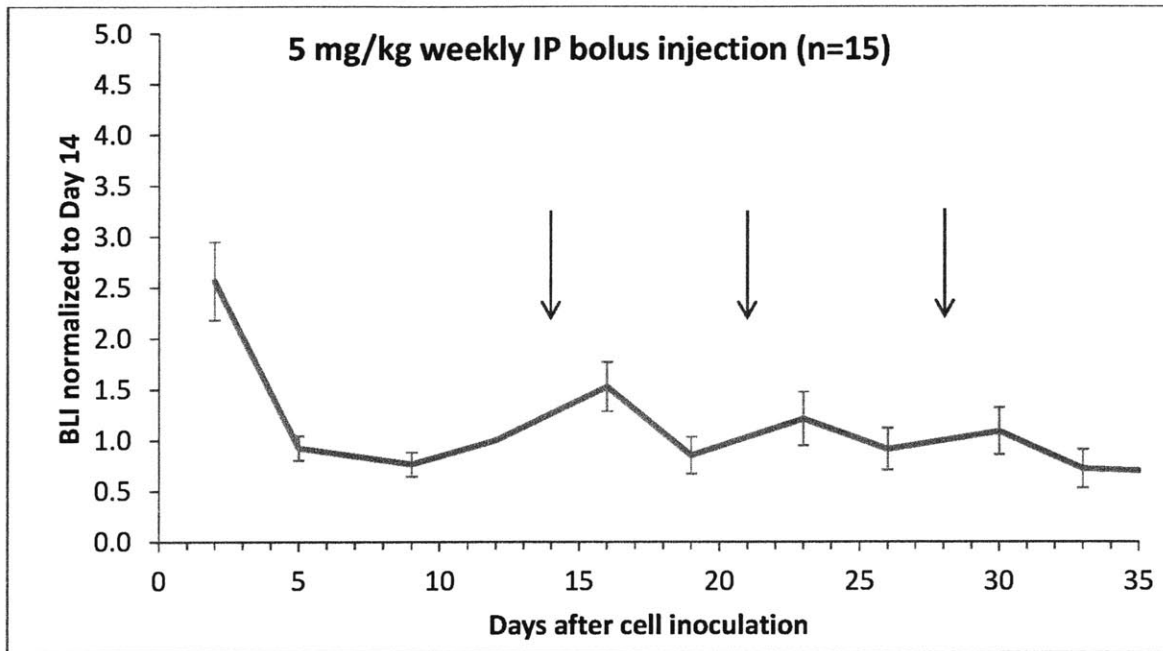
Figure 3.31 The normalized BLI (to the day of the start of treatment) showed the transient increase in luciferase activity following each IP bolus cisplatin injection (5 mg/kg). The red arrow marked the days of cisplatin dosing. A peak was observed in BLI two days after each cisplatin IP injection.

This page is intentionally left blank.

4 Future works

4.1 Human device design criteria and possible materials

The mouse device had shown great potential in the success of the new treatment regimen of having a low, sustained cisplatin concentration locally in the peritoneal cavity for ovarian cancer patients. A larger and more ergonomic human device needs to be designed and characterized for the larger animal pre-clinical trial and eventually the clinical trials. Discussions with gynecologic surgeon Dr Marcela Del Carmen concluded with the following design considerations for the human device:

1. The material has to be biocompatible to be used for an implantable device.

2. The mechanical properties of the material have to be compatible with the organs in the peritoneal cavity to minimize trauma and damage to the organs.

3. The material needs to be easy to be fabricated into a desirable shape and size.

4. The drug (cisplatin) needs to be permeable to the material chosen.

5. The design of the device must be easy to be inserted and removed through a laparoscopic port during implantation and at the end of the treatment. This will enhance physician acceptance.

6. The shape and size of the device should aid with the distribution of the drug within the peritoneal cavity.

There are numerous biocompatible materials; however, choosing the right material that could fulfill both the mechanical and chemical property requirements for designing this device may not be trivial. Figure 4.1 and 4.2 shows the mechanical properties of soft tissues and some commonly used biomaterials. Silicone rubber is the most suitable biomaterial for use with

soft tissues given its low modulus of 8 MPa and low tensile strength of 7.6 MPa. However, it was shown that silicone has a low permeability for cisplatin. Cisplatin is a small neutral molecule while silicone is highly hydrophobic. The release of cisplatin by permeation through a silicone reservoir would require a very large surface area. A smart design for engineering this large surface area into a device that would be easy to be inserted or removed through a laparoscopic port would be the next important milestone. Alternatively, a composite material that involves the mixing of silicone with another more hydrophilic biomaterial could bypass this.

Mechanical properties of soft tissues [22]

Soft tissue	Modulus (MPa)	Tensile strength (MPa)
Articular cartilage	10.5	27.5
Fibrocartilage	159.1	10.4
Ligament	303.0	29.5
Tendon	401.5	46.5
Skin	0.1–0.2	7.6
Arterial tissue (longitudinal direction)		0.1
Arterial tissue (transverse direction)		1.1
Intraocular lens	5.6	2.3

Figure 4.1 A table listing the mechanical properties of soft tissues. *Source: Biomedical applications of polymer-composite materials: a review by Ramakrishna et al.*

Mechanical properties of typical polymeric biomaterials [22]

Material	Modulus (GPa)	Tensile strength (MPa)
Polyethylene (PE)	0.88	35
Polyurethane (PU)	0.02	35
Polytetrafluoroethylene (PTFE)	0.5	27.5
Polyacetal (PA)	2.1	67
Polymethylmethacrylate (PMMA)	2.55	59
Polyethylene terepthalate (PET)	2.85	61
Polyetheretherketone (PEEK)	8.3	139
Silicone rubber (SR)	0.008	7.6
Polysulfone (PS)	2.65	75

Figure 4.2 A table of commonly used polymeric biomaterials and their mechanical properties. *Source: Biomedical applications of polymer-composite materials: a review by Ramakrishna et al.*

4.2   Other candidates for intraperitoneal drug delivery

Recent developments in targeted therapies had given hope to many diseases. Cisplatin, for instance, has been conjugated to targeting agents for targeted treatment of diseases such as breast cancer, colon cancer and prostate cancer[90-92]. However, most of these particles release their payloads in just 1-3 days[90,92]. A combination of a drug delivery platform used in this thesis and these particles would potentially bring about even more efficacious and less toxic treatment – having a continuous supply of the therapeutic agent only to the target site.

Cisplatin was discovered in the 1960s and had generated interest in the use of metal compound in cancer treatment since the 1970s[18]. It was shown to be a potent chemotherapeutic and many platinum compounds have since been synthesized to improve minimize its toxic side-effects

and/or to circumvent cisplatin resistance[93]. Among the recent discoveries, carboplatin evolved to be an equally potent but less toxic chemotherapeutic drug against advanced ovarian cancer compared to cisplatin when administered intraperitoneally[94,95]. These promising results from the pre-clinical and clinical trials have led to two Phase III clinical trials being conducted by the Gynecologic Oncology Group in the United States and the National Cancer Institute of Canada.

The GOG 252 study was started in 2009 and is estimated to complete in Oct 2014[96]. If IP carboplatin is proven to be more beneficial to patients (similar or improved progression-free survival and/or overall survival) without the experiencing the toxicity of cisplatin, carboplatin could soon rise to become the standard-of-care in the IP treatment of ovarian cancer. This would enable carboplatin to become a good candidate for intraperitoneal release from this human device in the near future.

Paclitaxel is another drug that is currently approved for IP therapy. It has used in conjunction with cisplatin in the treatment of ovarian cancer[33,38,39]. It demonstrated a profound pharmacokinetic advantage for local delivery over systemic delivery. It was shown to achieve a 1000 fold higher drug concentration when delivered IP than IV[34]. However, in contrast to the platinum-based drugs, paclitaxel exhibits local toxicity rather than systemic ones. The dose-limiting side-effect was abdominal pain. A drug delivery device that releases paclitaxel slowly but continuously over a prolonged period of time may prove to be more beneficial for patients than the current bolus injection IP. Preclinical studies have shown that compared to intermittent delivery of paclitaxel IP, a sustained paclitaxel delivery from a novel formulation resulted in a significant reduction of tumor proliferation, enhanced apoptosis and increased survival times[97,98]. Paclitaxel, however, has a low aqueous solubility of less than 0.01 mg/mL[99]. This would pose a problem in releasing with this drug delivery platform which is aqueous diffusion driven.

Research on formulating the paclitaxel pro-drug with PEG had shown promising results[100-102].

These water-soluble formulations could also be a potential candidate for device release in the

near future.

This page is intentionally left blank.

5 Conclusion

Ovarian cancer is one of the most common gynecologic cancers in the United States. The intraperitoneal (IP) treatment regimen improves the treatment survival outcome significantly compared to the traditional intravenous (IV) cisplatin administration. The IP treatment, however, causes various drug-related toxicities, catheter-induced infection and discomfort to the patient. This results in the premature termination of treatment for a large proportional of the patients. A drug delivery platform was developed in this thesis as a tool to investigate the treatment outcome of a low constant cisplatin concentration over a long time versus periodic cisplatin concentration spikes in the peritoneal cavity. This drug delivery device demonstrated comparable efficacy to and less toxicity than cycles of IP bolus injections of cisplatin of a similar cumulative dose or area-under-curve (AUC). This revealed that the treatment efficacy for ovarian cancer is correlated to the AUC and not the peak drug concentration (C_{max}). This device treatment regimen where cisplatin is administered slowly but continuously to deliver the same AUC could potentially revolutionize the treatment of ovarian cancer in the near future.

References

1   Cancer, O. *Surveillance, Epidemiology and End Results (SEER) Program of the National Cancer Institute*.

2   Cannistra, S. A. Cancer of the ovary (vol 351, pg 2519, 2004). *N. Engl. J. Med.* **352**, 104-104 (2005).

3   Colombo, P. E. *et al.* Intraperitoneal administration of novel doxorubicin loaded polymeric delivery systems against peritoneal carcinomatosis: Experimental study in a murine model of ovarian cancer. *Gynecol. Oncol.* **122**, 632-640, doi:10.1016/j.ygyno.2011.05.032 (2011).

4   Laurie Ilit, T. K. O., Allan Covens, Janice Kwon, Michael Fung-Kee Fung, Holger W. Hirte, Amit M. Oza. Intraperitoneal Chemotherapy in the First-line Treatment of Women with Stage III Epithelial Ovarian Cancer. *Cancer* **109**, 692-702 (2007).

5   Guppy AE, N. P., Rustin GJ. Epithelial ovarian cancer: a review of current management. *Clinical Oncology* **17**, 399-411 (2005).

6   Memarzadeh, S. & Berek, J. S. Advances in the management of epithelial ovarian cancer. *J. Reprod. Med.* **46**, 621-629 (2001).

7   Roverts Ozols, T. C. H. Focus on epithelial ovarian cancer. *Cancer Cell* **5** (2004).

8   Fathalla, M. Incessant ovulation - a factor in ovarian neoplasia? *Lancet* **17** (1971).

9   Cramer, D. a. W., WR. Determinatnt of ovairan cancer risk. II. Inferences regarding pathogenesis. *J. Natl. Cancer Institute* **71**, 717-721 (1983).

10   Mannis GN, F. J., Creasman JS, Jacoby VL, Beattie MS. Risk-reducing salpingo-oophorectomy and ovarian cancer screening in 1077 women after BRCA testing *JAMA Intern Med* **173** (2012).

11   Berchuck, A. M. D. C., Frank M.D. Genetics of Ovarian Cancer. *Current Opinion in Endocrinology, diabetes and obesity* **7** (1997).

12   King, P. L. W. a. M.-C. BRCA1 and BRCA2 and the genetics of breast and ovarian cancer. *Human Molecular Genetics* **10**, 705-713 (2001).

13   Victor Grann, M., MPH; Maxine Ashby-Thompson, MPH. Role of Genetic Testing for Screening and Prevention for Ovarian Cancer. *SAMA Intern Med.* **173** (2013).

14   Victoria Cepeda1, M. A. F., Josefina Castilla2, Carlos Alonso1, Celia Quevedo3 and & Jose M. Pérez3. Biochemical Mechanisms of Cisplatin Cytotoxicity. *Anti-Cancer Agents in Medicinal Chemistry,* **7** 3-18 (2007).

15   Siddik, Z. H. Cisplatin: mode of cytotoxic action and molecular basis for resistance. *Oncogene* **22** (2003).

16   Amélie Rebillard*, 2, Dominique Lagadic-Gossmann1,2 and Marie-Thérèse Dimanche-Boitrel*,. Cisplatin Cytotoxicity: DNA and Plasma membrane targets. *Current Medicinal Chemistry* **15**, 2656 - 2663 (2008).

17   Hans C. Ehrsson, I. B. W., and Anita S. Anderson. Cisplatin, transplatin, and their hydrated complexes: Separation and identification using porous graphitic carbon and electrospray ionization mass spectrometry. *Analytical Chemistry* **67**, 3608-3611 (1995).

18   Rebecca A. Alderden, M. D. H., and Trevor W. Hambley. The discovery and development of cisplatin. *Journal of chemical education* **83** (2006).

19   Beyer, F. K. a. U. Serum Proteins as Drug Carriers of Anticancer Agents: A Review. *Drug delivery* **5** (1998).

20   Deconti, R. C., Toftness, B. R., Lange, R. C. & Creasey, W. A. CLINICAL AND PHARMACOLOGICAL STUDIES WITH CIS-DIAMMINEDICHLOROPLATINUM(II). *Cancer Research* **33**, 1310-1315 (1973).

21   Ivanov, A. I. *et al.* Cisplatin binding sites on human albumin. *Journal of Biological Chemistry* **273**, 14721-14730, doi:10.1074/jbc.273.24.14721 (1998).

22   Andrews, P. A., Wung, W. E. & Howell, S. B. A HIGH-PERFORMANCE LIQUID-
        CHROMATOGRAPHIC ASSAY WITH IMPROVED SELECTIVITY FOR CISPLATIN AND ACTIVE
        PLATINUM(II) COMPLEXES IN PLASMA ULTRAFILTRATE. *Analytical Biochemistry* **143**, 46-56,
        doi:10.1016/0003-2697(84)90556-6 (1984).

23   Ishida, S. I., S); Lee, J (Lee, J); Thiele, DJ (Thiele, DJ); Herskowitz, I (Herskowitz, I). Uptake of the
        anticancer drug cisplatin mediated by the copper transporter Ctr1 in yeast and mammals.
        Proceedings of he National Academy of Sciences of the United States of America **99** (2002).

24   Davies, M. D., MS); Berners-Price, SJ (Berners-Price, SJ); Hambley, TW (Hambley, TW). Slowing of
        cisplatin aquation in the presence of DNA but not in the presence of phosphate: Improved
        understanding of sequence selectivity and the roles of monoaquated and diaquated species in
        the binding of cisplatin to DNA. *Inorganic Chemistry* **39**, 5603-5613 (2000).

25   Kelland, L. R. Preclinical perspectives on platinum resistance. *Drugs* **59**, 1-8,
        doi:10.2165/00003495-200059004-00001 (2000).

26   Chu, G. CELLULAR-RESPONSES TO CISPLATIN - THE ROLES OF DNA-BINDING PROTEINS AND DNA-
        REPAIR. *Journal of Biological Chemistry* **269**, 787-790 (1994).

27   Kelland, L. R. NEW PLATINUM ANTITUMOR COMPLEXES. *Critical Reviews in
        Oncology/Hematology* **15**, 191-219, doi:10.1016/1040-8428(93)90042-3 (1993).

28   Furuta, T. *et al.* Transcription-coupled nucleotide excision repair as a determinant of cisplatin
        sensitivity of human cells. *Cancer Research* **62**, 4899-4902 (2002).

29   Chaney, S. G. & Sancar, A. DNA repair: Enzymatic mechanisms and relevance to drug response.
        Journal of the National Cancer Institute **88**, 1346-1360, doi:10.1093/jnci/88.19.1346 (1996).

30   Hills, C. A. *et al.* BIOLOGICAL PROPERTIES OF 10 HUMAN OVARIAN-CARCINOMA CELL-LINES -
        CALIBRATION INVITRO AGAINST 4 PLATINUM COMPLEXES. *British Journal of Cancer* **59**, 527-534,
        doi:10.1038/bjc.1989.108 (1989).

31   McGuire WP, H. W., Brady MF, et al. Cyclophosphamide and cisplatin compared with paclitaxel
        and cisplatin in patients with stage III and stage IV ovarian cancer. *N. Engl. J. Med.* **334**, 1-6
        (1996).

32   Piccart MJ, B. K., James K, et al. Randomized intergroup trial of cisplatin-paclitaxel versus
        cisplatin-cyclophosphamide in women with advanced epithelial ovarian cancer: Three-year
        results. *Journal of National Cancer Institute* **92** (2000).

33   Armstrong, D. K. *et al.* Intraperitoneal cisplatin and paclitaxel in ovarian cancer. *N. Engl. J. Med.*
        354, 34-43 (2006).

34   Markman, M. Intraperitoneal antineoplastic drug delivery: rationale and results. *The Lancet
        Oncology* **4**, 277-283 (2003).

35   Walker, J. L. *et al.* Intraperitoneal catheter outcomes in a phase III trial of intravenous versus
        intrapentoneal chemotherapy in optimal stage III ovarian and primary peritoneal cancer: A
        Gynecologic Oncology Group study. *Gynecol. Oncol.* **100**, 27-32,
        doi:10.1016/j.ygyno.2005.11.013 (2006).

36   Casper, E. S., Kelsen, D. P., Alcock, N. W. & Lewis, J. L. IP CISPLATIN IN PATIENTS WITH
        MALIGNANT ASCITES - PHARMACOKINETIC EVALUATION AND COMPARISON WITH THE IV
        ROUTE. *Cancer Treatment Reports* **67**, 235-238 (1983).

37   Walter H. Gotlieb, M., PhD. Intraperitoneal Chemotherapy - Why the Fuzz? *International Journal
        of Gynecological Cancer* **20** (2010).

38   Alberts DS, L. P., Hannigan EV, et al. Intraperitoneal cisplatin plus intravenous cyclophosphamide
        versus intravenous cisplatin plus intravenous cyclophosphamide for stage III ovarian cancer. *N.
        Engl. J. Med.* **335**, 1950-1955 (1996).

39   Markman M, B. B., Alberts DS et al. Phase III trial of standard-dose intravenous cisplatin plus
        paclitaxel versus moderately high-dose carboplatin followed by intravenous paclitaxel and

intraperitoneal cisplatin in small-volume stage III ovarian carcinoma: an intergroup study of the Gynecologic Oncology Group, South-western Oncology Group and Eastern Cooperative Oncology Group. *Journal of Clinical Oncology* **19**, 1001-1007 (2001).

40   Grady, D. Widespread Flaws Found in Ovarian Cancer Treatment. *New York Times* (2013).

41   Bristow, R. E. *et al.* Disparities in Ovarian Cancer Care Quality and Survival According to Race and Socioeconomic Status. *Jnci-Journal of the National Cancer Institute* **105**, 823-832, doi:10.1093/jnci/djt065 (2013).

42   Paul A. Zieske, M. K., Jeffery L. Hinese, Cory C. Knight et al. Characterization of cisplatin degradation as affected by pH and light. *AJHP* **48**, 1500-1506 (1991).

43   Deanna N Bell, J. J. L., Mark J MacKeage et al. Comparative protein binding, stability and degradation of satraplatin, JM118 and cisplatin in human plasma in vitro. *Clinical and Experimental Pharmacology and Physiology* **35**, 1440-1446 (2008).

44   Anita Andersson, H. E. Stability of cisplatin and its monohydrated complex in blood, plasma and ultrafiltrate - implications for quantitative analysis. *Journal of Pharmaceutical and Biomedical Analysis* **13**, 639-644 (1995).

45   McIntosh, D. P., Cooke, R. J., McLachlan, A. J., DaleyYates, P. T. & Rowland, M. Pharmacokinetics and tissue distribution of cisplatin and conjugates of cisplatin with carboxymethyldextran and A5B7 monoclonal antibody in CD1 mice. *Journal of Pharmaceutical Sciences* **86**, 1478-1483, doi:10.1021/js960282u (1997).

46   Newman, M. S., Colbern, G. T., Working, P. K., Engbers, C. & Amantea, M. A. Comparative pharmacokinetics, tissue distribution, and therapeutic effectiveness of cisplatin encapsulated in long-circulating, pegylated liposomes (SPI-077) in tumor-bearing mice. *Cancer Chemotherapy and Pharmacology* **43**, 1-7, doi:10.1007/s002800050855 (1999).

47   V Augey, M. C., M Galtier, R Yearoo, V Pinsani, F Bressolle. High-performance liquid chromatographic determination of cis-dichlorodiammineplatinum(II) in plasma ultrafiltrate. *Journal of Pharmaceutical and Biomedical Analysis* **13**, 1173-1178 (1995).

48   A Lopez-Flores, R. J., P Garcia-Lopez. A high-performance liquid chromatographic assay for determination of cisplatin in plasma, cancer cell and tumor samples. *Journal of Pharmacological and Toxicological Methods* **52**, 366-372 (2005).

49   WRL Cairns, L. E., SJ Hill. *Analytical Proceedings* **31**, 295-297 (1994).

50   WRL Cairns, L. E., SJ Hill. *Frensenius Journal of Analytical Chemistry* **355**, 202-208 (1996).

51   S.Hann, Z. S., K Lenz, G Stingeder. *Analytical and Bioanalytical Chemistry* **381**, 405-412 (2005).

52   S Hann, G. K., Zs Stefanka, G Stingeder, M Furhacker, W Buchberger, RM Mader. *Journal of Analytical Spectrometry* **18**, 1391-1395 (2003).

53   M. Espinosa Bosch, A. R. S., F Sanchez Rojas, C Bosch Ojeda. Analytical methodologies for the determination of cisplatin. *Journal of Pharmaceutical and Biomedical Analysis* **47**, 451-459 (2008).

54   Iwano, S. *et al.* Development of simple firefly luciferin analogs emitting blue, green, red, and near-infrared biological window light. *Tetrahedron* **69**, 3847-3856, doi:http://dx.doi.org/10.1016/j.tet.2013.03.050 (2013).

55   Hensley, D. C. C. a. H. H. Xenograft and transgenic mouse models of epithelial ovarian cancer and non-invasive imaging modalities to monitor ovarian tumor growth in situ: applications in evaluating novel therapeutic agents. *Current Protocols in Pharmacology* (2009).

56   Choy, G. *et al.* Comparison of noninvasive fluorescent and bioluminescent small animal optical imaging. *Biotechniques* **35**, 1022-+ (2003).

57   Araki, H., Tani, T. & Kodama, M. Antitumor effect of cisplatin incorporated into polylactic acid microcapsules. *Artificial Organs* **23**, 161-168 (1999).

58   Ding, D. *et al.* Nanospheres-Incorporated Implantable Hydrogel as a Trans-Tissue Drug Delivery System. *Acs Nano* **5**, 2520-2534, doi:10.1021/nn102138u (2011).

59   Leite, E. A. *et al.* Acute toxicity of long-circulating and pH-sensitive liposomes containing cisplatin in mice after intraperitoneal administration. *Life Sciences* **84**, 641-649, doi:10.1016/j.lfs.2009.02.002 (2009).

60   Coimbra Araujo, J. G. *et al.* Biodistribution and antitumoral effect of long-circulating and pH-sensitive liposomal cisplatin administered in Ehrlich tumor-bearing mice. *Experimental Biology and Medicine* **236**, 808-815, doi:10.1258/ebm.2011.011038 (2011).

61   Canta, A. *et al.* In vivo comparative study of the cytotoxicity of a liposomal formulation of cisplatin (lipoplatin (TM)). *Cancer Chemotherapy and Pharmacology* **68**, 1001-1008, doi:10.1007/s00280-011-1574-3 (2011).

62   De Stefano, I. *et al.* Hyaluronic acid-paclitaxel: effects of intraperitoneal administration against CD44(+) human ovarian cancer xenografts. *Cancer Chemotherapy and Pharmacology* **68**, 107-116, doi:10.1007/s00280-010-1462-2 (2011).

63   Balthasar, D. K. S. J. V. R. J. B. J. P. Evaluation of combined bevacizumab and intraperitoneal carboplatin or paclitaxel therapy in a mouse model of ovarian cancer. *Cancer Chemother Pharmacol* **68**, 951–958 (2011).

64   · Daniela Gallo, I. D. S. A. B. G. F. Z. M. G. P. A. F. D. T. S. B. D. R. G. S. C. F. Hyaluronic acid–paclitaxel effects of intraperitoneal administration against CD44(+) human ovarian cancer xenografts. *Cancer Chemother Pharmacol*, 107–116 (2011).

65   Carozzi, V. A. *et al.* Neurophysiological and neuropathological characterization of new murine models of chemotherapy-induced chronic peripheral neuropathies. *Exp. Neurol.* **226**, 301-309, doi:10.1016/j.expneurol.2010.09.004 (2010).

66   S. Hann, G. K. e. a. Application of HPLC-ICP-MS to speciation of cisplatin and its degradation products in water containing different chloride concentrations and in human urine. *J. Anal. At. Spectrom.* **18**, 1391-1395 (2003).

67   LifeSciences, C.

68   Wang, Y. D., Ameer, G. A., Sheppard, B. J. & Langer, R. A tough biodegradable elastomer. *Nat. Biotechnol.* **20**, 602-606, doi:10.1038/nbt0602-602 (2002).

69   Ma, J. *et al.* PHARMACOKINETIC-DYNAMIC RELATIONSHIP OF CISPLATIN IN-VITRO - SIMULATION OF AN IV BOLUS AND 3 H AND 20 H INFUSION. *British Journal of Cancer* **69**, 858-862, doi:10.1038/bjc.1994.166 (1994).

70   B Royer, E. G., E polycape, G Hoizey, D Delroeux et al. Serum and intraperitoneal pharmacokinetics of cisplatin within intraoperative intraperitoneal chemotherapy: influence of protein binding. *Anti-Cancer Drugs* **16**, 1009-1016 (2005).

71   Kristin M Nieman1, H. A. K., Carla V Penicka1, Andras Ladanyi1, Rebecca Buell-Gutbrod2,, Marion R Zillhardt1, I. L. R., Mark S Carey3, Gordon B Mills3, Gökhan S Hotamisligil4, S Diane Yamada1, & Marcus E Peter5, K. G. E. L. Adipocytes promote ovarian cancer metastasis and provide energy for rapid tumor growth. *Nature Medicine* **17**, 1498 - 1503 (2011).

72   Rebillard, A., Lagadic-Gossmann, D. & Dimanche-Boitrel, M. T. Cisplatin Cytotoxicity: DNA and Plasma Membrane Targets. *Curr. Med. Chem.* **15**, 2656-2663, doi:10.2174/092986708786242903 (2008).

73   An, Y., Xin, H., Yan, W. & Zhou, X. X. Amelioration of cisplatin-induced nephrotoxicity by pravastatin in mice. *Experimental and Toxicologic Pathology* **63**, 215-219, doi:10.1016/j.etp.2009.12.002 (2011).

74   Fujieda, M. *et al.* Effect of pravastatin on cisplatin-induced nephrotoxicity in rats. *Human & Experimental Toxicology* **30**, 603-615, doi:10.1177/0960327110376551 (2011).

75   Ozer, M. K. *et al.* Effects of misoprostol on cisplatin-induced renal damage in rats. *Food and Chemical Toxicology* **49**, 1556-1559, doi:10.1016/j.fct.2011.03.051 (2011).

76   Kwon, H. N. *et al.* Predicting idiopathic toxicity of cisplatin by a pharmacometabonomic approach. *Kidney International* **79**, 529-537, doi:10.1038/ki.2010.440 (2011).

77   Travlos, G. S. Normal structure, function, and histology of the bone marrow. *Toxicologic Pathology* **34**, 548-565, doi:10.1080/01926230600939856 (2006).

78   Kondo, M., Weissman, I. L. & Akashi, K. Identification of clonogenic common lymphoid progenitors in mouse bone marrow. *Cell* **91**, 661-672, doi:10.1016/s0092-8674(00)80453-5 (1997).

79   Akashi, K., Traver, D., Miyamoto, T. & Weissman, I. L. A clonogenic common myeloid progenitor that gives rise to all myeloid lineages. *Nature* **404**, 193-197, doi:10.1038/35004599 (2000).

80   Laiosa, C. V., Stadtfeld, M. & Graf, T. in *Annual Review of Immunology* Vol. 24 *Annual Review of Immunology*   705-738 (2006).

81   Travlos, G. S. Histopathology of bone marrow. *Toxicologic Pathology* **34**, 566-598, doi:10.1080/01926230600964706 (2006).

82   Vanputten, L. M. THE LIFE SPAN OF RED CELLS IN THE RAT AND THE MOUSE AS DETERMINED BY LABELING WITH DFP32 INVIVO. *Blood* **13**, 789-794 (1958).

83   MF., S. Cytomegalovirus promoter for expression in mammalian cells. *Gene expression systems: using nature for the art of expression. San Diego (CA): Academic Press;*, 211-233 (1999).

84   Chen, J. P. & Stinski, M. F. Role of regulatory elements and the MAPK/ERK or p38 MAPK pathways for activation of human cytomegalovirus gene expression. *Journal of Virology* **76**, 4873-4885, doi:10.1028/jvi.76.10.4873-4885-2002 (2002).

85   Johnson, R. A., Huong, S. M. & Huang, E. S. Activation of the mitogen-activated protein kinase p38 by human cytomegalovirus infection through two distinct pathways: a novel mechanism for activation of p38. *Journal of Virology* **74**, 1158-1167, doi:10.1128/jvi.74.3.1158-1167.2000 (2000).

86   Ramanathan, M., Hasko, G. & Leibovich, S. J. Analysis of signal transduction pathways in macrophages using expression vectors with CMV promoters: A cautionary tale. *Inflammation* **29**, 94-102, doi:10.1007/s10753-006-9005-z (2005).

87   Ursaka Kamensek, G. S., Suzana Vidic, Gregor Tevz, Simona Kranjc, Maja Cemazar. Irradiation, cisplatin and 5-azacytidine upregulate cytomegalovirus promoter in tumors and muscles: Implementation of non-invasive fluorescence imaging. *Molecular Imaging and Biology* **13**, 43-52 (2010).

88   Svensson, R. U., Barnes, J. M., Rokhlin, O. W., Cohen, N. B. & Henry, M. D. Chemotherapeutic agents up-regulate the cytomegalovirus promoter: implications for bioluminescence Imaging of tumor response to therapy. *Cancer Research* **67**, 10445-10454, doi:10.1158/0008-5472.can-07-1955 (2007).

89   Reinhardt, H. C., Aslanian, A. S., Lees, J. A. & Yaffe, M. B. p53-deficient cells rely on ATM- and ATR-mediated checkpoint signaling through the p38MAPK/MK2 pathway for survival after DNA damage. *Cancer Cell* **11**, 175-189, doi:10.1016/j.ccr.2006.11.024 (2007).

90   Valencia, P. M. *et al.* Synergistic cytotoxicity of irinotecan and cisplatin in dual-drug targeted polymeric nanoparticles. *Nanomedicine* **8**, 687-698, doi:10.2217/nnm.12.134 (2013).

91   Mi, Y., Zhao, J. & Feng, S. S. Targeted co-delivery of docetaxel, cisplatin and herceptin by vitamin E TPGS-cisplatin prodrug nanoparticles for multimodality treatment of cancer. *Journal of Controlled Release* **169**, 185-192, doi:10.1016/j.jconrel.2013.01.035 (2013).

92   Petersen, M. A., Hillmyer, M. A. & Kokkoli, E. Bioresorbable Polymersomes for Targeted Delivery of Cisplatin. *Bioconjugate Chemistry* **24**, 533-543, doi:10.1021/bc3003259 (2013).

93 Kelland, L. R. *et al.* Mini-review: discovery and development of platinum complexes designed to circumvent cisplatin resistance. *Journal of Inorganic Biochemistry* **77**, 111-115, doi:10.1016/s0162-0134(99)00141-5 (1999).

94 Mangioni, C. *et al.* RANDOMIZED TRIAL IN ADVANCED OVARIAN-CANCER COMPARING CISPLATIN AND CARBOPLATIN. *Journal of the National Cancer Institute* **81**, 1464-1471, doi:10.1093/jnci/81.19.1464 (1989).

95 Stewart, L. A. CHEMOTHERAPY IN ADVANCED OVARIAN-CANCER - AN OVERVIEW OF RANDOMIZED CLINICAL-TRIALS. *British Medical Journal* **303**, 884-893 (1991).

96 Bevacizumab and Intravenous or Intraperitoneal Chemotherapy in Treating Patients With Stage II, Stage III, or Stage IV Ovarian Epithelial Cancer, Fallopian Tube Cancer, or Primary Peritoneal Cancer.

97 Vassileva, V. *et al.* Efficacy assessment of sustained intraperitoneal paclitaxel therapy in a murine model of ovarian cancer using bioluminescent imaging. *British Journal of Cancer* **99**, 2037-2043, doi:10.1038/sj.bjc.6604803 (2008).

98 Vassileva, V., Grant, J., Souza, R. D., Allen, C. & Piquette-Miller, M. Novel biocompatible intraperitoneal drug delivery system increases tolerability and therapeutic efficacy of paclitaxel in a human ovarian cancer xenograft model. *Cancer Chemothera Pharmacol* **60**, 907-914 (2007).

99 Madhu S. Surapaneni, S. K. D., and Nandita G. Das. Designing Paclitaxel Drug Delivery Systems Aimed at Improved Patient Outcomes: Current Status and Challenges. *International Scholarly Research Network Pharmacology* **2012** (2012).

100 Greenwald, R. B., Pendri, A., Bolikal, D. & Gilbert, C. W. HIGHLY WATER-SOLUBLE TAXOL DERIVATIVES - 2'-POLYETHYLENEGLYCOL ESTERS AS POTENTIAL PRODRUGS. *Bioorganic & Medicinal Chemistry Letters* **4**, 2465-2470, doi:10.1016/s0960-894x(01)80411-x (1994).

101 Greenwald, R. B. *et al.* Drug delivery systems: Water soluble taxol 2'-poly(ethylene glycol) ester prodrugs - Design and in vivo effectiveness. *Journal of Medicinal Chemistry* **39**, 424-431, doi:10.1021/jm950475e (1996).

102 Li C, Y. D., Inoue T, Yang DJ, Milas L, Hunter NR, Kim EE, Wallace S. Synthesis and evaluation of water-soluble polyethylene glycol-paclitaxel conjugate as a paclitaxel prodrug. *Anticancer drugs* **7**, 642-648 (1996).